# COMPARATIVE PHARMACOKINETICS OF MATRINE: PURE MATRINE *VS.* CRUDE CHEMICAL IN ACAPHA®

by

Guanghua Gao
Bachelor of Medicine, Beijing Medical University, 1988
Master of Medicine, Beijing Medical University, 1991

THESIS SUBMITTED IN PARTIAL FULFILLMENT OF
THE REQUIREMENTS FOR THE DEGREE OF

DOCTOR OF PHILOSOPHY

In the
Department
of
Biological Sciences

© Guanghua Gao 2007

SIMON FRASER UNIVERSITY

Spring, 2007

# APPROVAL

Name: Guanghua Gao

Degree: Doctor of Philosophy

Title of Thesis:

Comparative pharmacokinetics of matrine: Pure matrine vs. crude chemical in Acapha®

Examining Committee:

Chair: Dr. A. Plant, Associate Professor

Dr. F.C.P. Law, Professor, Senior Supervisor
Department of Biological Sciences, S.F.U.

Dr. C.J. Kennedy, Associate Professor
Department of Biological Sciences, S.F.U.

Dr. P.C.H. Li, Associate Professor
Department of Chemistry, S.F.U.

Dr. R.A. Nicholson, Associate Professor
Department of Biological Sciences, S.F.U.
Public Examiner

Dr. W. Riggs, Professor
Faculty of Pharmaceutical Sciences, U.B.C.
External Examiner

December 18, 2006
Date Approved

# SIMON FRASER UNIVERSITY library

# DECLARATION OF PARTIAL COPYRIGHT LICENCE

The author, whose copyright is declared on the title page of this work, has granted to Simon Fraser University the right to lend this thesis, project or extended essay to users of the Simon Fraser University Library, and to make partial or single copies only for such users or in response to a request from the library of any other university, or other educational institution, on its own behalf or for one of its users.

The author has further granted permission to Simon Fraser University to keep or make a digital copy for use in its circulating collection (currently available to the public at the "Institutional Repository" link of the SFU Library website <www.lib.sfu.ca> at: <http://ir.lib.sfu.ca/handle/1892/112>) and, without changing the content, to translate the thesis/project or extended essays, if technically possible, to any medium or format for the purpose of preservation of the digital work.

The author has further agreed that permission for multiple copying of this work for scholarly purposes may be granted by either the author or the Dean of Graduate Studies.

It is understood that copying or publication of this work for financial gain shall not be allowed without the author's written permission.

Permission for public performance, or limited permission for private scholarly use, of any multimedia materials forming part of this work, may have been granted by the author. This information may be found on the separately catalogued multimedia material and in the signed Partial Copyright Licence.

The original Partial Copyright Licence attesting to these terms, and signed by this author, may be found in the original bound copy of this work, retained in the Simon Fraser University Archive.

Simon Fraser University Library
Burnaby, BC, Canada

**SIMON FRASER UNIVERSITY library**

# STATEMENT OF ETHICS APPROVAL

The author, whose name appears on the title page of this work, has obtained, for the research described in this work, either:

(a) Human research ethics approval from the Simon Fraser University Office of Research Ethics,

or

(b) Advance approval of the animal care protocol from the University Animal Care Committee of Simon Fraser University;

or has conducted the research

(c) as a co-investigator, in a research project approved in advance,

or

(d) as a member of a course approved in advance for minimal risk human research, by the Office of Research Ethics.

A copy of the approval letter has been filed at the Theses Office of the University Library at the time of submission of this thesis or project.

The original application for approval and letter of approval are filed with the relevant offices. Inquiries may be directed to those authorities.

Simon Fraser University Library
Burnaby, BC, Canada

# ABSTRACT

Acapha[®], an herbal product used for treating esophageal cancer in China, is undergoing clinical trials as a chemopreventive agent for lung cancer at the B.C. Cancer Agency (BCCA). Little is known of the pharmacokinetics (PK) of Acapha[®] because most of the PK tools available today are developed for a single chemical entity not a chemical mixture such as Acapha[®]. The purposes of the present study were to demonstrate the feasibility of using matrine as a chemical marker to study the PK of Acapha[®], to compare the PK of pure matrine with the PK of crude matrine in Acapha[®], to elucidate the underlying mechanism of matrine absorption and metabolism, and to develop and validate a physiologically based pharmacokinetic (PBPK) model of matrine for rats and humans.

A generic matrine PBPK model consisting of 12 compartments was developed and validated in the rat. The rat model was then scaled to the model of a standard human by replacing the parameters in the rat model with those of humans. The human PBPK model was able to describe closely the time course of matrine concentrations in plasma (or urine) reported in the literature or from a human study at the BCCA. The BCCA datasets also were fitted to a 2-compartment, clearance-volume classical PK model. Model-derived PK parameters showed that about 35-48% of the matrine administered orally was absorbed by humans, which was consistent with the results of the *in vitro* Caco-2 cell transport study. The PBPK model also predicted that matrine was not metabolized significantly by humans confirming the results of the *in vitro* liver

microsomal incubation studies. When the various CYP1A2, 2C19, 3A4, 2C9, and 2D6 probe substrates were incubated separately with human liver microsomes in the presence or absence of Acapha® extract, the metabolic rates of the CYP probes were not found to change significantly. Results of the present studies demonstrate that Caco-2 cell monolayer and PBPK model can provide important insights to the kinetics of Acapha® in humans. These scientific tools should be integrated with the herbal product development paradigm because they may render the development processes more rational and efficient.

**Keywords:**

Acapha®, matrine, pharmacokinetics (PK), classical model, two compartmental model, PBPK model, Caco-2 cell, metabolism, P450 isoenzyme inhibition, PK parameters, extrapolation

# DEDICATION

This work is dedicated to my mom Enxia Xu, my husband Taiping Wu and my son Yuxiang Wu.

# ACKNOWLEDGEMENTS

# TABLE OF CONTENTS

# LIST OF FIGURES

# LIST OF TABLES

# GLOSSARY

| | |
|---|---|
| Acapha® | Anti-cancer and preventive herbal agent |
| PK | Pharmacokinetics |
| PBPK | Physiologically based pharmacokinetic model |
| A to B | Transport from apical side to basolateral side of Caco-2 cells |
| B to A | Transport from basolateral side to apical side of Caco-2 cells |
| $P_{app}$ | Apparent permeability coefficient |
| TEER | Transepithelial electrical resistance |
| P-GP | P-glycoprotein |
| Crude matrine | Matrine in the mixture of Acapha® |
| $IC_{50}$ | The concentration of drug (chemical) producing 50% of inhibition of the CYP isoenzyme |
| LOQ | The limit of quatitation |
| TEF | The toxic equivalency factor |
| LL | Log-likelihood |
| Vc | Distribution volume in the central compartment |
| Vt | Distribution volume in the peripheral compartment |
| CL | The volume of blood or plasma cleared of drug per unit time |
| CLD | Inter-compartmental clearance and distribution volume |
| KA | Absoption rate constant |
| TLAG | Lag time for absorption |
| PC | Tissue/blood partition coefficient |

# CHAPTER 1:
# PROJECT OVERVIEW

## 1.1 Cancer and carcinogenesis

Cancer development is a multi-step process which can be arbitrarily subdivided into initiation, promotion, and progression steps that are required in transforming a normal cell into a neoplastic or tumor cell. Cancer is also characterized by a period that is often 20 years or more between the initiation event and the onset of invasive or metastatic disease. Chemoprevention refers to the use of food, beverages, or pharmacological agents that are used for other clinical applications (Tosetti *et al.*, 2002) to inhibit, delay or reverse the progression of carcinogenesis (Hong and Sporn, 1997). The aim of chemoprevention is to lower the risk of developing invasive or life threatening cancers (Kelloff, 2000; Sporn and Suh, 2000). Thus, chemoprevention is based on the concept that cancers do not arise as the result of a single initiating event but rather represent a multi-step process *i.e.*, the disease to be treated is not cancer *per se* but the process of carcinogenesis.

## 1.2 Acapha®, a chemopreventive agent?

Acapha® has been used in China to treat esophageal cancer for many years. It has been introduced recently into Canada as a potential chemopreventive agent for lung cancer and is undergoing phase IIa clinical trials at the B.C. Cancer Agency.

Despite advances in detection and treatment, lung cancer patients still have a very

poor prognosis. Thus, prevention is an important strategy of controlling lung cancer, especially for the high-risk populations such as former smokers. Several drugs and natural chemicals including tamoxifen (Fisher *et al.*, 1999), non-steroidal anti-inflammatory drugs (Steinbaach *et al.*, 2000), and retinoids such as 13-*cis* retinoic acid (Hong *et al.*, 1990), have undergone clinical trials for lung cancer chemoprevention. The results of these clinical trials have been disappointing (Van Zandwijk et al., 2000; Hennekens *et al.*, 1996; Omenn *et al.*, 1996). In contrast, Acapha® has shown great promise as a lung cancer chemoprevention agent (Zhang *et al*, 2004). Acapha® is prepared from six common Chinese herbs which include *Sophora tonkinensis, Polygonum bistorta, Prunella vulgaris, Sonchus brachyotus, Dictamnus dasycarpus and Dioscorea bulbifera.* Two of the herbal components, *Sophora tonkinensis and Prunella vulgaris*, have been shown to possess significant anticancer activities (Zhang and Gong, 1998; Ji *et al.*, 1999; Xu *et al.*, 2000; Bo *et al.*, 2002).

## 1.3  Pharmacokinetics (PK) and its importance in Acapha® development

PK is the branch of science, which deals with the time course of a drug in the body. Specifically, it is the study of drug absorption, distribution, metabolism and elimination (ADME). These will be described briefly as follows: (a) Absorption is the first step by which a drug gains entry into the body. It is defined as the net transfer of drug from the site of absorption into the circulating fluids of the body. For an orally administered drug, it involves at least two steps: i) to cross the gastrointestinal tract either by transcellular or paracellular mechanisms and enter the bloodstream *via* the capillaries; ii) to pass through the hepatoportal system into systemic circulation with or without

biotransformation. (b) Distribution is defined as the net transfer of drug from the blood into the various tissues and organs. (c) Metabolism is the bioconversion of a drug into other chemical forms or metabolites, mostly by the P-450 system of the liver. (d) Excretion is the removal of drug from the body primarily *via* urine and occasionally *via* feces, bile, sweat, or exhaled air (Schoenwald, 2002). Whether a botanical drug is absorbable by animals *in vivo* or the Caco-2 cell preparation *in vitro* would have great influence on the decision if the agent will be developed into a marketable product. This will be discussed in Chapter 3. Drug biotransformation also is another factor in deciding whether a new therapeutant should be further developed because if the drug is not metabolized, it will accumulate in the body and cause toxicity. This will be examined in Chapter 4.

In contrast to the conventional drug paradigm, Acapha® has been approved as an anticancer drug by the State Food and Drug Agency of China without conducting any preclinical or clinical PK studies. Probably, this is related to the following unresolved problems on herbal product research: (a) it is very difficult to establish a dose-response relationship for an herbal product because most commonly used PKtools are designed for a single pure chemical whereas Acapha® is a mixture, (b) many pharmacologically active chemicals of herbal products still remain to be identified, and (c) there is no established method to study the PK of an herbal mixture. Without the benefits of a PK study, the quantitative relationship between an oral dose of Acapha® and the amount of Acapha® delivered to and deposited in the target organs (*e.g.*, lung and esophagus) will remain largely unknown.

In the present study, I have chosen matrine as a marker chemical or surrogate to

study the PK of Acapha® in rats and humans. There are at least 3 reasons why matrine was chosen to represent Acapha®: (a) a high matrine concentration is often found in the *Sophora* roots, (b) matrine has been shown to possess anticancer activities (Zhu *et al*, 2001; Wang, 1983) and (c) a matrine analytical standard can be purchased from commercial sources.

Hitherto, only one matrine PK study has been published in humans (Wang *et al.*, 1994). In this study, healthy volunteers were infused *i.v.* with 6 mg/kg matrine for 0.5 hr and their serum was sampled at different time points post-dosing. Unchanged matrine in the serum samples were quantitated using a high performance liquid chromatography-ultraviolet detection (HPLC/UV). The time course of serum matrine concentrations in the volunteers could be described by a classical 2-compartment, open PK model. The elimination half-life ($t_{1/2}$) and the renal clearance of matrine were $184 \pm 54$ min and 144 ml/min, respectively. About 52% of the administered dose was excreted unchanged in the urine within 32 hours. No matrine metabolite could be found in the serum or urine (Wang *et al.*, 1994).

Although both animal studies and *in vitro* testing are still considered essential to support the development of a new botanical drug, these tests are too costly and time consuming to be applied to the full range of natural health products (NHPs) available today. Therefore, computer based models especially the PK models, have been used to solve problems in the development of new conventional drugs. PK modeling is a means of expressing a working hypothesis for the primary mechanism of drug distribution and disposition. PK models also are useful to relate the PK of a chemoprevention agent with its pharmacodynamics because the maximal effects of the agent in the target tissue(s) can

4

only be achieved by maintaining a sufficiently high level of the agent for tumor inhibition and the PK models are able to provide such information (Dedrick *et al.*, 1973). PK models also are useful in interpreting the results of toxicokinetic experiments during pre-clinical botanical drug development and supporting dose-finding and dose-escalation studies during clinical trials.

In general, there are two types of PK modeling approaches, namely, one that is data-based and another that is physiologically-based: (a) The data-based PK models divide the animal system into a series of compartments, which do not represent real, identifiable anatomical regions of the body. Since data-based PK models are typically based on the curve fitting of multi-exponential model equations to plasma-concentration time data, they are useful only in interpolation and they have limited use for extrapolation. Moreover, although the data-based models have been used widely and successfully in the development of conventional drugs, they do not explicitly describe the physiological system that determines the PK behaviour. They also do not provide information on, for example tissue-to-tissue concentration differences, the effect of diffusion limitations, changes in protein binding, etc. The plasma PK of matrine in human will be examined in the Chapter 5 of this thesis. (b) Physiologically-based PK (PBPK) models are aimed toward the prediction and characterization of the therapeutic and toxic effects of an agent because these models often represent the real physical structures of the organism *i.e.*, organ or tissue groups with realistic weights and blood flows. Also, they can provide quantitative information on the relationship between the administered dose and the "delivered" or "effective" dose in the tissues and excreta of the organism at any time post-dosing (Clewell and Andersen, 1985). An excellent review has been published

on PBPK modeling (Gerlowski and Jain, 1983). A generic PBPK model of matrine for rat and human will be presented in the Chapter 6 of this thesis.

## 1.4    Research objectives

The long-term objectives of the present study are:

- To develop and validate a generic PBPK model for pure matrine and crude matrine (matrine in Acapha®) in rats and humans based on kinetic data published in the literature and empirical blood, urine and tissue data collected in our laboratory.

- To compare pure matrine PK with those of crude matrine (matrine in Acapha®) in the rat using a volume-clearance PK and a PBPK model.

- To use Caco-2 cell monolayers to elucidate the modes of Acapha® absorption and compare the transport and uptake of pure matrine with that of crude matrine (matrine in Acapha®) *in vitro*.

- To study Acapha® inhibition of human liver CYP1A2, 2C19, 3A4, 2C9, and 2D6 in order to get an idea about potential interaction between Acapha® and western drugs using probe CYP substrates.

## 1.5 References

Bo, Q.M., Wu, Z.Y., Shun, Q.S., Bao, X. S., Mao, Z.S., Ha, S.Q., Lu, S.Y.and Huang, J.M. (2002) A selection of the Illustrated Chinese Anti-Cancer Herbal Medicines. Shanghai Science and Technology Literature Press, Shanghai.

Clewell, H.J. and Andersen, M.E. (1985) In J.F. Stara et al. (Eds). Advances in Health Risk Assessment for Systemic Toxicants and Chemical Mixtures. Princeton Scientific Publishing Co, Princeton, New Jersey.

Dedrick, R.L. Zaharko, D.S.and Lutz, R.J. (1973) Transport and binding of methotrexate *in vivo*. Journal of Pharmaceutical Sciences. 62(6):882-890.

Fisher, B., Costantino, J.P., Wickerham, D.L. Redmond, C.K., Kavanah, M., Cronin, W.M., Vogel, V., Robidoux, A., Dimitrov, N., Atkins, J., Daly, M., Wieand, S., Tan-Chiu E; Ford, L.and Wolmark, N. (1998) Tamoxifen for prevention of breast cancer: report of the National Surgical Adjuvant Breast and Bowel Project P-1 Study. Journal of the National Cancer Institute. 90(18):1371-1388.

Gerlowski, L.E.and Jain, R.K. (1983) Physiologically based pharmacokinetic modeling: principles and applications. Journal of Pharmaceutical Sciences. 72(10):1103-1127.

Hennekens, C.H., Buring, J.E., Manson, J.E., Stampfer, M., Rosner, B., Cook, N.R., Belanger, C., LaMotte, F., Gaziano, J.M., Ridker, P.M., Willett, W. and Peto, R. (1996) Lack of effect of long-term supplementation with beta carotene on the incidence of malignant neoplasms and cardiovascular disease. New England Journal of Medicine. 334(18):1145-1149.

Hong, W.K. and Sporn, M.B. (1997) Recent advances in chemoprevention of cancer, Science. 278:1073-1077.

Hong, W.K., Lippman, S.M., Itri, L.M., Karp, D.D., Lee, J.S., Byers, R.M., Schantz, S.P., Kramer, A.M., Lotan, R. and Peters, L.J. (1990) Prevention of second primary tumors with isotretinoin in squamous-cell carcinoma of the head and neck. New England Journal of Medicine. 323(12):795-801.

Ji, Y.B., He, S. W., Ma, Y.L., Li, J., Yang, C. and Liu, L.L. (1999) Pharmacological Action and Application of Anticancer Traditional Chinese Medicines. Heilongjiang Science and Technology Publishing House, Ha'erbin, China

Kelloff, G.J. (2000) Perspective on cancer chemoprevention research and drug development. Advances in Cancer Research. 78:199-334.

Nestorov, I.A., Aarons, L.J. and Rowland, M. (1997) Physiologically based pharmacokinetic modelling of a homologous series of barbiturates in the rat: a sensitivity analysis. Journal of Pharmacokinetics and Biopharmaceutics. 25(4):413-447.

Omenn, G.S., Goodman, G., Thornquist, M., Barnhart, S., Balmes, J., Cherniack, M., Cullen, M., Glass, A., Keogh, J., Liu, D., Meyskens, F. Jr., Perloff, M., Valanis, B. and Williams, J. Jr. (1996) Chemoprevention of lung cancer: the beta-Carotene and Retinol Efficacy Trial (CARET) in high-risk smokers and asbestos-exposed workers. IARC Scientific Publications. 136:67-85.

Poulin, P.and Theil, F.P. (2002) Prediction of pharmacokinetics prior to *in vivo* studies. II. Generic physiologically based pharmacokinetic models of drug disposition, Journal of Pharmaceutical Sciences, 91(5):1358-1370.

Sporn, M.B. and Suh, N. (2000) Chemoprevention of cancer. Carcinogenesis. 21:525-530.

Steinbach, G.; Lynch, P.M.; Phillips, R.K.; Wallace, M.H.; Hawk, E., Gordon, G.B., Wakabayashi, N., Saunders, B., Shen, Y., Fujimura, T., Su, L.K. and Levin, B. (2000). The effect of celecoxib, a cyclooxygenase-2 inhibitor, in familial adenomatous polyposis. New England Journal of Medicine. 342(26):1946-1952.

Tosetti, F., Ferrari, N., Flora, S.D. and Albini, A. (2002) 'Angioprevention': angiogenesis is a common and key target for cancer chemopreventive agents. The FASEB Journal. 16(1):2-14.

Van Zandwijk, N., Dalesio, O., Pastorino, U., de Vries, N. and van Tinteren, H. (2000) EUROSCAN, a randomized trial of vitamin A and *N*-acetylcysteine in patients with head and neck cancer or lung cancer. For the European Organization for Research and Treatment of Cancer Head and Neck and Lung Cancer Cooperative Groups. Journal of the National Cancer Institute. 92(12):977-986.

Wang, P.Q., Lu, G.H., Zhou, X.B., Shen, J.F., Chen, S.X., Mei, S.W., Chen, M.F. (1994) Pharmacokinetics of matrine in healthy volunteers. Acta Pharmaceutica Sinica. 29 (5):326-329.

Xu, G.J., Wang, Q., Yu, B.Y., Pang, M.J., Han, L., Chen, T., Wang, T.Z., Zeng, J.H. and Li, P. (2000) Coloured Illustrations of Antitumor Chinese Traditional and Herbal Drugs (2rd). Fujian Science and Technology Publishing House, Fuzhou, China.

Zhang, Q.M. and Gong, H.M. (1998) Clinical Practice of Anticancer Traditional Chinese Medicines. People's Health Publishing House, Beijing.

Zhang, Z, Wang, Y, Yao, R, Li, J., Yan, Y., La Regina, M., Lemon, W.L., Grubbs, C.J., Lubet, R.A. and You, M. (2004) Cancer preventive activity of a mixture of Chinese herbs (antitumor B ) in mouse lung tumor models. Oncogene. 23:3841-3850.

8

# CHAPTER 2:
# PRELIMINARY STUDIES ON CHEMICAL
# COMPOSITION OF ACAPHA®

## 2.1 Introduction

It is estimated that there are about 250,000 species of flowering plants in the

world and at least 11,000 of them are used as foods, spicies, flavouring or therapeutic

agents. Thus, plants are a major source of macronutrients (fat, carbohydrate, and protein),

micronutrients (vitamins and trace metals) and non-nutrient constituents (natural products

or secondary metabolites). Although the natural products (secondary metabolites) are

only a small group of these naturally occurring chemicals, they are the main sources of

many therapeutic agents (Tyler, et al, 1976). Table 2.1 shows the detailed classification

of the secondary metabolites in plants.

**Table 2.1:    Subclassification of the secondary metabolites in plants**

| | |
|---|---|
| **Terpenoids** | Monoterpenoid, iridoids, sesquiterpeneoids, sesquiterpene, lactones, diterpenoids, triterpenoid, saponins, steroid, saponins, cardenolides and bufadienolides, phytosterols, cucurbitacins, nortriterpenoids, other triterpenoids, carotenoids |
| **Alkaloids** | Amaryllidaceae, betalain, indole, diterpenoid, isoquinoline, lycopodium, monoterpene, sesquiterpene, peptide, pyrrolidine and piperidine, pyrolizidine, quinoline, quinolizidine, steroidal, tropane |
| **Other nitrogen containing chemicals** | Non- protein amino acids, amines, cyanodenic glycosides, glucosinolates, purines and pyrimidines |
| **Phenolic constituents** | Anthocyanins, anthochlors, benzofurans, chromones, coumarins, Minor flavonoids, flavones and flavonols, isoflavonoids, lignans, phenols and phenolic acids, phenolic ketones, phenylpropanoids, quinonoids, stilbenoids, tannins, xanthenes |

The functional role of natural products in the plants in which they are found is not always obvious. However, these chemicals are believed to play the same or similar role in plants and animals. For example, plant antioxidants such as flavone derivatives, isoflavones, catechins, coumarins, polyfunctional organic acids, ascorbic acid, carotene, *etc.* have been shown to act as reducing chemicals, as free radical chain interrupters, as quenchers or inhibitors of the formation of singlet oxygen and as inactivators of pro-oxidant metals in animals (Simic and Karel, 1980; Hudson, 1990). These natural product chemicals also have been shown to possess anticarcinogenic, anti-inflammatory, and antimutagenic activities in humans (Cai, 2004).

## 2.1.1 Chemical components in Acapha®

Table 2.2 shows the six Chinese herbs that are used to formulate Acapha® and the natural chemicals that may be found in these herbs. As Acapha® will be used as a chemopreventive agent, a brief description on the herbs for their potential contribution to the anticancer, anti-inflammatory, antiviral and immuno-modulation activities of Acapha® should help selecting a marker chemical for Acapha®:

(1) *Sophora tonkinensis*. This herb has been shown to inhibit the growth of mouse S-180 sarcoma cells (Wang, 1983) and increase tumor immunity in laboratory animals (Mori *et al.*, 1989).

(2) *Prunella vulgaris*. It has been shown to possess antiviral, anti-inflammatory, anti-allergic, antimicrobial and immuno-modulation effects. The anti-allergic and anti-inflammatory effects of the herb may be related to the triterpenes such as betulinic acid, ursolic acid, 2-α, 3-α-dihydroxyurs-12-ene-28-oic acid, 2-α-hydroxyursolic acid (Ryu, et al, 2000). Another triterpene, osmarinic acid has been found to possess anti-microbial activity on gram-positive bacteria (Psotova, *et al*, 2003). It also has inhibitory effects on T cell activation and proliferation (Won, *et al*, 2003). The antiviral effects are attributed to a polysaccharide fraction, which down-regulates the expression of herpes simplex virus antigen in Vero cells (Chiu *et al*, 2004). An extract of *Prunella vulgaris* also has been shown to inhibit replication at reverse transcription *in vitro* (Kageyama, *et al*, 2000; Yamasaki, *et al*, 1993; Yao, *et al*, 1992).

**Table 2.2:** Chemical components in the six herbs of Acapha

| Herb | Active components | Reference |
|---|---|---|
| *Sophora tonkinensis* | Quinolizidine alkaloids: cytisine, sophocarpine, matrine, lehmannine, sophoranol, oxymatrine, oxysophocarpine | Ding, et al., 2005<br>Ding, et al., 2006<br>Song, et al., 1999 |
| *Polygonum bistorta* | Flavanoid aglycones: taxifolin, quercetin, quercetin-3-methylether, kaempferol, myritcetin, luteolin, isorhamnetin, rhamnetin | Smolarz, 2002 |
| *Prunella vulgaris* | Polysaccharide: prunelline<br>Triterpenes: betulinic acid, ursolic acid, 2-alpha, 3-alpha-dihydroxyurs-12-ene-28-oic acid, 2-alpha-hydroxyursolic acid, oleanolic acid | Tabba, et al., 1989<br>Ryuet, et al., 2000<br>Yan, et al., 1999 |
| | Triperpenoid saponins | Wang, 2000 |
| | Phenolic acids: rosmarinic acid, caffeic acid | Skottova, et al., 2004<br>Won, et al., 2003<br>Markova,et al., 1997 |
| *Sonchus brachyotus* | Phenolic compounds: gallic acid, protocatechuic acid, chologenic acid, caffeic acid, m-hydroxybenzolic acid, p-coumaric acid, cinnamic acid<br>Diosgenin, sinigrin, oleanolic acid, β-sitosterol, villoside, campesterol | Kim, et al., 2005 |
| *Dictamnus dasycarpus* | 6β-hydroxyfraxinellone, fraxinellone, isofraxinellone, calodendrolide, dictamine, haplopine | Zhao, et al, 1998<br>Yu,et al., 1992 |
| | Rutavin | Wang, et al., 1992 |
| | Skimmianine, gamma-fagarine, beta-sitosterol, obacunone, limonin disophenol, fraxinellonone, wogonin, kihadinin B, dasycarine | Du, et al., 2005 |
| | Terpene glycosides, phenolic glycosides, Sequesterpene glycodisides | Chang, et al., 2002<br>Chang, et al., 2001 |
| *Dioscorea bulbifera* | Sitosterol, tetracosanoic acid, 1-(tetracosanoyl-glycerol, trans-tetracosanylferulate, bafoudiosbulbins A and B | Teponno, et al., 2006<br>Gao, et al., 2002 |
| | Kaempferol-3,5-dimethyl ether, caryatin, catechin, amricetin, quercetin-3-O-galactopyranoside, mericetin-3-O-glucopyranoside, diosbulbin 3,7-dimethoxy-5,4'-dihydroxyfalvone, 3,7-dimethoxy-5,3'4'-trihydroxyflavone, emodin | Li, et al., 2000 |

12

(3) *Dictamnus dasycarpus*. This herb has been shown to possess cytotoxic activity to human lung adenocarcinoma (A-549) cells (Chang, *et al*, 2002). The phenolic glycosides of *Dictamnus dasycarpus* have been found to inhibit T-cells proliferation *in vitro* (Chang, *et al*, 2002). The alkaloid and limonoid derivatives of *Dictamnus dasycarpus* have been shown to possess antifungal effects in plant (Zhao, *et al*, 1998).

(4) *Dioscorea bulbifera*. The roots of *Dioscorea bulbifera* have been used in Chinese medicine as a remedy for sore throat and for struma. Recently, Gao *et al* (2002) have shown that the ethyl acetate fraction of *Dioscorea bulbifera* inhibits the tumor promotion of JB6 cells induced by a promoter–TPA. The research of Komori (1997) also has shown that diosbubin glycoside can significantly inhibit the growth of solid sarcoma 180 tumor.

(5) *Polygonum bistorta* (Quanshen) and (6) *Sonchus brachyotus*. These herbs are not commonly used. Only scanty information is available on the chemical components and the pharmacological effects of these herbs.

As discussed before, many natural chemicals in Acapha® may contribute to the chemoprevention effects of the herbal product. These natural chemicals usually are formed by modifying the same biosynthetic pathways that produce carbohydrates, fats and proteins for the plant. Therefore, the content and concentration of natural chemicals may vary greatly in a specific herb because of the difference in genetic and/or environmental factors that affect their biosynthesis. The manufacturing process is another factor which may affect the levels of natural products in the herbs. The goals of this Chapter were to identify a few of the major natural chemicals in Acapha® using both high performance liquid chromatography (HPLC) and gas chromatography-mass spectrometry

(GC/MS) and to select a marker chemical(s) which might be useful for studying the PK of Acapha® in laboratory animals and humans.

## 2.2    Materials and methods

### 2.2.1    Preparation of Acapha® extract and matrine standard solution

Acapha® powders (100 mg) were weighed and dissolved in 1 ml of 70% ethanol. The final solution was ultrasonicated for 1 hr and centrifuged at 2000 rpm for 5 min. The supernatant was removed, filtered with a 0.45 µm filter unit (Millipore, Carrigtwohill, Co. Cork, Ireland). An aliquot of the filtrate (1 µl) was injected into a GC/MS or HPLC.

### 2.2.2    Determination of Acapha® chemical profile

The chemical profiles of the ethanolic extract of Acapha® were obtained using HPLC and GC/MS under the following chromatographic conditions:

(a) GC/MS. A Hewlett-Packard 5890 series II gas chromatograph coupled to a 5971 mass spectrometric detector was used in the study. Chromatographic separation was performed using a 5% diphenyl-95% dimethylpolysiloxane capillary column (30 m X 0.25 mm X 0.25 µm, HP-5 MS). Helium was used as the carrier gas under a head pressure of 50 psi. The injector and transfer line temperatures were set at 260 °C and 280 °C, respectively. The initial oven temperature was set at 80 °C, maintained for 3 min and then increased to 310 °C at a rate of 8 °C /min and maintained for 6 min. Ionization was performed under electron impact ionization with 70 eV. The GC/MS was scanned from a mass range of 50-500 m/z. Preliminary identities of the mass spectral peaks were examined by comparing their mass spectra with those stored in the Wiley library of the

instrument.

(b) HPLC. A Hewlett-Packard 1090 Liquid Chromatograph was also used to obtain the chemical profile of Acapha® extract. The HPLC was equipped with a Phenomenex LUNR phenyl-hexyl column (4.6 mm x 250 mm, 5μm) and a DAD UV detector. The column was eluted with a mobile phase consisting of solution A (methanol:acetonitrile, 58:42) and solution B (0.3% phosphoric acid aqueous solution pH2) in the following gradient composition: 10% A and 90% B for the first 8 min, increased to 40% A from 8 min to 18 min, 100% A from 18 min to 23 min and maintained until 25 min. The flow rate of the mobile phase was 1.0 ml/min and the injection volume was 20 μl. The HPLC eluent was monitored simultaneously at 215 nm, 260 nm and 330 nm wavelengths.

## 2.3    Results

### 2.3.1   GC/MS profile of Acapha®

Figure 2.1 shows a typical GC/MS chromatogram of the Acapha® extract. The chemical profile was characterized by numerous small chromatographic peaks which could be identified initially by comparing the $R_t$ and the mass spectrum of the chromatographic peak with those stored in the Wiley library of the GC/MS instrument. As shown in Fig 2.1, the putative matrine chromatographic peak (see arrow) is the largest peak in the GC/MS chromatogram and has a $R_t$ of 24.12 min. Figure 2.2 shows the mass spectrum of the putative matrine peak which is identical to that of the standard pure matrine (data not shown). Besides matrine, several natural chemicals including 4-methylene-1-(1methylethyl)-cyclohexene, dictamine, hexadecanoic acid, sophocarpine,

and campesterol also have been identified in the extract based on their $R_t$ and mass spectra. Indeed, major natural chemicals that are documented in the individual herb (Table 2.2) also have been identified in Acapha®. For example, dictamine, sophocarpine, campesterol are found, respectively in *Dictamnus dasycarpus*, *Sophora tonkinensis*, and *Sonchus brachyotus*. Also, hexadecanoic acid has been shown as a component of the volatile oil in *Sonchus brachyotus* (Bi *et al*, 2006; Jing and Meng, 2004). No attempt has been made to obtain the pure standards of these chemicals because none of them will be used as a marker chemical for Acapha®. Nevertheless, results of the present studies suggest that a variety of chemicals are found in the extract of Acapha® and most of these compounds appear to remain intact after going through the extraction and manufacturing processes.

**Figure 2.1:** GC/MS profile of Acapha extract. The arrow points to a putative matrine peak



TIC M032905B.D
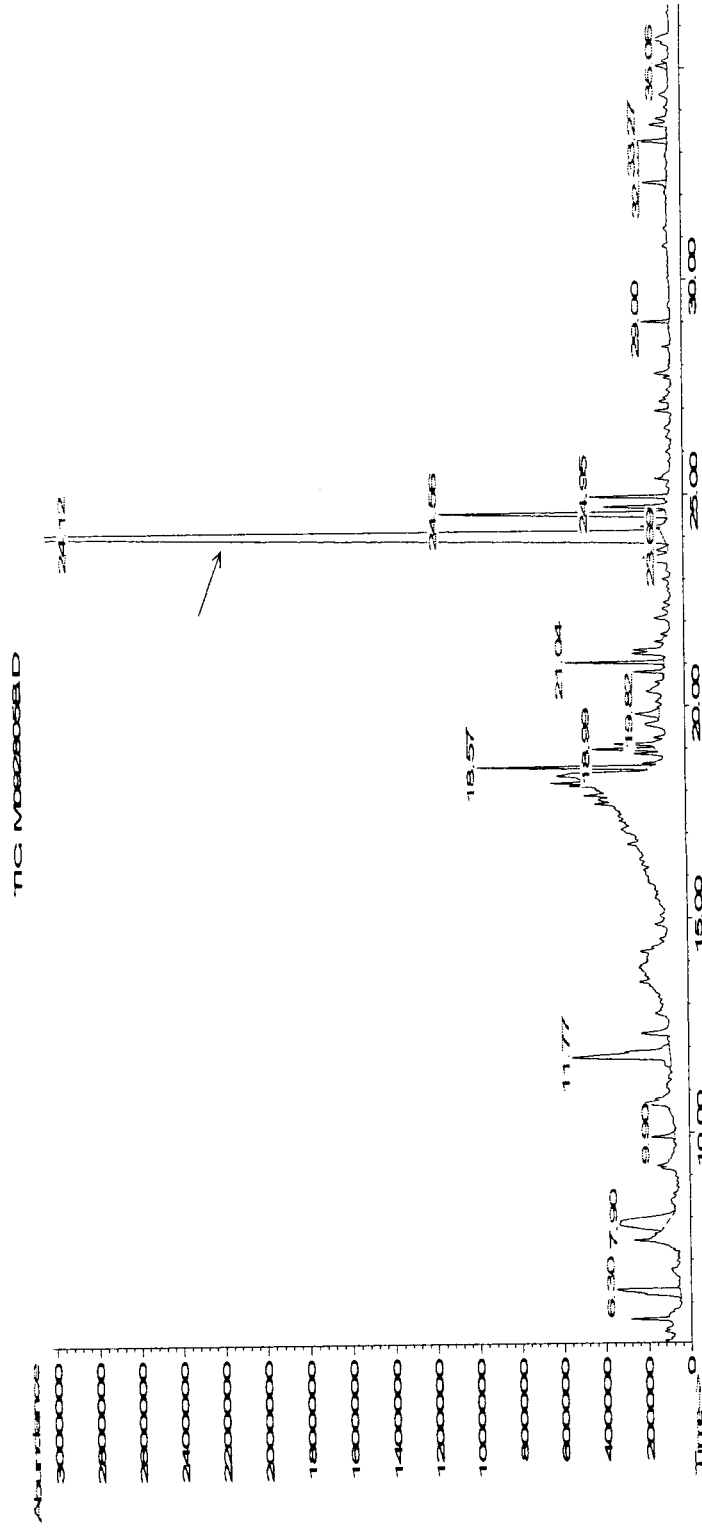
**Figure 2.2:** Mass spectrum of putative matrine peak in Acapha® extract. Molecular weight of matrine is 248.
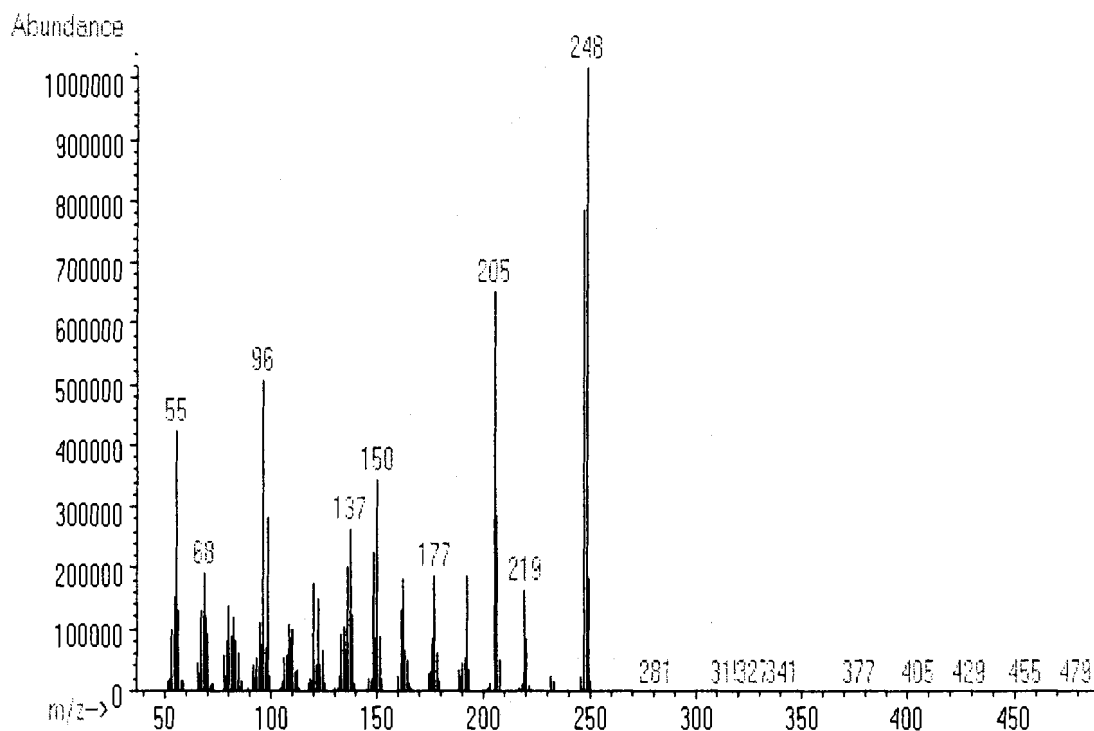


## 2.3.2 HPLC profiles of Acapha®

Fig.2.3 shows a typical HPLC chromatographic profile of the Acapha® extract which is monitored at 215 nm. A chromatographic peak with a $R_t$ of 7.8 min was found to co-elute with the matrine analytical standard (data not shown). Since the HPLC baseline began to drift at about 15 min after the start of the run and in many cases, the chromatographic peaks with $R_t > 20$ min became inseparable from one another, I also analysed the samples at 330 nm. Figure 2.4 shows a typical HPLC profile of the Acapha® extract monitored at 330 nm; it does not show any chromatographic peaks during the first 15 min of the run but a number of well separated peaks are observed at $R_t > 15$ min. It should be noted that the entire HPLC profile of the Acapha® extract can be obtained by monitoring the eluent at 215 nm between 0-15 min and at 330 nm between 15-30 min.

18

**Figure 2.3:** HPLC profile of Acapha® extract monitored at 215 nm. Matrine concentration was estimated to be 40 µg/ml in the Acapha® extract.
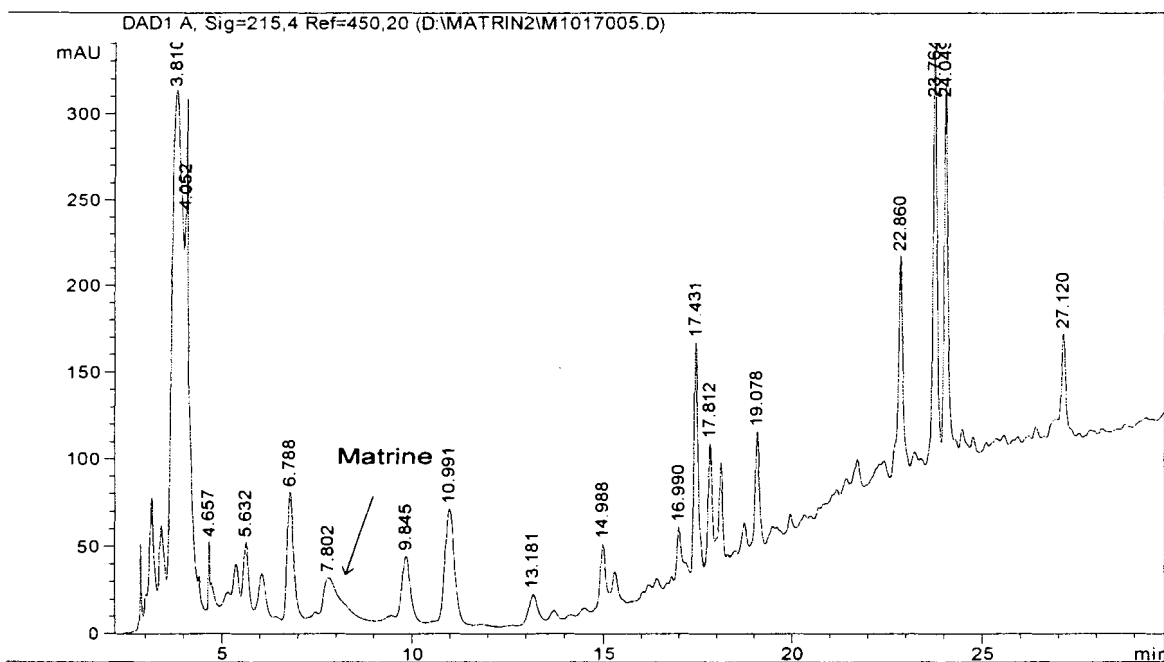


**Figure 2.4:** HPLC profile of Acapha® extract monitored at 330 nm. Matrine concentration was estimated to be 40 µg/ml in the Acapha® extract.
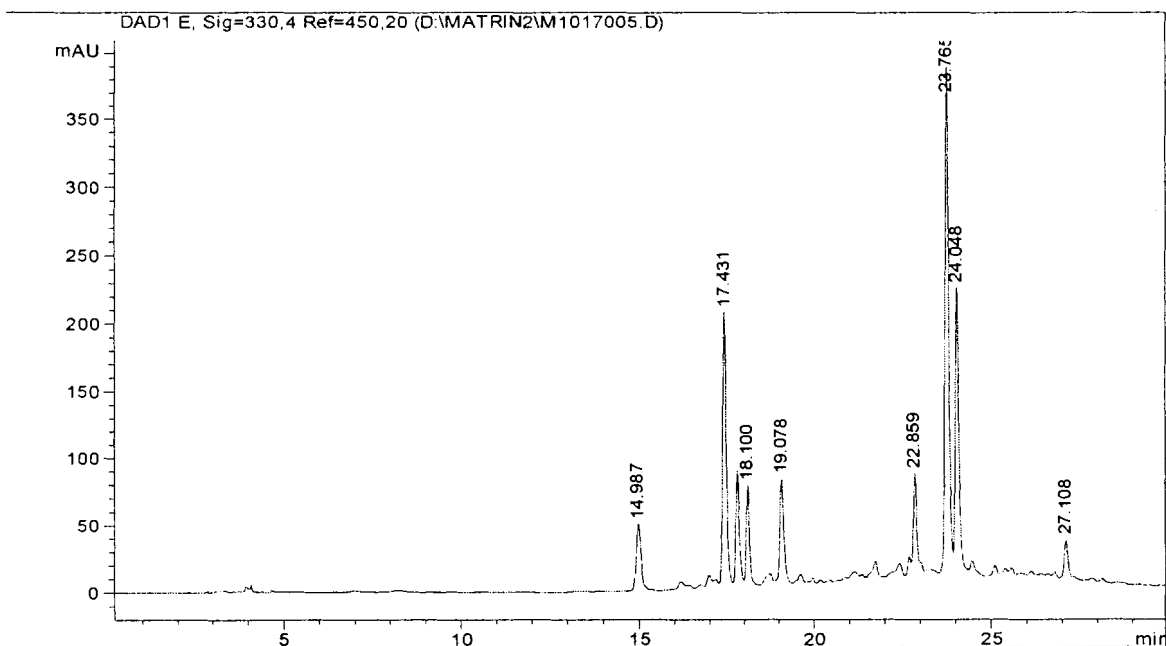
Acapha® extract should be monitored with two different UV wavelengths because

matrine absorbs maximally at 202 nm but does not show any absorption at 250 nm or

higher (Figure 2.5). In contrast, other unknown chemical components of Acapha® appear

to absorb maximally at >250 nm wavelength.

**Figure 2.5:    UV absorption spectrum of matrine**



DAD1, 7.157 (462 mAU, - ) of M1005005.D

matrine UV spectra
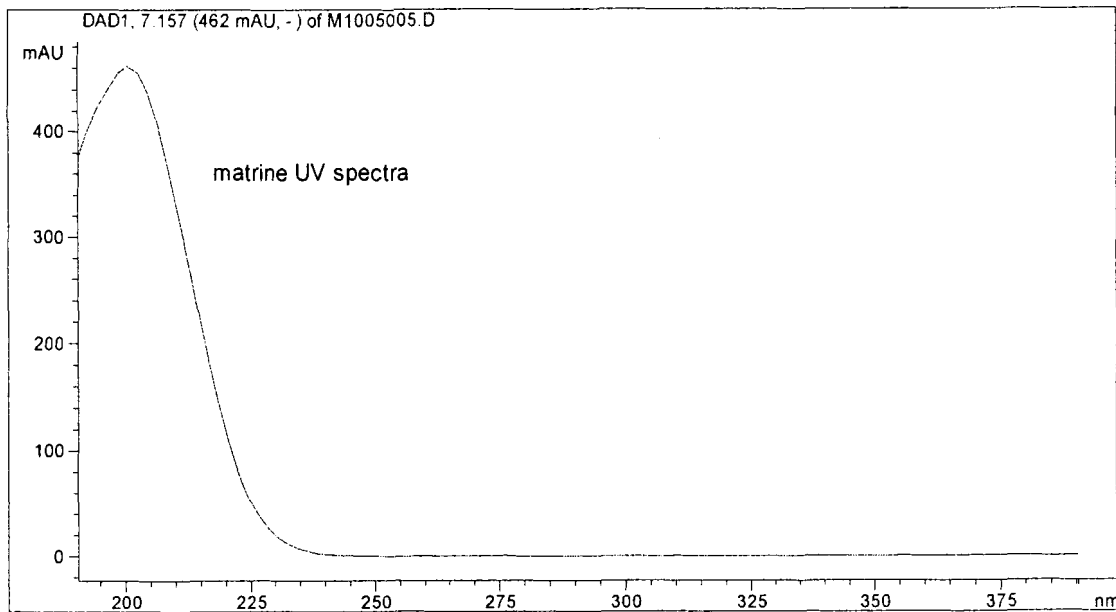
## 2.4    Discussion

Although matrine is not the largest peak in the HPLC profile, it is a major

chemical component in the GC/MS profile of Acapha® extract. A relatively high level of

matrine in Acapha® extract is consistent with the herbal composition of Acapha® which

includes *Sophora tonkinesis* (Table 2.2) because matrine has been shown to be a major

alkaloid in *Sophora tonkinesis* (Ding *et al.*, 2006).

### 2.4.1 Plant chemicals and chemoprevention

Carcinogenesis often is related to the overproduction of oxygen-centered free radicals and other oxygen species which may come from either the intrinsic physiological and biochemical processes in the human body or the foreign environment (Cai, *et al*, 2004; Halliwell, 1994; Niki, 1997). On the other hand, fruits, vegetable and herbs are the major sources of effective chemopreventive agents because they contain natural chemicals which possess antioxidative, antimutagenic and anticarcinogenic activities (Cai, *et al*, 2004). Because many chemicals in the growing plant can be modified during harvesting, storage, processing, and cooking, it is important to confirm the presence of some of these naturally occurring chemicals in Acapha® before embarking on a PK study.

### 2.4.2 Approaches to study chemical mixtures

The PK of a prescription drug usually is conducted using a pure active chemical. As such, there is no formal method available to study the PK of a multi-component, therapeutic agent consisting of a complex chemical mixture. Although a few PK studies have been reported for a chemical mixture but these studies are related mainly to environmental chemicals (Haddad et al. 1999). There are at least two different approaches used to study the PK of a chemical mixture in the environment: (a) the whole-mixture approach. It considers the chemical mixture as a single entity. A major problem of this approach is the lack of knowledge of the mixture components. Therefore, PK studies have been conducted without any knowledge on the concentration ratios of the components, the mechanism of action of the components, the existence of any synergistic or antagonistic interactions, or whether the pharmacological effects of the mixture is dominated by one or a limited number of chemicals. The inherent difficulty involving in

generating the required dose-response data for a chemical mixture also limits the utility of this method. An additional difficulty in applying the whole-mixture approach to study the PK of an herbal product is that the chemical components in the mixture could vary with the time of harvesting and the geographic location from which the herbs are collected. Therefore, PK results derived from the whole-mixture approach would only be applicable to situation where the major chemical components of the herbal extracts are fairly consistent. Because of all these difficulties, very few PK studies of herbal products have been conducted with this approach. (b) The component-based approaches. Most of the PK studies of environmental chemicals and herbal products are conducted using these approaches which rely on the pharmacological information available for the mixture constituents and assume that the shape of the dose-response curve for each component is not altered by the other components in the mixture. There are four commonly used component-based approaches, namely the marker chemical approach, dose addition approach, response addition approach and toxic equivalence factor approach (TEF): (i) The indicator chemical approach is the most common approach to study the PK of an herbal product; it assumes that a single component in a mixture accounts for most of the pharmacological activity of an herbal product quantitatively and qualitatively. This approach suffers from the obvious uncertainty that the other mixture components may also induce pharmacological effects either on an individual basis or following an interaction with the marker chemical. Therefore, care must be exercised when studying the actions of plant components in isolation because it can lead to incorrect assumptions about their modes of action and ultimate effects, (ii) The response- or effects-addition approach involes the summation of pharmacological activities attributed to each of the

mixture constituents. These approaches cannot be used if the dose-response relationship has not been established for the individual chemicals that constitute the mixture. (iii) The TEF approach (Safe, 1990) may be applied when the components of a mixture are congeners or isomers of a chemical. The TEF is the ratio of the potency of a given isomer to the "signature or reference" isomer in a particular assay. The TEF approach could be applicable to an herbal product when there is appropriate dose-response and mechanistic data.

### 2.4.3 Matrine as a chemical marker for Acapha®

Direct measurement of the chemical mixture in Acapha® is a complex and difficult task. In the absence of any practicable measures of the chemical mixture, the indicator chemical approach is the easiest and most widely used method to study the PK of an herbal mixture. The indicator chemical approach requires the identification of a chemical or class of compounds for monitoring that would be indicative of the presence and amount of an herb in a PK study. Such a chemical or class of compounds is called a chemical marker or proxy compound and matrine has been chosen as the chemical marker for the Acapha® PK studies. Figure 2.6 shows the chemical structure of matrine.

There are good reasons to choose matrine as the marker chemical of Acapha®: (a) matrine is an alkaloid, which is present at a relatively high level in the storage tissue (roots, fruits, and seeds) than in the green leaves of plants. Although the concentrations of alkaloids in plants are low, they usually possess high pharmacological activities (Harborne, 1999), (b) matrine is a unique alkaloid and a major constituent of *Sophora japonica* (*kushen*) and *Sophora subprostrta* (*shandougen*) roots; matrine constitutes about 2% of the dried root stock of *kushen* and 1% in *shandougen* and matrine has been

identified as a major chemical in the extract of Acapha®, (c) crude matrine in Acapha®
appears to be the only alkaloid which easily crosses the Caco-2 cell monolayer (see
Chapter 3), (d) a matrine analytical standard is available commercially and a sensitive
and specific GC/MS-SIM method has been developed, which permit accurate
measurement of matrine in biological fluids and tissues (Sit et al., 2004), and (e) matrine
has been used as an adjuvant to standard medical therapy of lung cancer (Chang, et al,
1992). It also has been shown to possess anti-neoplastic effects by helping leukemia cells
differentiate into mature and normal white blood cells (Zhu, 2001). Matrine also is
effective against Yoshida sarcoma and sarcoma 180 in the rat (Wang, 1983). In the
treatment of cancer, Sophora roots and matrine probably act by stimulating the immune
system rather than inhibiting the cancer cells directly (Xu and Jiang, 1998; Chang, et al,
1992).

Figure 2.6:   Chemical structure of matrine



24
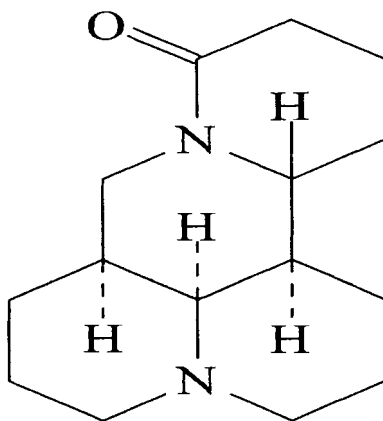
## 2.5 References

Bi, Y, Yang, G, Li, H, Zhang, G and Guo, Z. (2006) Characterization of the chemical composition of *lotus plumule* oil. Journal of Agricultural and Food Chemistry. 54(20):7672-7677.

Cai, Y., Luo, Q., Sun, M. and Corke, H. (2004) Antioxidant activity and phenolic compounds of 112 traditional Chinese medicinal plants associated with anticancer. Life Sciences. 74 (17):2157-2184.

Chang, M. Y. (1992) Anticancer Medicinal Herbs. Human Science and Technology Publishing House, Changsha, China.

Chang, J., Xuan, L.J., Xu, Y.M. and Zhang, J.S. (2001) Seven new sesquiterpene glycosides from the root bark of *Dictamnus dasycarpus*. Journal of Natural Products: 64(7):935-938.

Chang, J., Xuan, L.J., Xu, Y.M. and Zhang, J.S. (2002) Cytotoxic terpenoid and immunosuppressive phenolic glycosides from the root bark of *Dictamnus dasycarpus*. Planta Medica. 68(5): 425-429.

Chiu, L.C., Zhu, W. and Ooi, V. E. (2004) A polysaccharide fraction from medicinal herb *Prunella vulgaris* downregulates the expression of herpes simplex virus antigen in Vero cells. Journal of Ethnopharmacology. 93:63-68.

Ding, L.S. and Meng, Z.M. (2004) Phytochemistry. Eastern-Southern University Press, Nanjing, China.

Ding, P.L., Yu, Y.Q. and Chen, D.F. (2005) Determination of quinolizidine alkaloids in *Sophora tonkinesis* by HPCE. Phytochemical Analysis: PCA. 16(4):257-263.

Ding, P.L., Huang, H., Zhou, P. and Chen, D.F. (2006) Quinolizidine alkaloids with anti-HBV activity from *Sophora tonkinensis*. Planta Medica. 72(9): 854-856.

Du, C.F., Yang, X.X. and Tu, P.F. (2005) Studies on chemical constituents in bark of *Dictamnus dasycarpus*. Zhongguo Zhong Yao Za Zhi. 30(21):1663-1666.

Fan, Q. L. (2002) Science of Prescription. Shanghai TCM University Press, Shanghai. China.

Gao, H., Kuroyanagi, M., Wu., L., Kavahara, N., Yasuno, T. and Nakamura, Y. (2002) Antitumor-promoting constuents from *Dioscorea Bulbifera L.* in JB6 mouse epidermal cells. Biological & Pharmaceutical Bulletin. 25(9):1241-1243.

Haddad, S., Tardif, R., Charest, G. and Krishnan, K. (1999) Physiological modelling of the toxicokinetic interactions in a quaternary mixture of aromatic hudrocarbons. Toxicol. Appl. Pharmacol. 161: 249-257.

Halliwell, B. (1994) Free radicals, antioxidant, and human disease: curiocity, cause, or consequence? Lancet. 344(8924): 721-724.

Jia, W., Gao, W.Y., Yan, Y.Q., Wang, J., Xu, Z.H., Zheng, W.J. and Xiao, P.G. (2004) The rediscovery of ancient Chinese herbal formulas. Phytotherapy Research. 18 (8):681-686.

Kageyama, S., Kurokava, M. and Shiraki, K. (2000) Extract of Prunella vulgaris spikes inhibits HIV replication at reverse transcription *in vitro* and can be absorbed from intestine *in vivo*. Antiviral Chemistry & Chemotherapy. 11(2):157-164.

Kim, Y.O., Johnson, J.D. and Lee, E.J. (2005) Phytotoxic effects and chemical analysis of leaf extracts from three *Phytolaccaceae* species in South Korea. Journal of Chemical Ecology. 31(5):1175-86.

Komori, T. (1997) Glycosides from *Dioscorea bulbifera*. Toxicon. 35(10):1531-1536.

Li, S.S., Iliya, I.A., Deng, J.Z. and Zhao, S.X. (2000) Flavonoids and anthraquinone from *Dioscorea bulbifera L.* Zhongguo Zhong Yao Za Zhi. 25(3):159-160.

Markova, H., Sousek, J., and Ulrichova, J. (1997) *Prunella vulgaris L.-* a rediscovered medicinal plant. Ceská A Slovenská Farmacie (Ceska. Slov. Farm). 46(2):58-63.

Mori, H., Xu, Q., Sakamoto, O., Uesugi, Y., Koda, A. and Nishioka, I. (1989) Mechanisms of antitumor activity of aqueous extracts from Chinese herbs: their immunopharmacological properties. Japanese Journal of Pharmacology. 49(3):423-31.

Niki, E. (1997) Free radicals, antioxidants and cancer. In Ohigashi, H., Osawa, T., Terao, J., Wantanabe, S., Yoshikawa, T. (Eds.) Food Factors for Cancer Prevention. Springer, Tokyo, pp.55-57.

Psotova, J., Kolar. M., Sousek, J., Svagera, Z., Vicar, J. and Ulrichova, J. (2003) Biological activities of *Prunella vulgaris* extract. Phytotherapy Research. 17(9):1082-1087.

Ryu, S.Y, Oak, M. H., Yoon, S.K., Cho, D.I., Yoo, G.S., Kim, T.S. and Kim, K.M. (2000) Anti-allergic and anti-inflammatory triterpenes from the herb of *Prunella vulgaris*. Planta Medica. 66(4):358-360.

Safe, S. (1990) Polychlorinated biphenyls (PCBs), dibenzo-p-dioxins (PCDDs), dibenzofurans (PCDFs), and related compounds: environmental and mechanistic considerations which support the development of toxic equivalency factors (TEFs). Critical Reviews in Toxicology. 21 (1):51-88.

Skottova, N., Kazdova, L., Oliyarnyk, O., Vecera, R., Sobolova, L. and Ulrichova, J. (2004) Phenolics-rich extracts from *Silybum marianum* and *Prunella vulgaris* reduce a high-sucrose diet induced oxidative stress in hereditary hypertriglyceridemic rats. Pharmacological Research. 50:123-130.

Smolarz, H.D. (2002) Comparative study on the free flavonoid aglycones in herbs of different species of *Polygonum L.* Acta Poloniae Pharmaceutica. 59(2):145-148.

26

Song, J.Z., Xu, H.X., Tian, S.J. and But, P.P. (1999) Determination of quinolizidine alkaloids in traditional Chinese herbal drugs by nonaqueous capillary electrophoresis. Journal of Chromatography A. 857(1-2):303-311.

Tabba, H.D., Chang, R.S. and Smith, K.M. (1989) Isolation, purification, and partial characterization of prunellin, an anti-HIV component from aqueous extracts of *Prunella vulgaris*. Antiviral Research. 11(5-6):263-273.

Teppono, R.B., Tapondjou, A.L., Gatsing, D., Djoukeng, J.D., Abou-Mansour, E., Tabacchi, R., Tane, P., Stoekli-Evans, H. and Lontsi, D. (2006) Bafoudiosbulbins A, and B, two anti-salmonellal clerodane diterpenoids from *Dioscorea bulbifera* L. var sativa. Phytochemistry. 27 (Epub ahead of print).

Tyler, V.E., Brady, L.R., Robbers, J.E. (1976) Pharmacognosy. Lea & Febiger, Philadelphia.

Wang, Y.S. (1983) Pharmacology and Application of Chinese Materia Medica. People's Health Publisher, Beijing, pp.98-106.

Wang, Z., Xu, F. and An, S. (1992) Chemical constituents from the root bark of *Dictamnus Dasycarpus Turcz*. Zhongguo Zhong Yao Za Zhi. 17(9):551-552, 576.

Wang, Z.J., Zhao, Y.Y., Chen, Y.Y. and Ma, B.N. (2000) Triterpenoid compounds of *Prunella* genus and their features of 13C NMR spectroscopy. Zhongguo Zhong Yao Za Zhi. 25(10):583-588.

Won, J., Hur, Y.G., Hur, E.M., Park, S.H., Kang, M.A., Choi, Y., Park, C., Lee, K.H. and Yun, Y. (2003) Romarinic acid inhibits TCR-induced T cell activation and proliferation in an Lck-dependent manner. European Journal of Immunology. 33(4):870-879.

Xu, X, R. and J, J. K. (1998) Recent progress in anticancer bioactivity study of *Sophora flavescens* and its alkaloids. Chinese Journal of Integrative Traditional Chinese and Western Medicine. 4(3):235-239.

Yan, H., Zhao, L., Zhu, D. and Ding, L. (1999) Determination of oleanolic acid and ursolic acid in spica Prunellae by derivative GC method. Zhongguo Zhong Yao Za Zhi. 24(12):744-745, 764.

Yamasaki, K., Otake, T., Mori, H., Morimoto, M., Ueba, N., Kurokava, Y., Shiota, K. and Yuge, T. (1993) Screening test of crude drug extract on anti-HIV activity. Yakugaku Zasshi. 113(11):818-824.

Yao, X.J., Wainberg. M.A. and Parniak, M.A. (1992) Mechanism of inhibition of HIV-1 infection in vitro by purified extract of *Prunella vulgaris*. Virology. 187(1):56-62.

Yu, S.M., Ko, F.N., Su, M.J., Wu, T.S., Wang, M.L., Huang, T.F. and Teng, C.M. (1992) Vasorelaxing effect in rat thoracic aorta caused by fraxinellone and dictamine isolated from the Chinese herb *Dictamnus dasycarpus* Turcz: comparison with cromakalim and $Ca^{2+}$ channel blockers. Naunyn-Schmiedeberg's Archives of Pharmacology. 345(3):349-355.

Zhang, J.L. (2000) Study on Apoptosis induced by oxymatrine in cultured keratinocytes. Chinese Journal of Dermatology and Venereology. 14(6):367-368.

Zhao, W., Wolfender, J.L., Hostettmann, K., Xu, R. and Qin, G. (1998) Antifungal alkaloids and limonoid derivatives from *Dictamnus Dasycarpus*. Phytochemistry. 47(1):7-11.

Zheng, M.S. and Zhang, Y.Z. (1990) Anti-HBsAg herbs employing ELISA technique. Zhong Xi Yi Jie He Za Zhi. 10(9):560-562, 518.

Zhu N.X. (2001) Study on inducing and differentiating function and mechanism of matrine on leukemia cells. ACTA Traditional Chinese Medicine and Pharmacology (Shanghai). 15 (1):43-44.

# CHAPTER 3:
# *IN VITRO* TRANSPORT OF MATRINE AND CRUDE MATRINE BY CACO-2 CELLS

## 3.1 Introduction

As the oral route is by far the most convenient method of herbal product administration to humans, it is important to have an estimate of the rate and/or extent of intestinal absorption at an early stage of product development. An early intestinal absorption study may help reducing development time and costs of a product because if an herbal product were not absorbed by the gastrointestinal tract there would be no point in developing the product further.

Intestinal epithelial cell lines such as the Caco-2 cells are routinely cultivated as confluent monolayers on permeable filters to study the transepithelial transport of a therapeutic agent. Although Caco-2 cells are derived from colon cancer cells, they acquire many features of absorptive intestinal cells during culture and thus are capable of predicting drug absorption in humans (Artursson, *et al.*, 2001; Delie and Rubas, 1997). Therefore, the goal of an *in vitro* Caco-2 cell monolayer study can be to investigate whether a drug is actively or passively transported across the intestinal epithelium, and if the transport is active, to identify the relevant carrier. Previous studies on active drug transport in Caco-2 cell monolayers have investigated two transport systems: the dipeptide carrier and P-glycoprotein. These studies have shown that cell monolayers can be used to identify drugs with potential absorption problems and possibly to predict drug absorption *in vivo*. Since drug transport studies in cell monolayers are easy to perform

and require only a small quantity of a drug, they can be used to screen for drug absorption at an early stage of drug development (Artursson, *et al.*, 2001; Stoner, *et al.*, 2004).

The Caco-2 cell monolayer has many advantages over other drug absorption models such as the human *in vivo* study and intestine segment perfusion. These advantages include: a) a rapid evaluation of the permeability of a drug; b) an opportunity to study the mechanisms of drug transport under controlled conditions; c) a rapid evaluation of methods of improving drug absorption (by absorption enhancer or other pharmaceutical additives); d) an opportunity to perform studies on human cell line; e) an opportunity to minimize time-consuming, expensive, and sometimes controversial animal studies (Meunier *et al.*, 1995). The disadvantages of the Caco-2 cell preparation include low expression of metabolic enzymes and transporter, tight cells junctions, thick and unstirred water layer, and the production of homogeneous cells that cannot be used to study regional differences of intestinal drug absorption. An additional source of variability is the cell line itself; the properties of Caco-2 cell monolayer vary greatly among laboratories because of using different passage number, culture duration, extracellular (filter) support and culture medium. Therefore, caution must be exercised when comparing the permeability results of Caco-2 cells from different laboratories (Artursson *et al.*, 2001).

*In vivo* drug absorption is governed by various physiological and biochemical processes of the gastrointestinal tract *e.g.* pH, gastric emptying, intestinal transit time, active transport and microbial biotransformation. It is also controlled by the therapeutic agent's specific properties *i.e.*, lipophilicity, pKa, solubility, particle size, permeability, metabolic stability, formulation release kinetics, and dissolution kinetics. Among these,

the aqueous solubility and permeability of the chemical usually determine the rate of drug absorption (Artursson, *et al.*, 2001; Stoner *et al.*, 2004, Bergstrom, 2005). Therefore, it is important to select a cell line with the appropriate properties to mimic the biological barrier of the intestine. It should be noted that the transport and metabolic properties of cultured cells also may vary depending on the following factors: (a) the cell seeding density, (b) whether the cells have reached confluency, (c) the stage of differentiation, and (d) the presence or absence of essential nutrients and/or growth factors. During transport experiments, these properties may change depending on the composition of the transport media (*e.g.*, concentration of the solute, temperature, pH, presence or absence of a metabolic source of energy or ions, presence or absence of proteins that might bind the solute, presence or absence of competing solutes), and whether the solute is added to the apical or basolateral side of the monolayer. All of these factors need to be carefully optimized and regulated in order to best mimic the biological barrier *in vivo* (Artursson *et al.*, 2001, Meunier *et al.*, 1995).

For rapidly and completely absorbed compounds, the permeabilities between the Caco-2 cell monolayer and human jejunum *in situ*, the most common drug permeation route in the intestine, differ only by 2 to 4 fold. However, for slowly and incompletely absorbed drugs, tested drugs can be transported at a 30-80-fold slower rate in the Caco-2 cell monolayers than in the human jejunum. For drugs transported by active transporters such as L-dopa, permeability can be >100 fold lower in Caco-2 cell monolayer than that *in vivo*. The differences in transport rates may be related to the fact that Caco-2 cell line and intestine tissue are basically very different: Caco-2 cells have a lower permeability for paracellular transport than the intestinal tissue because the tight junction between the

31

cells in a Caco-2 cell preparation. In addition, Caco-2 cells also express lower level of active transporters (Artursson *et al*, 2001).

The transport of drugs across the intestinal epithelium occurs by one or more of the following mechanisms: passive transcellular and paracellular mechanisms, carrier mediated (passive or active) mechanisms and transcytosis mechanisms. Drugs are transported by different mechanisms depending on their intrinsic properties such as lipophilicity and hydrophilicity. The following are examples of a drug's intrinsic properties and its associated absorption mechanisms: (1) rapidly and completely absorbed drugs are generally lipophilic and distribute readily into the cell membranes of the intestinal epithelium by the passive transcellular route, (2) drugs that are slowly and incompletely absorbed are passively absorbed and distribute poorly into cell membrane; they are usually hydrophilic drugs and peptides because these drugs are transported through the water-filled pores of paracellular pathway across the intestinal epithelium, (3) if the structure of the hydrophilic drugs is similar as some nutrients, beside passive transport, active, carrier-mediated transport can also be involved in the transport process, and (4) transcytosis route happens only when the the size of the drugs is large (*e.g.* peptide antigens). The transport of vitamin $B_{12}$ is perhaps the best example of naturally occurring receptor–mediated endocytosis/transcytosis across enterocytes in the mucosal to serosal direction (Artursson, *et al*, 2001).

Because drug absorption is dependent on the clinical dose and the solubility and permeability of the drug, the US FDA (2000) has proposed a Biopharmaceutical Classification System (BCS) in predicting oral drug absorption. Drug substances are grouped into the following 4 classess: Class I: high permeability and high solubility drugs

(A drug substance is considered highly soluble when the highest dose strength is soluble in $\leq$ 250 ml water over a pH range of 1 to 7.5, a drug substance is considered highly permeable when the extent of absorption in humans is determined to be $\geq$ 90% of an administered dose, based on mass-balance or in comparison to an intravenous reference dose). Those compounds are well absorbed and their absorption rate is usually higher than excretion; Class II: high permeability and low solubility drugs, the bioavailability of those products is limited by their solvation rate; Class III: low permeability and high solubility drugs, the absorption is limited by the permeation rate but the drug is solvated very fast; Class IV: low permeability and low solubility drugs. Those compounds have a poor bioavailability. Usually they are not well absorbed across the intestinal mucosa and a high variability is expected. The BCS information may help screening of new drugs at an early stage of their development. For example, a biowaiver can be requested for solid, orally administered immediate-release products (>85% release in 30 min), containing drugs with a high solubility over the pH range from 1-7.5 and a high permeability (Lindenberg, *et al.*, 2004; FDA, 2000).

Previous Caco- 2 cells monolayer studies have focused on the effects of herbal products on the transport of conventional drugs (Nishimura, 2005; Spahn-Langguth and Langguth, 2001). In the present study, the rates and extents of absorption were compared between pure matrine and crude matrine (in Acapha®) to provide some information about their intestinal absorption. Results of these studies also may help developing a PBPK model of matrine for humans (see Chapter 6).

33

## 3.2    Materials and methods

### 3.2.1    Reagents and supplies

Caco-2 cells were obtained from the American Type Culture Collection (Rockville, MD). Dulbecco's modified Eagle medium (DMEM), fetal bovine serum (qualified), MEM non-essential amino acids, Dulbecco's phosphate-buffered saline (PBS), trypsin-EDTA (0.25% trypsin, 1 mM EDTA-4 Na), Hanks Balanced Salt solution (HBSS) and penicillin and streptomycin solution (10,000 units for penicillin and 10 mg streptomycin per ml) were all purchased from Gibco-Life Technologies (Gaithersburg, MD , USA). N-2-hydroxy-ethylpiperazine-N'-2 ethansulfonic acid (HEPES) was perchased from Sigma Chemical Co. (St Louis, MO). Cell culture dishes (100 x 20 mm) were obtained from Sarstedt AG & Co. (Postfach, Germany), 12-well flat-bottom plates and inserts (12 wells, pore size 0.45 μm, pore density $1.0 \times 10^8$) from Becton Dickinson labware (Franklin Lakes, NJ, USA). EVOM™ Epithelial Voltohmmeter for the trans-epithelial electric resistance (TEER) measurements was from World Precision Instruments, Inc. (FL, USA) and the Cell Culture Incubator was a Model 3110, Series II Water Jacket $CO_2$ Incubator from ThermoForma, MA, USA.

### 3.2.2    Insert preparation

Caco-2 cells were cultured in DMEM (pH 7.4) supplemented with 10% fetal bovine serum (qualified), 1% MEM non-essential amino acid, 100 IU/ml penicillin and 0.1 mg/ml streptomycin. The cells were cultured in an atmosphere of 95% relative humidity and 5% $CO_2$ at 37 °C. The culture medium was changed every two days. Subculture was conducted every week; the cells were washed with PBS and then

detached by 0.25% trypsin-EDTA. The number of cells was counted and seeded onto new dishes at the density of 0.5 x 10 $^6$/ml for the subculture (Maeng *et al*, 2002; Zhou *et al*, 2003).

**Figure 3.1:   Schematic diagram for Caco-2 cell transport**

A to B          B to A

Insert

Plate well

Apical chamber

Caco-2 cell
monolayer

Filter

Basolateral
chamber
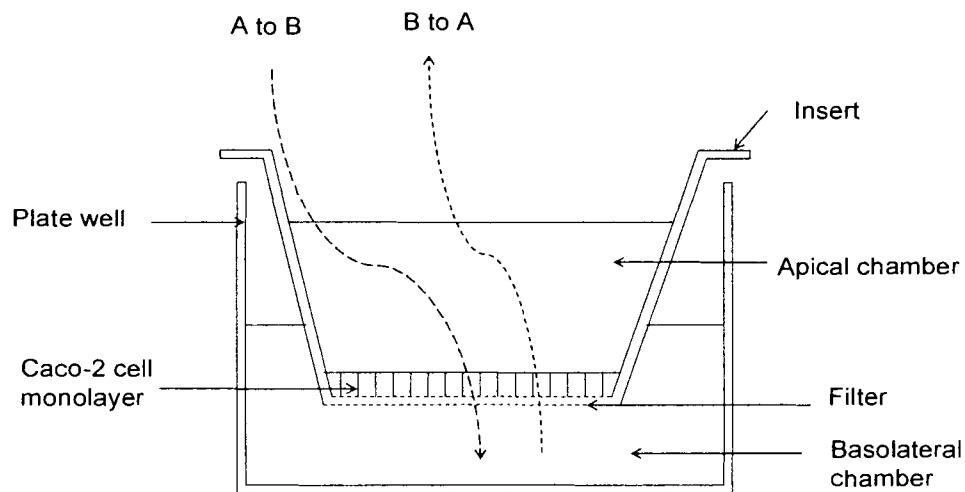
A transport study usually was conducted with a monolayer cultured for 21 days when the cell passage number was about 50-80 (Figure 3.1) as follows: An aliquot (0.5 ml) of the cell suspension was added in the insert after the insert had been incubated for 30 min with 0.1 ml DMEM medium in the upper compartment and 1.5 ml DMEM medium in the bottom compartment of the insert. The DMEM medium in the upper compartment was replaced after 4 hr when the cells were attached to the insert bottom. The incubation medium was changed every other day in the first 2 weeks and then every day. Only Caco-2 cell monolayers with a trans-epithelial electrical resistance (TEER) value greater than 400 $\Omega$ cm$^2$ were used for the transport study.

### 3.2.3    Caco-2 cell monolayer transport of pure matrine

#### 3.2.3.1    Pure matrine transport studies

The transport medium was the DMEM medium (pH 7.4) without the addition of fetal bovine serum, amino acid or antibiotics. Prior to an experiment, the Caco-2 cells monolayer was washed twice with the transport medium. Bidirectional transport studies were initiated by adding 0.4 ml of transport medium containing matrine either to the apical side (for apical to basolateral; A to B in Fig 3.1) or 1.5 ml to the basolateral side (for basolateral to apical transport ; B to A in Fig 3.1) of the monolayer. At predetermined time points: 25, 40, 60, and 90 min, a sample (150 µl for A to B transport; 40 µl for B to A transport) was removed from the opposite receptor compartment and replaced immediately by an equal volume of fresh DMEM medium. Matrine concentration range of the study was limited by the following factors: (a) a preliminary study was conducted to determine the matrine concentration range used in the study; the highest matrine concentration should not decrease the TEER because it was an indicator of the Caco-2 cell integrity; (b) the concentration range for pure matrine and that for crude matrine in Acapha® should overlap for comparison purposes; (c) transport samples for the lowest matrine concentration must be quantifiable by the GC/MS-SIM method. Final matrine concentrations chosen for transport study were 25, 100, 400, 800, and 1600 µg/ml for A to B transport and 25, 100, 400, and 800 µg/ml for B to A transport. All transport studies were conducted in triplicate. Results are expressed as transport mass of matrine per mg protein to account for the different number of Caco-2 cells used in each study.

36

### 3.2.3.2 Effects of temperature and pH on pure matrine transport.

The effects of transport temperature (0, 24 and 37 °C) and pH (5.0, 6.8 and 8.5) on matrine transport from A to B, was examined with only 1 pure matrine concentration (400 μg/ml). In this study, the inserts were kept on ice (0 °C), at room (24 °C) or 37 °C temperature. In the pH effect study, DMEM medium with 400 μg/ml matrine at the apical side was adjusted to pH 5.0, 6.8 or 8.5 when the basolateral side remained at pH 7.4.

### 3.2.3.3 Effects of p-glycoprotein inhibition

Verapamil is an inhibitor of p-glycoprotein and can inhibit the effux of drugs induced by p-glycoprotein if the drug is a substrate of p-glycoprotein. These studies were conducted with preincubation or coincubation with verapamil as follows: (a) Preincubation with verapamil. All monolayers were incubated for 30 min after replacing the culture DMEM with blank DMEM. Preincubation was initiated by adding 50 μM verapamil to the apical chamber at 37 °C. At the conclusion of a 0.5-hour incubation, the plate was washed twice with blank DMEM medium. The monolayers were transferred to a new plate. DMEM with matrine was added to the apical side (or basolateral side) and blank DMEM was added to the opposite side. At predetermined time points: 20, 40, 60, 90, and 120 min, an aliquot of the incubation medium was removed from the basolateral side (150 μl) or the apical chamber (40 μl). They were replaced immediately with the same volume of blank DMEM. (b) Coadminstration with verapamil. This was conducted by incubating the cell monolayer with matrine and verapamil in the apical chamber at the same time. Two different verapamil concentrations (50 μM and 200 μM) were used. The studies were carried out similar to the procedure described in (a). A TEER reading was taken after the last sample was removed. The monolayer was washed with cold blank

DMEM twice before being transferred to a new plate. After the addition of NaOH (0.5ml 1M) to the apical chamber, the plate was incubated at 37 °C for 30 min. An aliquot of the solution in the apical chamber was collected for protein analysis.

### 3.2.3.4 Determination of matrine using GC/MS

The samples were extracted and analyzed by GC/MS for matrine according to the procedure of Sit *et al.* (2004) with modification. Briefly, a Hewlett-Packard 5890 series II gas chromatograph coupled to a 5971 mass spectrometric detector was used to analyse matrine in DMEM. Chromatographic separation was performed using a 5% diphenyl-95% dimethylpolysiloxane capillary column (30m x 0.25mm x 0.25μm, HP-5 MS). Helium was used as the carrier gas under a head pressure of 50 psi. The injector and transfer line temperatures were set at 250 °C and 280 °C, respectively. The initial oven temperature was set at 110 °C, maintained for 1 min and then increased to 220 °C at a rate of 30 °C /min and maintained for 1 min. The temperature was further increased to 300 °C at a rate of 15 °C/min and maintained for 3 min. Ionization was performed under electronic impact ionization with 70 eV. Matrine and deuterated matrine were analyzed in the selective ion monitoring (SIM) mode. The ions *m/z* 248 and m/z 250 were selected to monitor matrine and deuterated matrine, respectively due to their abundance and specificity. The ion *m/z* 249 also was recorded but was not used in matrine quantification. Details of the GC/MS-SIM method can be found in **Appendix I**.

### 3.2.4 Caco-2 cell monolayer transport of crude matrine in Acapha®

#### 3.2.4.1 Preparation of Acapha® extracts

Acapha® powder was weighed and mixed with 70% ethanol to prepare a 100

mg/ml soultion. After the solution was ultrasonicated for 60 min, it was filtered through a filter paper (Whatman, International Ltd, Maidstone, England) following a 0.22μm Millipore filter unit (Carrigtwohill, Co.Cork, Ireland). The filtrate was concentrated to about 33% of its original volume in a vaccum centrifuge (Jouan, Trouin, France). The filtered extract was divided into several vials and stored in a -20°C freezer. Before transport study, the extract was diluted with blank DMEM to the corresponding matrine concentrations. To analyze the matrine concentration in the original extract, the sample from one vial was diluted 100 fold with DMEM and extracted with toluene/butanol (9:1) following the procedure described in the paper of Sit *et al.* (2004). The final toluene/butanol extract was injected into a GC/MS and analyzed for matrine in the SIM mode.

### 3.2.4.2   Transport of crude matrine in Acapha® by Caco-2 cells

The rationale behind the selection of a range of crude matrine (in Acapha®) concentrations is the same as that of pure matrine (see 3.2.3.1). The following crude matrine concentrations were used in the studies: 6.7, 13.4, 26.8, 53.7, and 107.4 μg/ml for A to B transport and 13.4, 26.8, and 53.7 μg/ml for B to A transport. The A to B transport study was initiated by washing the Caco-2 cell monolayer with the DMEM medium before adding the Acapha® extract (5 μl) to the apical side of the cells. A sample of DMEM (100 μl) was taken from the basolateral side at different time points up to 90 minutes. The samples were analysed for unchanged martrine using GC/MS-SIM (see 3.2.3.4). Transport of matrine across the cells (bioavailability) was expressed as a fraction of the initial amount of crude matrine applied to the apical side. A similar procedure was used for the B to A transport study.

### 3.2.4.3    HPLC chemical profile of Acapha®

The transport samples of Acapha® extract which contained 23.6 μg/ml matrine after crossing Caco-2 cell monolayer were chosen to get HPLC profiles of Acapha®. The profiles were obtained using a 1090 Liquid Chromatograph (Hewlett Packard Ltd, USA) equipped with a DAD UV detector and a Phenomenex LUNR phenyl-hexyl column (4.6 mm x 250 mm, 5μm) (USA). The mobile phase consisted of solution A: methanol and acetonitrile (58:42, v:v) and solution B: 0.3% phosphoric acid aqueous solution(pH 2) with the following gradient elution: 10% A and 90% B from the beginning to 8 min, increased to 40% A from 8 min to 18 min, 100% A from 18 min to 23 min and same gradient until 25 min. The flow rate was 1.0 ml/min and injection volume was 20 ul. The Acapha® extract profiles were obtained by setting the DAD UV detector at three wavelengths: 215, 260 and 330 nm.

### 3.2.5    Protein analysis

This assay followed a modification of the Lowry method (Peterson, 1977).

### 3.2.6    Calculation of transport rate

Transport rate was expressed as matrine mass per milligram protein per minute (μg/mgp/min). Permeability coefficient (Papp) was calculated according to the following equations: $P_{app}$ = (dc/dt) * Vr/(A*60*Cd), where (dc/dt) * Vr  is the flux of the test compound across the monolayer and Vr (ml) is the volume of the receptor compartment. The flux is estimated from the slope of the transported mass (μg/mgp) v.s. time plot. A (cm$^2$) is the surface area of the cell monolayer, and Cd is the initial concentration in the donor compartment. The $P_{app}$ values were expressed as nm/s.

### 3.2.7　Statistical analysis

Comparisons between different groups (more than two groups) were performed using one factor ANOVA following the post-hoc test if the significant difference was found among groups at $P<0.05$. Students' $t$ test was performed to compare $P_{app}$ or transport rate between two groups with a significance level of $P< 0.05$.

## 3.3　Results

### 3.3.1　Transport of pure matrine across Caco-2 cells

Transport of pure matrine across the Caco-2 cell monolayers was evaluated from A to B (apical side to basolateral side; Figure 3.2) and from B to A (basolateral side to apical side; Figure 3.3). Matrine was found to pass through the Caco-2 cell monolayers rapidly. Transported mass increased with incubation time linearly for 0.5 to 1 hr, the trendline $R^2$ value for transport data in 1 hour (Fig 3.2) is 0.99 for all concentrations except the 1600 µg/ml concentration which has a correlation coefficient, $R^2 = 0.94$. The flux for the highest concentration showed the trend to slow down after 0.5 hour. For B to A transport (Fig 3.3), a linear relationship was also observed between incubation time and transported mass for 1 hour with a correlation coefficient, $R^2 = 0.99$ for the 25, 100, 400 µg/ml concentrations and a $R^2 = 0.97$ for the 800 µg/ml concentration.

Figure 3.2:    Matrine flux across Caco-2 cell from A to B. Values are expressed as the mean ● S.E.of three determinations. If the error bar is not shown, the error is smaller than the symbol.
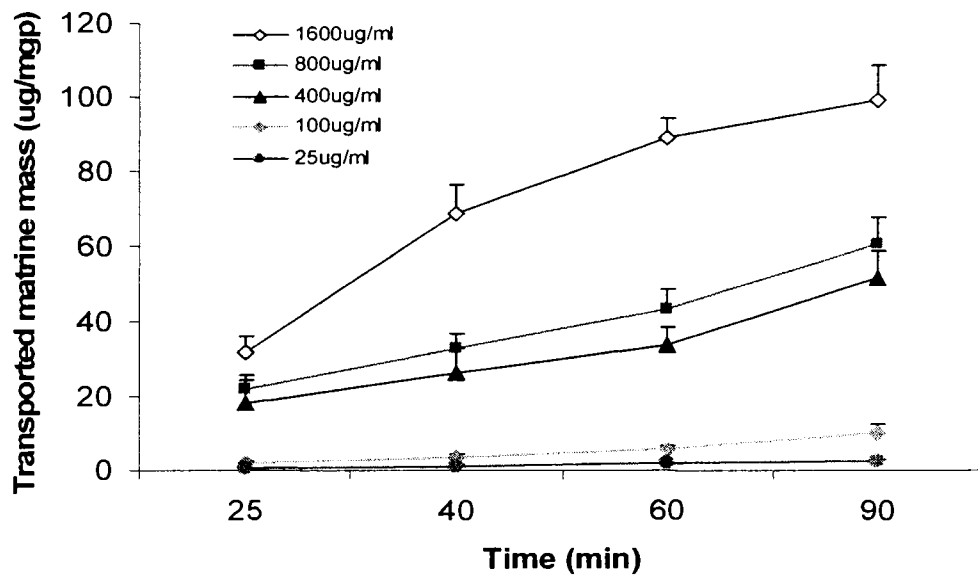


Figure 3.3:    Matrine efflux across Caco-2 cell monolayer from B to A. Values are expressed as the mean ● S.E. of three determinations. If the error bar is not shown, the error is smaller than the symbol.
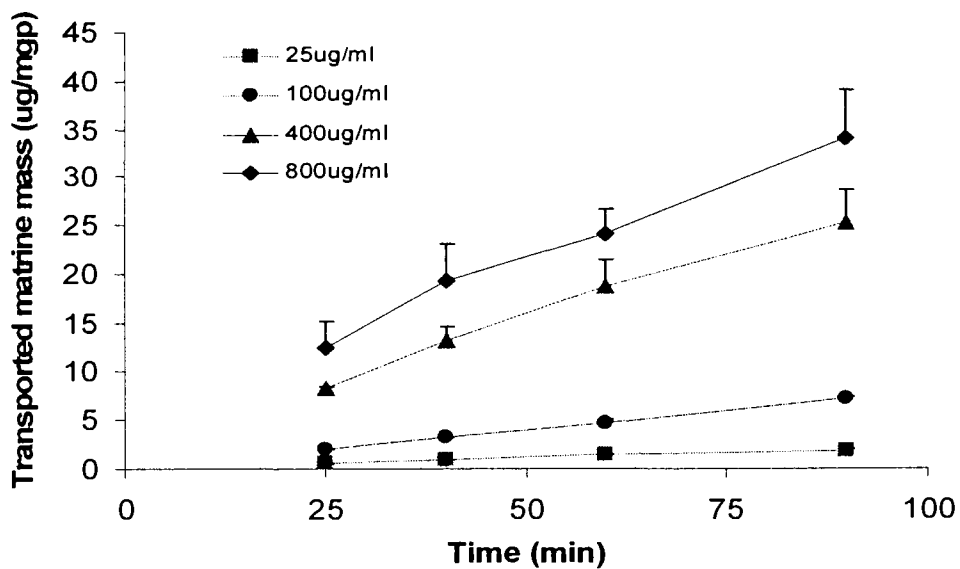
In order to compare the flux of matrine from A to B and that from B to A, transport rates were calculated based on the mass of matrine transported in 1 hr (0.5 hour for 1600 µg/ml from A to B). Figure 3.4 shows the relationship between the transport rate and initial concentration. At a donor concentration range of 25-1600 µg/ml for A to B and 25-400 µg/ml for B to A, the transport rates for both directions were very similar and a linear relationship existed between the transport rate and the initial matrine concentration, indicating that passive diffusion was involved in both directions of matrine transport. For B to A transport, the transport rate did not increase linearly with initial matrine concentrations when the concentration was higher than 400 µg/ml. A plausible explanation may be that matrine transport across the Caco-2 cell monolayers has become saturated at this concentration. A similar observation on a saturable diffusion transport process also has been reported for the uptake of ginsenoside Rb1 by Caco-2 cells (Han et al, 2006).

Figure 3.4:    Effects of concentration on matrine transport rate for both direction. Values are expressed as the mean ± S.E. (n=3). If the error bar is not shown, the error is smaller than the symbol.
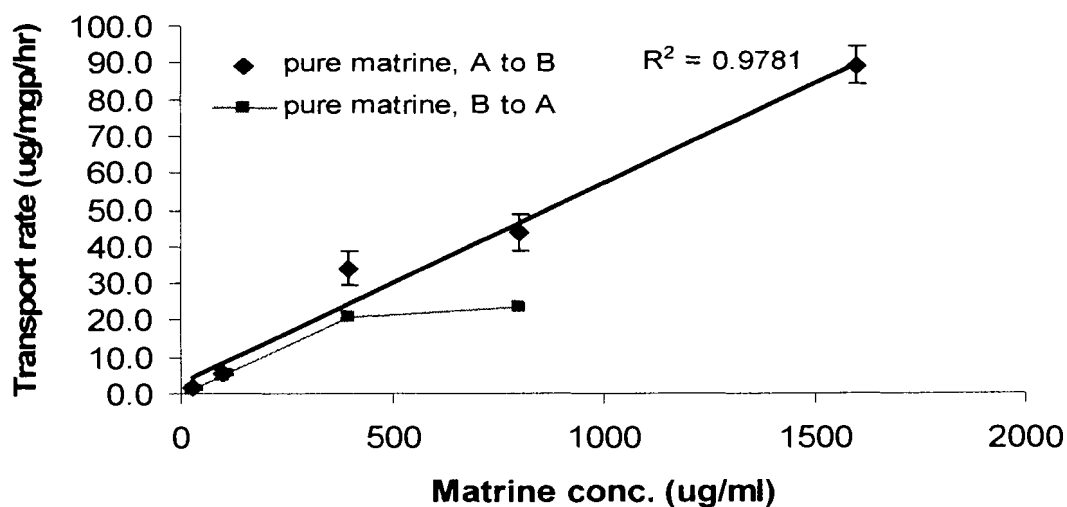
The transport of matrine from A to B and from B to A also was compared using $P_{app}$ calculated by the equation, $(dc/dt) * Vr/(A*60*Cd)$. $P_{app}$ is often used to compare the permeation of different chemicals or the same chemical under different experimental conditions because it incorporates the effects of donor concentration, transport area and transport rate. The $P_{app}$ for A to B transport was not found to be significantly greater than that of B to A transport for same donor concentrations (Table 3.1). For both transport directions, $P_{app}$ also did not change significantly within the concentration range of 25-1600 µg/ml for A to B and 25-400 µg/ml for B to A. The only exception was B to A transport at 800 µg/ml of which the $P_{app}$ was significantly higher (P=0.006) than that of 25 µg/ml. These results suggest that $P_{app}$ are relative stable within the concentration range of 25-1600 µg/ml for A to B and 25-400 µg/ml for B to A. Results of the studies also support passive diffusion as the mechanism of transport for both directions but with the possibility of saturation at a high matrine concentration for B to A transport.

Table 3.1:    Effects of matrine concentration on $P_{app}$ for both directions ($10^{-5}$ cm/s)

| Matrine conc. (µg/ml) | A to B | B to A |
|---|---|---|
| 25 | 2.22± 0.74 | 1.70± 0.35 |
| 100 | 2.00±0.36 | 1.24±0.34 |
| 400 | 2.06±0.44 | 1.39±0.36 |
| 800 | 1.43±0.07 | 0.76±0.13* |
| 1600 | 1.58±0.29 | NA |

Values are expressed as the mean ± S.E (n=3). NA: data is not available.
 * P=0.006 compared with the 25µg/ml group for the same transport direction (B to A).
$P_{app}$ comparison was performed between different conc. for the same transport direction
or between two different transport directions but at the same conc.

### 3.3.2 Acapha® extract transport across Caco-2 cell monolayer

The transport of Acapha® extract across Caco-2 cell monolayer also was evaluated bi-directionally (A to B and B to A). Figure 3.5 shows a typical HPLC profile of Acapha® extract after it passes through the Caco-2 cells monolayer (note: Acapha® extract profiles before passing through the Caco-2 cell monolayers are shown in Figure 2.3 and 2.4). At UV absorbance of 215 nm, matrine (see arrows in the figures) and a small number of unidentified chemicals were able to pass through the Caco-2 cell monolayers in both directions (Figures 3.5 I and III). As shown in the HPLC profile at UV absorbance of 330 nm, most chemicals with a Rt of 15 min or higher appeared to cross the Caco-2 cell monolayer freely (Figure 3.5 II and IV). It should be noted that the profile of Acapha® extract decreased in peak number and peak size after crossing the Caco-2 cell monolayers (Figure 2.3 *v.s* Figure 3.5 I and II, Fig 2.4 *v.s* Figure 3.5 III and IV). These results suggest that Caco-2 cell monolayer is a useful tool to screen for the intestinal absorption of a chemical mixture. In the case of Acapha®, it appears only a few chemicals cross the Caco-2 cell monolayer.

Figure 3.5:    HPLC profiles of Acapha® extract after crossing the Caco-2 cell monolayer. The profiles come from 90 min transport samples of Acapha® extract which contains 23.6 µg/ml matrine. The arrows point at the matrine peak. I and III profiles are monitored at 215 nm. II and IV are monitored at 330 nm. I and II: after transport from A to B; III and IV: after transport from B to A. All the profiles have been rescaled in order to show the peaks clearly.

DAD1 A, Sig=215,4 Ref=450,20 (D:\MATRIN2\M1017013.D)

**I**

mAU

After Caco-2 cell ( 215nm), A to B

120

100

80

60

40

Matrine

20

0

2.857
4.024
4.588
7.873
15.220

5    10    15    20    25    min

---

DAD1 E, Sig=330,4 Ref=450,20 (D:\MATRIN2\M1017013.D)

**II**

mAU

1.2

After Cac-2 cell (330nm), A to B

1

0.8

0.6

0.4

0.2

0

-0.2

2.815
2.943
3.371
4.243
14.929
16.926
17.373
17.757
18.049
19.016
22.330
23.737
24.005
27.754

5    10    15    20    25    min

mAU

III

After Caco-2 cell (215nm), B to A

80

60

4.035

40

3.813

4.626

Matrine

20

3.081

5.637

7.898

15.274

19.075

0

0          5          10         15         20         25        min

mAU

IV

After Caco-2 cell (330nm), B to A

22.372

23.783

1.2

17.426

1

24.042

0.8

19.070

0.6

17.697
18.093

22.754

2.821

25.420

0.4

14.982

21.740

24.772

25.986

27.792

4.235

0.2

4.674

0

3.102

-0.2

2.939

5          10         15         20         25        min

### 3.3.3 Transport of crude matrine in Acapha®

As shown in Fig 3.5, crude matrine (in Acapha®) was found to cross the Caco-2 cell monolayers. Based on the GC/MS-SIM analysis, matrine constituted about 0.4 % of

48

Acapha® by weight. This mass ratio was used to calculate the amount of crude matrine in the Acapha®extract used in the Caco-2 cell monolayer transport studies. Figures 3.6 and 3.7 show that crude matrine transport is linearly related to incubation time for about 1 hour in both directions (A to B and B to A); the correlation coefficients were found to range from 0.97 to 0.999 for different Acapha® concentrations. It is interesting to note that the transport rates in both directions are linearly related to the matrine concentrations (Fig 3.8), they are very similar at the same donor concentration.

**Figure 3.6:** The flux of crude matrine in Acapha® from A to B. Values are expressed as the mean ± S.E. If the error bar is not shown, the error is smaller than the symbol.
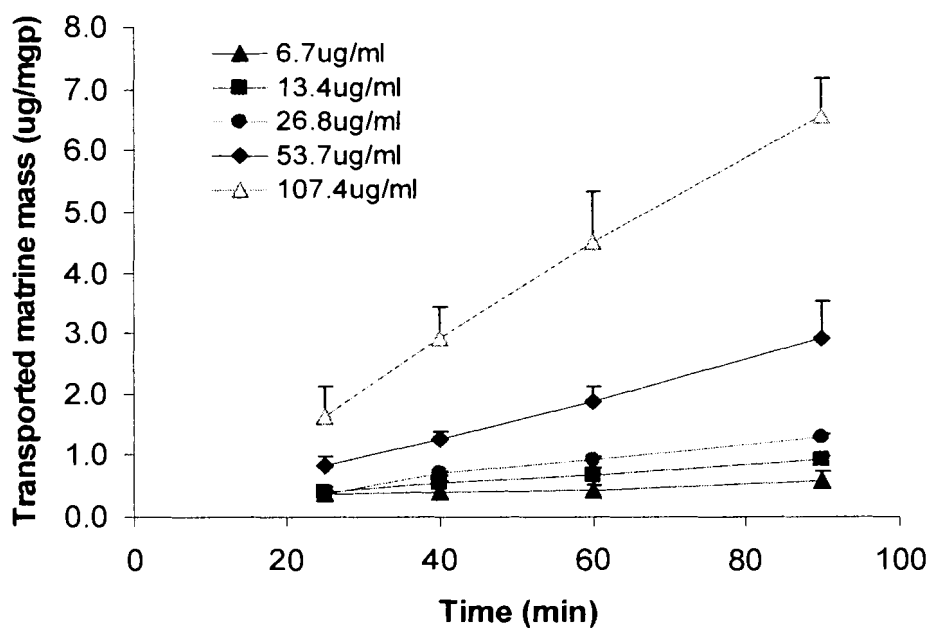
**Figure 3.7:** The efflux of crude matrine in Acapha® from B to A. Values are expressed as the mean ± S.E (n=3). If the error bar is not shown, the error is smaller than the symbol.
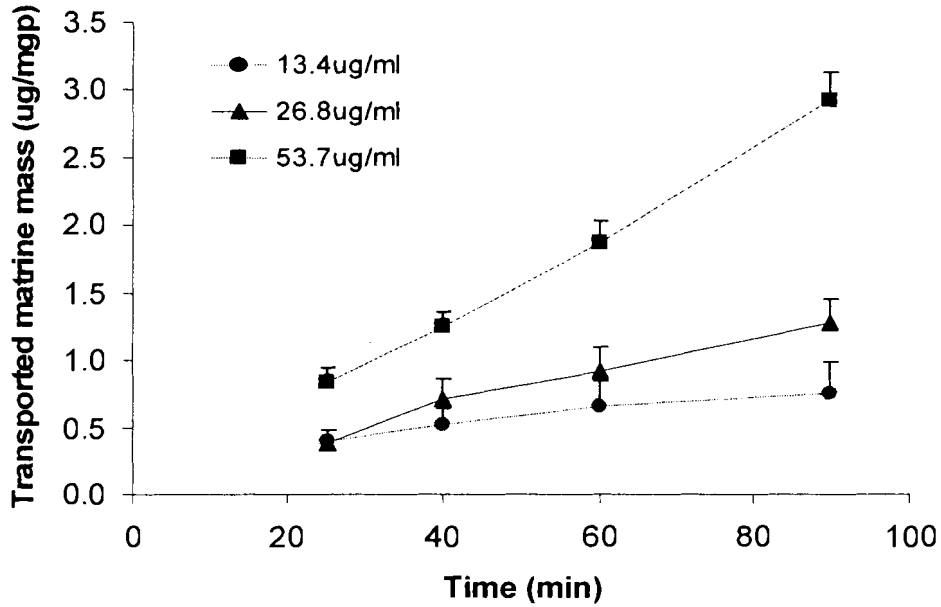


**Figure 3.8:** Effects of concentration on transport rate of matrine in Acapha® for both directions. Values are expressed as the mean ± S.E (n=3). If the error bar is not shown, the error is smaller than the symbol.



50
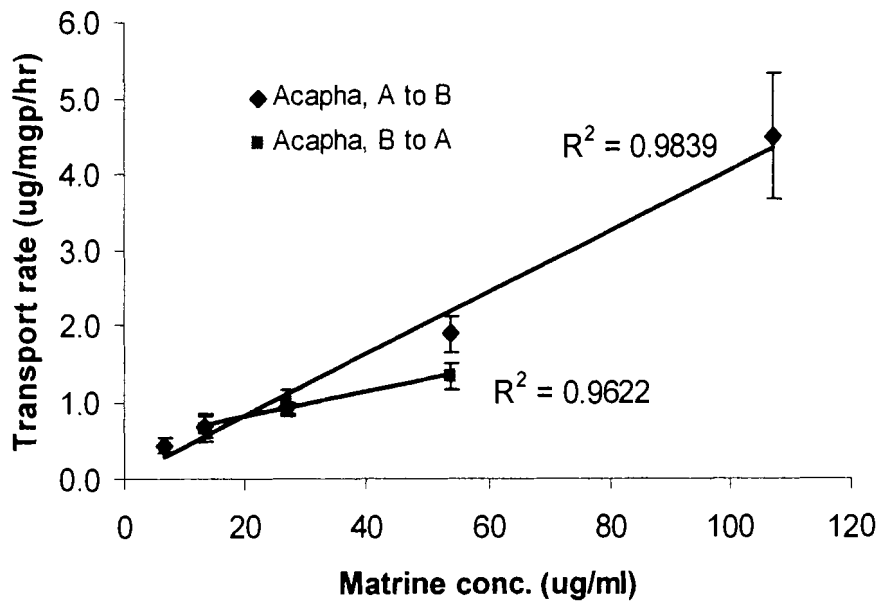
Table 3.2 shows the $P_{app}$ for the bi-directional transport of crude matrine at different donor concentrations. Similar to the results of pure matrine, $P_{app}$ for A to B transport was not much higher than that of B to A transport at all donor concentrations with the exception of the 53.6 µg/ml group. As with pure matrine, crude matrine $P_{app}$ is relative stable in the concentration range used in this study. These results also suggest that crude matrine is transported by the Caco-2 cell monolayers *via* a passive diffusion process.

Table 3.2: Concentration effects on $P_{app}$ of crude matrine transport for both directions

| Matrine conc. in Acapha® (µg/ml) | A to B | B to A |
|---|---|---|
| 6.7 | 0.84± 0.72 | NA |
| 13.4 | 1.08±0.07 | 1.02±0.49 |
| 26.8 | 0.91±0.06 | 0.85±0.23 |
| 53.6 | 1.12±0.32 | 0.58±0.08* |
| 107.2 | 1.31±0.09 | NA |

Values are expressed as the mean ± S.E (n=3). NA: data is not available.
* Significantly different to the A to B transport group, P= 0.05.
$P_{app}$ comparison was performed between different conc. for the same transport direction or between two different transport directions but at the same conc.

### 3.3.4 Comparison of pure matrine and crude matrine transport

Transport of pure matrine at a donor concentration range of 25-100 µg/ml (see 3.3.1.) are compared with the transport of crude matrine at a donor concentration range of 26.8 -107.4 µg/ml (see 3.3.3). Figures 3.9 and 3.10 show that pure matrine is always transported at a higher rate than crude matrine whether it is from A to B or B to A. These results clearly demonstrate that crude matrine transport across the Caco-2 cells monolayers is retarded by the matrix in Acapha®.

Figure 3.9:    A to B transport of pure matrine vs crude matrine in Acapha® Data were taken from Figs. 3.1 and 3.6. Values are expressed as the mean ± S.E (n=3). If the error bar is not shown, the error is smaller than the symbol.
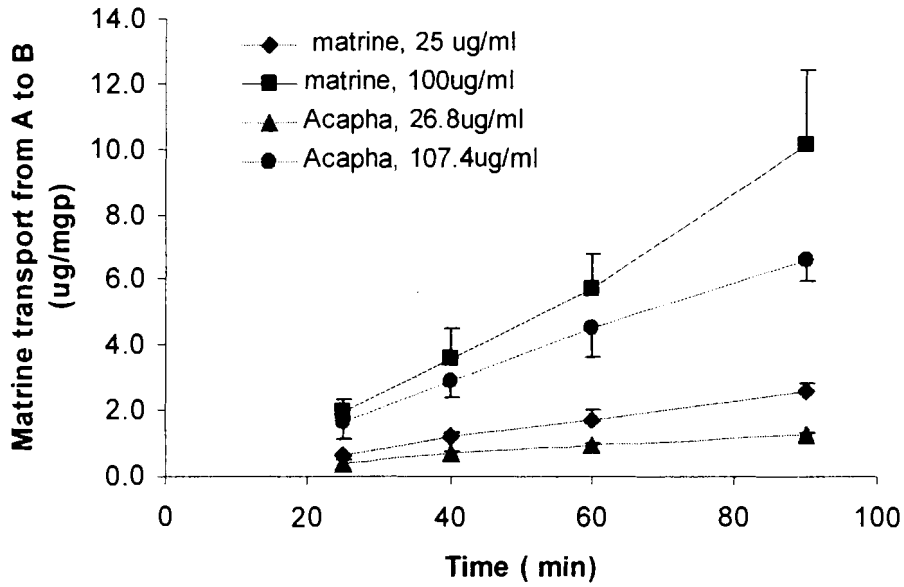


Figure 3.10:    B to A transport of pure matrine vs crude matrine in Acapha® Data were taken from Figs. 3.2 and 3.7. Values are expressed as the mean ± S.E. If the error bar is not shown, the error is smaller than the symbol.
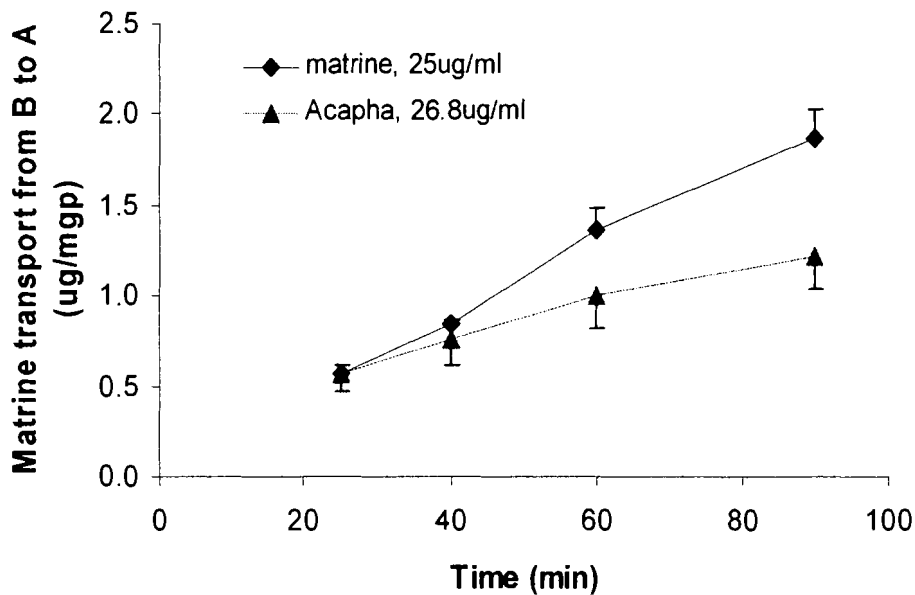
Table 3.3 shows that the transport rate and the $P_{app}$ values of pure matrine also are always higher than those of crude matrine in both transport directions. These results render further support to our hypothesis that crude matrine transport across the Caco-2 cells monolayers is retarded by the matrix and/or other known and unknown chemicals in Acapha®.

**Table 3.3:** Transport rate and $P_{app}$ for pure matrine and crude matrine in Acapha®

| Matrine conc. (µg/ml) | Matrine | Acapha | Matrine | Acapha |
|---|---|---|---|---|
| | A to B | A to B | B to A | B to A |
| **Transport rate (µg/mgp/hr)** | | | | |
| 25 /26.8 | 1.69± 0.33 | 0.93± 0.07*[a] | 1.27± 0.12 | 1.00± 0.17*[b] |
| 100/ 107.4 | 5.73± 1.07 | 4.49± 0.82 | NA | NA |
| **$P_{app}$ ( $10^{-5}$ cm/s)** | | | | |
| 25 /26.8 | 2.22± 0.74 | 0.91± 0.06*[c] | 1.70± 0.35 | 0.85± 0.23*[d] |
| 100/ 107.4 | 2.00± 0.36 | 1.31± 0.09*[e] | NA | NA |

NA: for B to A transport, the data for 107.4 µg/ml crude matrine in Acapha was not available.
Student's T-test was used to compare the transport rate and Paff between two groups.
*Significantly different to the corresponding pure matrine group of similar concentration.
* P values for a, b, c, d and e are 0.02, 0.04, 0.02, 0.01 and 0.03.

### 3.3.5 Factors affecting Caco-2 cell transport

#### 3.3.5.1 Effects of temperature on pure matrine transport

Matrine transport across the Caco-2 cell monolayers also was examined at different incubation temperatures (0 °C, 24 °C and 37 °C) to determine if the transport involved an energy-dependent process. Figure 3.11 shows that the mass of matrine transported increases with an increasing incubation temperature. Moreover, the flux from A to B at 0 °C and 20 °C was significantly lower than that of 37 °C (P< 0.01).

53

Figure 3.11:    Effects of temperature on pure matrine transport. Values are expressed as the mean ± S.E of three to six determinations. An asterisk denotes a significant difference (P<0.01) from the 37°C group at same samping time.

Temperature (degree)

■ 0     □ 24     □ 37



Time (min)
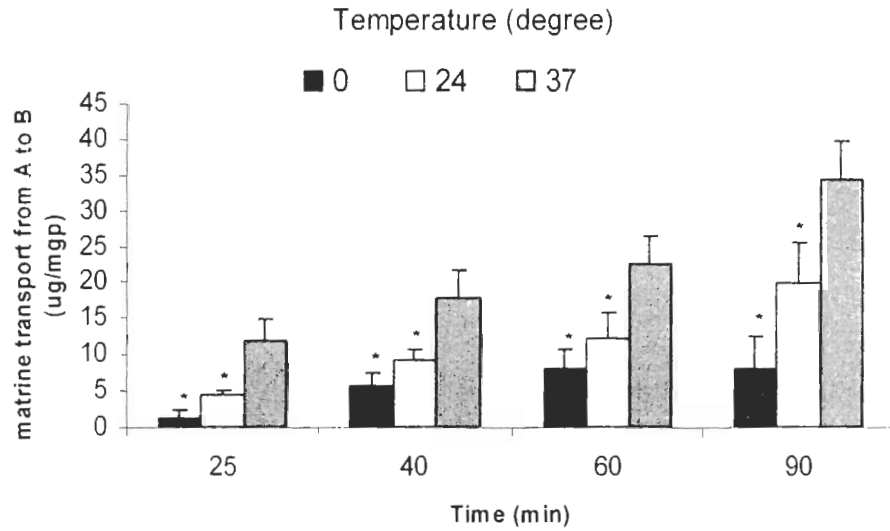
## 3.3.5.2    Effects of pH on pure matrine transport

Figure 3.12:    Effects of pH on pure matrine transport. Values are expressed as the mean ± S.E. of three to six determinations. The letters a,b,c represent the groups of pH 5.0, 6.8 and 8.5 respectively. The letters above each column bar indicate the significance (P<0.01) from other groups at same sampling time.



■ pH5.0     □ pH6.8     □ pH8.5

Time(min)

54
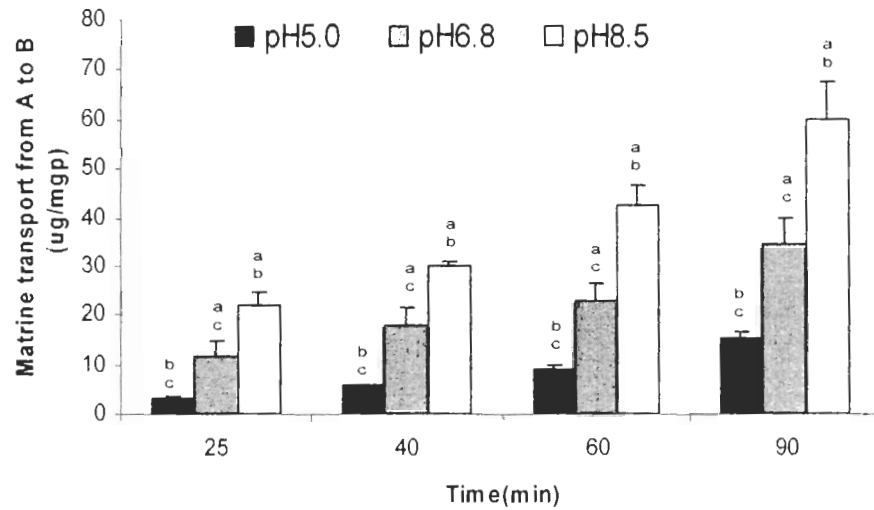
Matrine transport also was studied using different buffer pH values. Figure 3.12 shows that matrine transport increases with an increasing buffer pH value. The flux from A to B at a higher pH was significantly faster than that at a lower pH (p<0.01). Since matrine is an alkaloid or a nitrogen-containing chemical, different buffer pH might influence the nonionized/ionized ratio of matrine in an aqueous solution affecting its absorption by the Caco-2 cell monolayers. A higher buffer pH might favor the matrine molecule to remain in the unionized form, making it easier to pass through the Caco-2 cell membrane.

### 3.3.5.3    Effects of P-glycoprotein inhibition on pure matrine transport

P-glycoprotein (P-GP) is an active transporter which carries a foreign chemical out of the intestine cell and pumps the chemical back to the GI tract lumen. To determine if P-GP is involved in the transport of matrine, a P-GP inhibitor, verapamil was used to inhibit the transporter. If matrine is the substrate of P-GP, its transport will be changed by the administration of verapamil, the final effect is to increase matrine transport from A to B and decrease that for B to A from this *in vitro* study; if matrine is not the substrate of P-GP, the administration of verapamil might not influence matrine transport. Figures 3.13 and 3.14 show the effects of verapamil on matrine transport. The transport of matrine in both directions (A to B and B to A) was not affected significantly by verapamil whether it was added before or at the same time with matrine into the apical side of the Caco-2 cell monolayers. Matrine transport also was unchanged when the concentration of verapamil was increased by four fold (coadministration 2). This result suggests that P-gp might not be involved in matrine transport and confirms the results observed in pure matrine and crude matrine transport (section 3.3.1 and 3.3.2) in which A to B and B to A transport

rates are not very different suggesting a passive diffusion mechanism  for matrine

transport (Maeng, et al, 2002; Zhou, et al, 2005).

Figure 3.13:  Inhibitory effect of verapamil on matrine transport from A to B. Transport was conducted from A to B, matrine concentration for all groups were 400 μg/ml. Verapamil and matrine were administered into the A side. Control: 400 μg/ml matrine without verapamil. Preincubation: matrine was administered after 30 min incubation with verapamil.Coadministration: matrine was administered in the A side same time as verapamil. Coadministration: 1 and 2: the concentrations of verapamil were 50 μg/ml and 200 μg/ml.
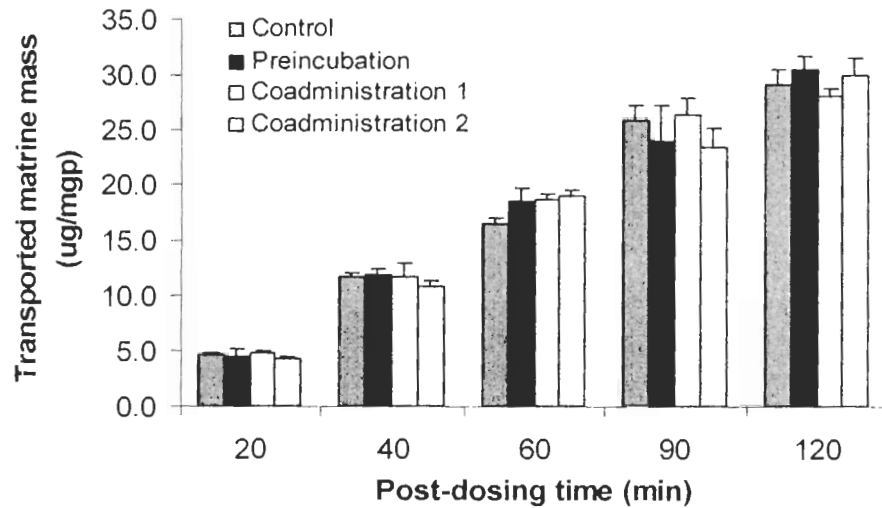


Figure 3.14:  Inhibitory effect of verapamil on matrine transport from B to A. Transport was conducted from B to A, matrine concentration for all groups were 400 μg/ml. Verapamil was administered into the A side, matrine into the B side. Control: 400 μg/ml matrine without verapamil. Preincubation: matrine was administered into the B side after 30 min incubation with verapamil. Coadministration: matrine was administered in the A side same time as verapamil. Coadministration 1 and 2: the concentrations of verapamil were 50 μg/ml and 200 μg/ml respectively.
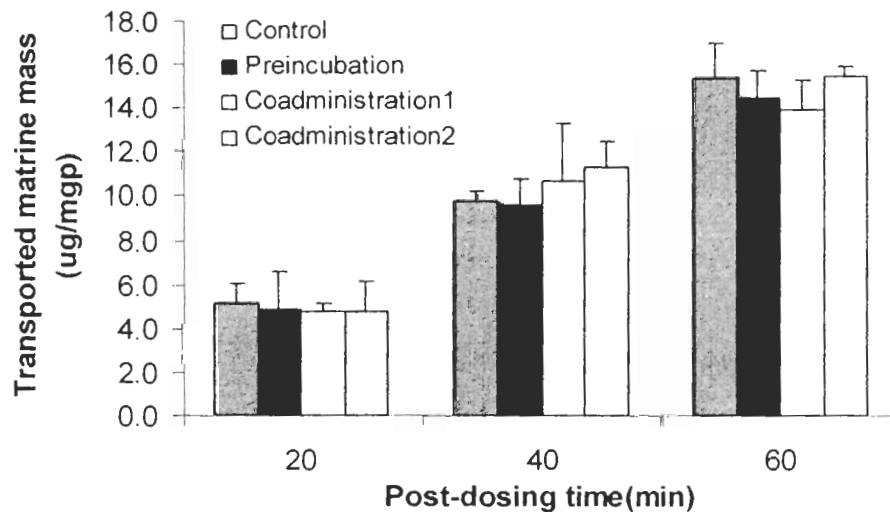
## 3.4　Discussion

### 3.4.1　Absorption of crude matrine by Caco-2 cells

Acapha® is a brownish powder with some small granules which do not dissolve completely in water or common organic solvents. Therefore, Acapha® extracts are used in the present Caco-2 cell transport studies. Results of the studies show that the Caco-2 cell monolayer is permeable to both pure matrine and crude matrine. These results also provide the first indication that Acapha® most likely is absorbed by the gastrointestinal tract of human *in vivo*.

In our preliminary transport studies, pure matrine was found to be less toxic to the Caco-2 cells than crude matrine since TEER (an indicator of membrane integrity) decreased after adding 8000 µg/ml and about 200µg/ml, respectively of pure matrine and crude matrine to apical side of the Caco-2 cell monolayer. Also, a higher concentration of matrine can be added to the apical side than the basolateral side of the Caco-2 cell before TEER begins to decrease. Therefore, different concentration ranges of pure matrine and crude matrine were used in our transport study; the highest concentration in the range is limited by TEER whereas the lowest concentration is dictated by the LOQ of the GC/MS analytical method. Because both TEER and LOQ of the marker chemical can limit the concentration range used in the study, a preliminary range finding study is conducted before embarking on the actual transport study.

### 3.4.2　$P_{app}$ and matrine transport

$P_{app}$ is widely used to quantify the permeation of Caco-2 cell monolayers by different drugs. A completely absorbed drug usually has a high permeability coefficient

($P_{app} > 1 \times 10^{-6}$ cm/s) whereas an incompletely absorbed drug has a low permeability coefficient ($P_{app} < 1 \times 10^{-7}$ cm/s) in the Caco-2 cell monolayer (Artursson, et al, 2001). Matrine is a highly permeable chemical since $P_{app}$ ranging from $0.6\text{-}2.2 \times 10^{-6}$ cm/s have been observed in the present transport study. The fraction of matrine which is absorbed from A to B is about 13-24% for pure matrine and 12-16% for crude matrine after 90 min. A relatively high $P_{app}$ and a reasonable fraction of transport from A to B indicate matrine has a relatively high oral bioavailability *in vivo* (Zhou, 2003, Maeng, 2002).

Our results suggest that matrine transport involves a passive diffusion process. This is based on the following lines of evidence: 1) Transport rate was linearly related to pure matrine concentrations from 25-1600 μg/ml for A to B transport and from 25-400 μg/ml for B to A transport. B to A transport became saturated at concentrations greater than 400 μg/ml. The transport rate of crude matrine also is linearly related to crude matrine concentrations in the study. 2) No obvious polarized transport was found. The $P_{app}$ for both directions is very similar when they are compared at the same matrine concentration (Maeng, et al, 2002). 3) Verapamil, a P-GP inhibitor did not affect the transport of matrine in either direction. Therefore, P-GP might not involve in the transport of matrine (Fricker, et al, 1996; Wu and Rominson, 1999). Although our results support a passive diffusion mechanism of transport without the involvement of active transporter for matrine, two recently published papers have reported that chemicals with basic nitrogen atoms are very likely to be the substrates of P-GP (Pearce et al, 1989; Ford, et al, 1988). Therefore, we cannot rule out completely that matrine transport involves an active process.

### 3.4.2.1  Temperature effects

The transport of pure matrine from A to B was studied at 3 different temperatures: 0°C, 24 °C and 37 °C. There are at least two possible reasons that matrine transport is a temperature or energy-dependent process: 1) Active transport processes may be involved in either A to B direction or B to A direction. Some drugs are transported across the Caco-2 cell monolayers from A to B by an active process, for example the transport of thalidomide (Zhou, 2003; 2005), quinidine (Ishida, *et al,* 2005), and genistein (Oitate *et al.,* 2001). An active transport process also may be involved in B to A transport, for example the P-glycoprotein which is the most commonly studied transporter. A variety of drugs (verapamil, cyclosporine D analog, and valspodar) or phytochemicals (piperine, curcumin, and capsaicin) are substrates of P-gp (Han, Y., et al, 2006). However, no study has demonstrated the involvement of the active transport processes in both transport directions, and 2) Another reason that matrine transport is a temperature and energy-dependent process may be related to the fact that chemical diffusion across the Caco-2 cell membrane is decreased by (i) a reduction of membrane fluidity related phase transitions of the lipid bilayer or (ii) a high membrane rigidity at low temperature (Han et al, 2006; Zhou et al, 2005). Our results suggest a passive diffusion mechanism for matrine transport which is consistent with the assumption of a small molecule such as matrine can easily diffuse across the cell membrane. The reduction of matrine transport from A to B probably is best explained by 2) above.

### 3.4.2.2  pH effects

The media used in the Caco-2 experiments are buffered at pH 7.4 on both sides of the monolayer because the pH in the cellular interstitial fluid and blood compartment is

known to be about 7.4. In contrast, the pH in the upper GI tract under fasting conditions may range from 5.0-6.5, with an acidic microclimate condition above the the epithelial cell layer estimated to be 5.8-6.3. Ingels and Augustijns (2003) have demonstrated that transport media with pH values ranging from 5.0-8.0 are compatible with the Caco-2 cell monolayer. The DMEM medium used in our transport studies of pure matrine and crude matrine is at pH 7.4 whereas pH values ranging from 5.0-8.5 have been chosen to observe the effects of pH on matrine transport. Our results show that matrine transport from A to B increases with decreasing pH values, which is consistent with the fact that matrine is an alkaloid and a higher buffer pH might favour the formation of unionized matrine in the medium and further increase the partitioning of matrine into the cell membrane.

### 3.4.2.3 Culture medium effects

Initially, the Hanks balance salt solution (HBSS) is used as the transport media in the Caco-2 cells transport study since most published Caco-2 cell transport studies have been conducted in HBSS buffer with HEPES supplemented with glucose. HBSS was replaced by blank DMEM with glucose (without the addition of serum, non-essential amino acids and antibiotics) as the transport medium (see Methods) because a satisfactory TEER could not be obtained for the Caco-2 cell monolayers. Blank DMEM contains amino acids and vitamins (Xu and E, 1994) which are essential nutrients for the growth of Caco-2 cells. Hitherto, saline buffer such as tris buffer (Mao et al, 2005, Alsenz et al., 2003) and Ringer medium (Brunet et al, 2004) and non-saline buffer such as Opti MEM (Han, et al. 2006) also have been used in Caco-2 cell transport studies. There are shortcomings associated with the use of saline buffers for Caco-2 experiments; these include limited solubility for lipophilic drugs, adsorption and/or non-specific

binding to the device surfaces or to the cells and poor physiological relevance of the

media used (Ingles and Augustijns, 2003).

## 3.5 References

Alsenz, J and Harnel, E. (2003) Development of a 7-day, 96-well Caco-2 permeability assay with high-throughput direct UV compound analysis. Pharmaceutical Research. 20(12):1961-1969.

Artursson, P., Palm, K. and Luthman, K. (2001) Caco-2 monolayers in experimental and theoretical predictions of drug transport. Advanced Drug Delivery Reviews. 46:27-43.

Bergström, C.A.S. (2005) In silico predictions of drug solubility and permeability: two rate-limiting barriers to oral drug absorption. Basic and Clinical Pharmacology and Toxicology, 96:156-161.

Brunt, J., Maresca, M., Fantini, J. and Belzunces, L.P. (2004) Human intestinal absorption of imidacloprid with Caco-2 cells as enterocyte model. Toxicology and Applied Pharmacology. 194:1-9.

Delie, F., and Rubas, W. (1997) A human colonic cell line sharing similarities with enterocytes as a model to examine oral absorption: advantages and limitations of the Caco-2 model. Critical Reviews in Therapeutic Drug Carrier System. 14(3):221-286.

D'Emanuele, A., Jevprasesphant, R., Penny, J. and Attwood, D. (2004) The use of dendrimer-propranolol prodrug to bypass efflux transporters and enhance oral bioavailability. Journal of Controlled Release. 95:447-453.

Food and Drug Administration (2000). http://www.fda.gov/cder/OPS/BCS_guidance.htm.

Ford, J. M., Prozialeck, W. C. and Hait, W. N. (1988) Structural features determining activity of phenothiazines and related drugs for inhibition of cell growth and reversal of multidrug resistance. Molecular Pharmacology. 35: 105-115.

Fricker, G., Drewe, J., Huwyler, J., Gutmann, H. and Beglinger, C. (1996) Relevance of p-glycoprotein for the enteral absorption of cyclosporine A: in vitro-in vivo correlation. British Journal of Pharmacology. 118:1841-1847.

Han, Y., Tan, T. and Lim, L.Y. (2006) Effects of capsaicin on P-GP function and expression in Caco-2 cells. Biochemical Pharmacology. 71:1727-1734.

Ingles, F.M. and Augustijns, P.F. (2003) Biological, pharmaceutical, and analytical considerations with respect to the transport media used in the absorption screening system, Caco-2. Journal of Pharamceutical Sciences. 92 (8): 1545-1558.

Ishida, K., Takaai, M. and Hashimoto, Y. (2006) Pharmacokinetic analysis of transcellular transport of quinidine across monolayers of human intestinal epithelial Caco-2 cells. Biological & Pharmaceutical Bulletin. 29(3):522-526.

Lindenberg, M., Kopp, S. and Dressman, J.B. (2004) Classification of orally administered drugs on the World Health Organization Model List of Essential Medicines according to the biopharmaceutics classification system. European Journal of Pharmaceutics and Biopharmaceutics. 58:265-278.

Maeng, H.J., Yoo, H.J., Kim, I.W., Song, I.S., Chung, S.J. and Shim, C.K. (2002) P-glycoprotein-mediated transport of berberine across Caco-2 cell monolayer. Journal of Pharmaceutical Sciences, 91(12):2614-2621.

Mao, S., Germershaus, O., Fischer, D., Linn, T., Schnepf, R., Kissel, T. (2005) Uptake and transport of PEG-graft-trimethyl-chitosan copolymer-insulin nanocomplexes by epithelial cells. Pharmaceutical Research. 22(12):2058-2068.

Meunier, V., Bourrié, M., Berger, Y. and Fabre, G. (1995) The human intestinal epithelial cell line Caco-2; pharmacological and pharmacokinetic applications. Cell Biology and Toxicology. 11:187-194.

Nishimura, N. (2005) Effects of Chinese herbal medicines on intestinal drug absorption. Yakugaku Zasshi. 125(4):363-369.

Oitate, M., Nakaki, R., Koyabo, N., Takanaga, H., Matsuo, H., Ohtani, H., and Sawada, Y. (2001) Transcellular transport of genistein, a soybean-derived isoflavone, across human colon carcinoma cell line (Caco-2). Biopharmaceutics and Drug Disposition. 22:23-29.

Pearce, H. L., Safa, A. R., Bach, N. J., Winter, M.A. and Cirtain M.C. (1989) Essential features of the P-glycoprotein pharmacophore as defined by a series of reserpine analogs that modulate multidrug resistance. Proceedings of the National Academy of Sciences of the United States of America. 86: 5128-5132.

Peterson, G.L. (1977) A simplification of the protein assay method of Lowry et al. which is more generally applicable. Analytical Biochemistry. 83(2):346-356.

Sit, D.S., Gao, G., Law, F.C. and Li, P.C. (2004) Gas chromatography-mass spectrometry determination of matrine in human plasma. Journal of Chromatography B. 808(2):209-214.

Spahn-Langguth, H. and Langguth, P. (2001) Grapefruit juice enhances intestinal absorption of the P-glycoprotein substrate talinol. European Journal of Pharmaceutical Sciences. 12:361-367.

Stoner, C.L., Cleton, A., Johnson, K., Oh, D.M., Hallak, H., Brodfuehrer, J., Surendran, N. and Han, H.K. (2004) Integrated oral bioavailability projection using *in vitro* screening data as a selection tool in drug discovery. International Journal of Pharmaceutics. 269:241-249.

Taetz, S., Baldes, C., Mürdter, T.E., Piochowska, K., Bock, U., Haltner-Ukomadu, E., Mueller, J., Huwer, H., Schaefer, U.F., Klotz, U., and Lehr, C.M. (2006) Biopharmaceutical characterization of the telomerase inhibitor BRACO19. Pharmaceutical Research. 23(5):1031-1037.

Wu, S.and Robinson, J.R. (1999) Transport of human growth hormone across Caco-2 cells with novel delivery agents: evidence for P-glycoprotein involvement. Journal of Controlled Release. 62:171-177.

Xu, X.L. and E, Z. (1994) Cell culture medium In Tissue Culture and Molecular and Cellular Techniques. Eds. E, Z., Beijing Press, Beijing, pp.57-60.

Zhang, J., Huang, M., Guan, Su., Bi, H.C., Pan, Y., Duan, W., Chan, S.Y., Chen, X., Hong, Y.H., Bian, J.S., Yang, H.Y. and Zhou, S. (2006) A mechanism study of the intestinal absorption of cryptotanshinone, the major active constituent of *Salvia miltiorriza*. Journal of Pharmacology and Experimental Therapeutics. 317(3):1285-1294.

Zhou, S., Feng, X., Kestell., P., Paxton, J.W., Baguley, B.C. and Chan, E. ( 2005) transport of the investigational anti-cancer drug 5,6-dimethylxanthenone-4-acetic acid and its acyl glucuronide by human intestinal Caco-2 cells. European Journal of Pharmaceutical Sciences. 24:513-524.

Zhou, S., Li, Y., Kestell, P. and Paxton, J.W. (2003) Determination of thalidomide in transport buffer for Caco-2 cell monolayer by high-performance liquid chromatography with ultraviolet detection. Journal of Chromatography B. 785:165-173.

# CHAPTER 4:
# *IN VITRO* MATRINE METABOLISM BY HUMAN LIVER MICROSOMES AND POTENTIAL INTERACTION OF ACAPHA® WITH PRESCRIPTION DRUGS

## 4.1 Introduction

Botanical products have been used to maintain human health and treat diseases since the dawn of civilization and are still used as medicines by more than 80% of the world's population today. Although botanical products are often promoted as natural and therefore harmless, many botanical products may cause serious interaction when used concomitantly with a conventional drug (Fugh-Berman, 2000; Heck *et al.*, 2000). This is termed drug/herb interactions.

The general consequences of drug/herb interactions are either an enhancement or a minimization of the drug's pharmacological or toxicological effects. The consequence is particularly serious for drugs with a narrow therapeutic window because an increase in the actions of these drugs may lead to toxicity or lethality. Several recent reviews have examined the metabolic and pharmacokinetic interactions of prescription drugs with herbal agents (Sweeney and Bronilow, 2006; Isso, 2004; Pal and Mitra, 2006; Singh, 2005). These reports have focused on drug interactions with top selling botanicals such as St John's wort, garlic, ginkgo biloba, ginseng and milk thistle that are used to treat conditions ranging from depression to high blood pressure, from diabetes to general improvement of health outcome. Therefore, when St John's wort is combined with oral

contraceptives (ethynylestradiol/desogestrel), loperamide, or selective serotonin-reuptake inhibitors (sertaline, paroxitine, nefazodone), it may cause inter-menstrual bleeding, delirium, or mild serotonin syndrome respectively. Ginkgo may raise blood pressure when combined with a thiazide diuretic and induce coma when combined with trazodone. Garlic may produce hypoglycaemia when taken with chlopropamide. Kava can cause a semicomatose state when given concomitantly with alprazolam (Zhou *et al.*, 2005).

Among the various mechanisms that are responsible for the occurrence of drug/herb interaction, the most common mechanism may be pharmacokinetic interaction *i.e.*, the competition of a drug and an herb for the same active site(s) on the hepatic cytochrome P-450 (CYP) isoenzymes (Zhou *et al.*, 2005).

Xenobiotics and drugs are broken down by the drug metabolizing enzymes, most of which are found in the liver. These enzymes are designated as being either Phase I or Phase II enzymes. Phase I enzymes consist of cytochrome P450 enzymes, previously known as mixed-function oxidase enzymes and are responsible for reactions (mainly oxidation and hydroxylation) that alter the existing functional groups to increase water solubility. The cytochrome (CYP) isoenzymes are a family of haemoproteins that are the terminal oxidases of the mixed function oxidase system found on the membranes of the endoplasmic reticulum. The present system of nomenclature for various CYP isoenzymes employs a three-tiered classification based on the conventions of molecular biology: a numeral and a capital letter designate the amino-acid sequence, with a final number indicating the individual enzyme. In humans there are about 30 CYP enzymes which are responsible for drug metabolism and these belong to families 1-4 (Dostalek *et al.*, 2005; Sweeney and Bromilow, 2006). It has been estimated that about 90% of drug oxidation

can be attributed to six enzymes: CYP 1A2, 2C9, 2C19, 2D6, 2E1 and 3A4. The most

significant CYP isoenzymes in terms of quantity are CYP 3A4 and CYP 2D6. Table 4.1

is a summary of the CYP P450 isoenzymes and their substrates (Sweeney and Bromilow,

2006; Moody, *et al*; 1999):

Table 4.1:    CYP P450 isoenzymes and important drug substrates

| CYP form | Substrate |
| --- | --- |
| CYP1A2 | Caffeine, amitryptyline, clomipramine, clozapine, propanolol, ropivicaine, lignocaine, theophylline, verapamil, phenecetin |
| CYP2C9 | S-warfarin, tamoxifen, losartan, glipzide, fluoxetine, fluvastatin, ibuprofen, diclofenac, phenytoin, tubutamide, losartan, naproxen |
| CYP2C19 | Diazepam, phenytoin, omeprazole, pantoprazol, clomipramine, propranolol, citalopram, indomethacin, progesterone |
| CYP2D6 | Flecanide, haloperidol, thioridazine, paroxitine, imipramine, sparteine, carvedilol, codeine, tramadol, dextromethophan |
| CYP2E1 | Alcohol, euflurane, theophilline, sevoflurane, halothane, isoflurane, ethrane, ropivicaine, chlorzoxazone, paracetamol |
| CYP 3A4 | Midazolam, triazolam, diazepam, bupivicaine, ropivicaine, quinidine, diltiazem, nifedipine, amiodarone, erythromycin |

Phase II reactions involve conjugation reactions occurring primarily in the

endoplasmic reticulum. The process of solubilization of the metabolites is continued by

phase II metabolism. The conjugation of polar compounds occurs *via* a number of

reactions involving sulphotransferases, N-acetyltransferases (NAT-1,2), methyl

transferases, e.g. thiopurine methyl transferase, glutathione transferase and, most

commonly, by glucurononyl-transferases (UDPGT), more commonly know as UGT

(Sweeney and Bromilow, 2006).

In the present study, the metabolism of matrine, a marker chemical of Acapha[®],

was examined. Also, the inhibitory effects of Acapha® extract on drug metabolism enzymes were studied with 5 of the most common CYP isoforms, CYP1A2, CYP3A4, CYP2D6, CYP2C9 and CYP2C19.

## 4.2    Materials and methods

### 4.2.1    Chemicals and biochemicals

Pooled human liver microsome was purchased from BD Gentest™ Products and Services (Woburn, MA, USA). β–NADPH cofactors (β-nicotinamide adenine dinucleotide phosphate), non-radiolabeled caffeine, erythromycin, dextromethorphan, diazepam, naproxen were all purchased from Sigma Chemical Co. (St Louis, MO, USA). $^{14}$C Labeled probe substrates[3-methyl-$^{14}$C]caffeine (specific radioactivity 55 mCi/mmol, conc. 0.1 mCi/ml), [$O$-methyl-$^{14}$C]dextramethorphan (specific radioactivity 55 mCi/mmol, conc. 0.1 mCi/ml) , [$N$-methyl-$^{14}$C]diazepam (specific radioactivity 55 mCi/mmol, conc. 0.1mCi/ml) and [$O$-methyl-$^{14}$C]naproxen(specific radioactivity 55 mCi/mmol, conc. 0.1 mCi/ml) were purchased from American Radiolablled Chemical Inc (St Louis, MO, 63146, USA) [$N$-methyl-$^{14}$C]erythromycin (specific radioactivity 48.8 mCi/mmol) was obtained from Perkin Elmer Life Sciences Inc (Boston, MA 02118, USA). DMSO was purchased from Caledon Laborotories Ltd (Georgetown, ON. Canada). Potassium phosphate dibasic (K$_2$HPO$_4$. 3 H$_2$O) and potassium dihydrogen orthophosphate (KH$_2$PO$_4$) were obtained from BDH Chemicals Ltd., Poole England and BDH Chemicals Ltd., Toronto, respectively.

### 4.2.2    Matrine metabolism

Incubation buffer was prepared by adding 0.1 M KH$_2$PO$_4$ into 0.1M K$_2$HPO$_4$ until

the pH reached 7.4. Matrine and NADPH cofactor solutions were prepared in the above phosphate buffer. A typical reaction mixture contained matrine 1000 ng/ml, NADPH 0.25mM and human microsomes 0.4 mg/ml in a final incubation volume of 1 ml. The solution was incubated for 5 min before the addition of NADPH to inititate the reaction. Incubations were conducted in duplicates for 60 min at 37 °C in a shaking water bath before they were stopped by adding 50 µl trichoroacetic acid (10% w/v) (Kim, et al, 2006; Bu, et al, 2005). The incubations were extracted and analyzed for matrine using GC/MS-SIM.

### 4.2.3 Cytochrome P-450 inhibition by Acapha

#### 4.2.3.1 Preparation of Acapha extracts

Acapha® powders (600 mg) were weighed accurately and dissolved in 10 ml of 70% ethanol. The mixture was extracted for 1 hr by ultrasonication and then centrifuged at 3000 rpm for 5 min. An aliquot of the supernatant (4 ml) was removed and dried under a gentle stream of nitrogen. The residues were reconstitued in 0.5 ml 55% ethanol. This stock solution was diluted 0.5, 0.25, 0.125, 0.063, 0.031, 0.0156 fold with 55% ethanol to prepare a series of Acapha® extract concentrations. These solutions were prepared by adding 100 µl of an Acapha® extract into a 0.6 ml microfuge tube and mixing for 10 seconds on a Fisher Scientific Vortex-Genie. Crude matrine conentrations in these solution series also were quantified using GC/MS-SIM.

#### 4.2.3.2 Radiometric CYP assays

[14C]-dextromethorphan O-demethylation (Rodrigues et al., 1994), [14C]-naproxen O-demethylation (Rodrigues et al., 1996), [14C]-erythromycin N-demethylation

(Riley and Howbrook, 1998), [$^{14}$C]-diazepam $N$-demethylation (Jung *et al.* 1997) and

[$^{14}$C]-caffeine $N$-demethylation (Bloomer *et al.*, 1995) assays were used, respectively as

probe reactions for CYP2D6, CYP2C9, CYP3A4, CYP2C19, and CYP1A2. All

incubations were conducted under the optimized conditions reported in the original

publications. The CYP probe concentrations were at or below the Michaelis-Menten

constant of the reaction and the turnover of the CYP probes was linearly dependent on

the incubation time. A typical incubation mixture consisted of 50 mM potassium

phosphate buffer (pH 7.4), human liver microsomes, NADPH (1.0 mM) and 0.1μCi of

[$^{14}$C]-naproxen (110μM) or [$^{14}$C]-erythromycin (60μM) or [$^{14}$C]-dextromethorphan (5

μM) or [$^{14}$C]-diazepam (20 μM) or [$^{14}$C]-caffeine (250 μM) as appropriate, in a final

volume of 0.? ml. An appropriate amount of cold substrate was mixed with the

radiolabelled chemical in 1% DMSO or ethanol to prepare the CYP probes for the

incubations. Blank incubation was prepared without an NADPH cofactor. Incubation was

conducted in a Dubnoff shaking water bath at 37°C for 20 min. These reactions can be

represented by the equation, $^{14}$C-CYP probe → $O$- or $N$-demethylated probe + [$^{14}$C]-

formaldehyde/[$^{14}$C]formic acid. The reaction was stopped by the addition of 50 μl cold

10% TCA.


### 4.2.3.3    Inhibition of CYP $^{14}$C-probe metabolism by Acapha®

The residues of the dried Acapha® extracts (see 4.2.3.1) were redissolved in

DMSO (final DMSO concentration in the incubation <2%). Inhibition of $^{14}$C-lableled

CYP probe substrate metabolism was examined by adding each serial dilution of the full

strength extract separately into the incubation mixture (see 4.2.3.2). An equal volume of

DMSO was added to the control. The mixture was incubated for 5 min. After the addition

of 20 µl NADPH cofactor (final concentration 1 mM), the mixture was incubated for an additional 20 min at 37 °C in a shaking water bath. The reaction was terminated by adding 50 µl 10% (w/v) trichloroacetic acid, followed by centrifugation for 5 min (Moody, 1999).

### 4.2.3.4 Solid phase extraction

An aliquot (150 µl) of the incubation mixture supernatant was applied to a pre-conditioned solid-phase extraction (SPE) column (Supelclean Envi-Carb®, 3 ml). The SPE column was pre-conditioned twice with 1 ml methanol followed twice by 1 ml of double distilled water. After adding the supernatant, the column was eluted with 1 ml of double distilled water twice and the elutant which contained [$^{14}$C]-formaldehyde/[$^{14}$C] formic acid, was collected into a liquid scintillation vial. The radioactivity in each vial was counted by Multi-Purpose Scintillation Counter (LS 6500, Beckman Coulter, USA) after adding 15 ml liquid scintillation fluid. The radioactivity represented the amount of [$^{14}$C]-formaldehyde/[$^{14}$C] formic acid formed in the radiometric CYP assay (Moody, 1999).

### 4.2.3.5 IC$_{50}$ determination

The quantity of [$^{14}$C]formaldehyde/[$^{14}$C]formic acid formed in each radiometric CYP assay was calculated from the net disintegrations per minutes (DPM) of the final water eluant from the SPE column, *i.e.*, sample DPM minus blank DPM. The $^{14}$C from the incubation without the addition of Acapha® extract was regarded as the 100% CYP isoform activity. Percent of remaining CYP activity was plotted against the logarithm of Acapha$^{@}$ dilution volume. The plot was analyzed by linear regression analysis. The IC$_{50}$

value of Acapha® extract was calculated and had the unit of percent volume (%) (Moody, 1999).

## 4.3    Results

### 4.3.1    Matrine is not metabolized by liver microsomes *in vitro*

When matrine (2µg/ml) was incubated with human liver microsomes in the presence of an NADPH cofactor, the amount of matrine recovered from the sample was about 98.5 % of the incubation without an NADPH cofactor (control). Moreover, the GC/MS profiles of the incubation with and without an NADPH cofactor were found to be very similar (data not shown). Based on the results of these studies, it is concluded that matrine is not metabolized by human liver microsomes *in vitro*.

### 4.3.2. Acapha® inhibition on CYP probe substrates

Five different CYP $^{14}$C-probe substrates were used to investigate the inhibitory effects of Acapha® extract on the CYP isozymes. These were conducted using the serial dilutions of the original, full strength extract of which matrine concentration was determined by GC/MS-SIM to be 2064 µM. Table 4.2 shows the $IC_{50}$ values of the Acapha® extract on the 5 CYP isozymes. Acapha® extract inhibited the CYP isozyme activities to different extent; the $IC_{50}$ ranged from a dilution factor of 0.11 (CYP3A4) to 0.36 (CYP1A2) which correspond to crude matrine concentration range from 2064-6960 µM (Table 4.2).

**Table 4.2:** IC$_{50}$ of Acapha® for the five CYP isoenzymes

| CYP | Substrate | IC$_{50}$ (% of full strength) | Matrine content (µM) |
|---|---|---|---|
| CYP3A4 | Erythromycin | 0.11 | 2064 |
| CYP1A2 | Caffeine | 0.36 | 6960 |
| CYP2C9 | Naproxen | 0.30 | 5760 |
| CYP2C19 | Diazepam | 0.14 | 2640 |
| CYP2D6 | Dextromethorphan | 0.16 | 3120 |

## 4.4   Discussion

### 4.4.1   Matrine metabolism

The present studies show that matrine is not metabolized by human liver microsomes *in vitro*. This result is consistent with the findings of Wang *et al.* (1994) that about 52% of the matrine infused *i.v.* to human volunteers is excreted in the urine as unchanged matrine and no matrine metabolite is identified either in the plasma or the urine. Our human PK study (Section 5.3.2) also shows that cumulative urine excretion of matrine in human volunteers after receiving Acapha® is 60-80% of the administered dose at 42 hrs post-dosing. Although matrine is not metabolized by human liver microsomes, it is rapidly eliminated and not accumulated in humans. These results are consistent with those of the multiple dosing studies in which matrine is not found to be accumulated by humans (Section 6.3.9).

## 4.4.2 CYP isoenzyme inhibitory assays

There are at least 2 approaches to determine the activities of CYP enzymes: (1) they can be evaluated by analysing the CYP proteins using techniques commonly employed in molecular biology. For example, the western blot analysis has been used to compare the effects of chemical treatment on the CYP enzyme levels in the liver microsomes (Jang, 2004). (2) CYP enzyme activity also can be quantified by assaying the drug metabolizing enzyme activities. This approach usually requires GC or HPLC to quantify the unchanged drug or its metabolites. For example, CYP P450 isoenzyme inhibition by *Scutellariae radix* (Kim *et al.* 2002), Kampo medicines (Takahashi *et al.* 2003) and St John's wort (Dostalek *et al.* 2005). Many CYP inhibition studies also have made use of fluorescence-based and radioactivity-based methods to quantify the parent drugs or their metabolites. However, these methods are non-specific and thus have limits in their general applicability (Zlokarnik *et al*, 2005).

In the present study, I have chosen the radioactivity-based method to examine the inhibition of Acapha® extract on CYP isoenzymes. The $^{14}$C-labled probe substrates produce a radioactive metabolite(s) which can be separated from the probe substrate by solid phase extraction and quantified using liquid scintillation counting. The advantages of the radiometric CYP assays are that they are simple, rapid, and sensitive. The disadvantages of the radiometric CYP assays are non-specific, expensive and generation of radioactive waste, which requires subsequent decontamination and disposal (Moody *et al*, 1999; Zlokarnik *et al*, 2005).

### 4.4.3 Drug/Acapha® interaction

In the present study, Acapha® extract inhibition on the metabolism of human CYP450 probe substrates was examined using CYP 1A2, 2C9, 2C19, 2D6 and 3A4. Results of the study show that the $IC_{50}$s of Acapha® for the various CYP isoforms are >2000 μM crude matrine concentration. Considering that matrine plasma levels in human volunteers are usually < 1 μM (see Chapter 5), it is unlikely that Acapha® will interact with conventional drugs (see Table 4.1) because plasma matrine concentration can never reach the interaction threshold of 2000 μM under normal dosing conditions. Results of the present study are consistent with the general guidelines proposed by Obach *et al* (2005): only drugs with an *in vitro* inhibition potency values (Ki or $IC_{50}$) < 1 μM generate concerns regarding the potential of causing drug/drug interactions whereas those greater than 10-30 μM are typically not associated with drug/drug interactions. My results also are in agreement with those of Kim, *et al.* (2002) who has proposed an $IC_{50}$ of 50 μM as the interaction threshold.

## 4.5 References

Bloomer, J.C., Clarke, S.E. and Chenery, R.J. (1995) Determination of P4501A2 activity in human liver microsomes using [3-$^{14}$C-methyl] caffeine. Xenobiotica. 25(9):917-927.

Bu, H.Z., Kang, P., Zhao, P., Pool, W.F., and Wu, E.Y. (2005) A simple sequential incubation method for deconvoluting the complicated sequential metabolism of capravirine in humans. Drug Metabolism and Disposition. 33(10):1438-1445.

Dostalek, M., Pistovcakova, J., Jurica, J., Tomandl, J., Linhart, J., Sulcova, A. and Hadasova, E. (2005) Effect of St John's wort on cytochrome P-450 activity in perfused rat liver. Life Sciences. 78:239-244.

Fugh-Berman, A. (2000) Herb-drug interactions. Lancet. 355 (9198):134-138.

Heck, A.M., DeWitt, B.A. and Lukes, A.L. (2000) Potential interactions between alternative therapies and warfarin. American Journal of Health-System Pharmacy. 57(13):1221-1227; quiz 1228-1230.

Izzo, A.A. (2004) Herb-drug interactions: an overview of the clinical evidence, Fundamental & Clinical Pharmacology. 19:1-16.

Jang, E.H., Park, Y.C. and Chung, W.G. (2004) Effects of dietary supplements on induction and inhibition of cytochrome P450s protein expression in rats. Food and Chemical Toxicology. 42:1749-1756.

Jung, F., Richardson, T.H., Raucy, J.L. and Johnson, E.F. (1997) Diazepam metabolism by cDNA-expressed human 2C P450s: identification of P4502C18 and P4502C19 as low K(M) diazepam N-demethylases. Drug Metabolism and Disposition. 25(2):133-139.

Kim, H, Kang, S., Kim, H. , Yoon, Y.J., Cha, E.Y.,Lee, H.S., Kim, J.H., Yea, S.S., Lee, S.S., Shin, J.G. and Liu, K.H. (2006) In vitro metabolism of a new cardioprotective agent, KR-32570, in human liver microsomes. Rapid Communications in Mass Spectrometry. 20(5):837-843.

Kim, J.Y., Lee, S.Y. and Kim, D.H.(2002) Effects of flavonoids isolated from Scutellariae radix on cytochrome P-450 activities in human liver microsomes. Journal of Toxicology and Environmental Health, Part A. 65:373-381.

Riley, R.J. and Howbrook, D. (1997) In vitro analysis of the activity of the major human hepatic CYP enzyme (CYP3A4) using [N-methyl-$^{14}$C]-erythromycin. Journal of Pharmacological and Toxicological Methods. 38(4):189-193.

Moody, G.C., Griffin, S.J., Matter, A.N., Mcginnity, D.F. and Riley, R.J. (1999) Fully automated analysis of activities catalysed by the major human liver cytochrome P450 (CYP) enzymes: assessment of human CYP inhibition potential. Xenobiotica. 29(1):53-75.

Obach, R.S., Walsky,R.L., Venkatakrishnan, H., Houstan, J.B. and Tremaine, L.M. (2005) *In vitro* cytochrome P450 inhibition data and the prediction of drug-drug interactions: Qualitative relationships, quantitative predictions, and the rank-order approach. Clinical Pharmacology and Therapeutics. 78:582-592.

Pal, D. and Mitra, A.K. (2006) MDR- and CYP3A4-mediated drug-herbal interactions. Life Sciences. 78:2131-2145.

Rodrigues, A.D., Kukulka, M.J., Roberts, E.M., Ouellet, D. and Rodgers, T.R. (1996) [O-methyl $^{14}$C]naproxen O-demethylase activity in human liver microsomes: evidence for the involvement of cytochrome P4501A2 and P4502C9/10. Drug Metabolism and Disposition. 24 (1):126-136.

Rodrigues, A.D., Kukulka, M.J., Surber, B.W., Thomas, S.B., Uchic, J.T., Rotert, G.A., Michel, G.,Thome-Kromer, B. and Machinist, J.M. (1994) Measurement of liver microsomal cytochrome P450 (CYP2D6) activity using [O-methyl-$^{14}$C] dextromethorphan. Analytical Biochemistry. 219 (2):309-320.

Singh, Y.N. (2005) Potential for interaction of kava and St. John's wort with drugs. Journal of Ethnopharmacology. 100:108-113.

Sweeney, B.P. and Bromilow, J. (2006) Liver enzyme induction and inhibition: implications for anaesthesia. Anaesthesia. 61:159-177.

Takahashi, K., Uejima, E., Morisaki, T., Takahashi, K, Kurukava, N. and Azuma, J. (2003) *In vitro* inhibitory effects of Kampo medicines on metabolic reactions catalyzed by human liver microsomes. Journal of Clinical Pharmacy and Therapeutics. 28:319-327.

Wang, P.Q., Lu, G.H., Zhou, X.B., Shen, J.F., Chen, S.X., Mei, S.W. and Chen, M.F. (1994) Pharmacokinetics of matrine in healthy volunteers. Acta Pharmaceutica Sinica. 29 (5):326-329.

Zhou, S., Huang, M., Xu, A, Yang, H., Duan, W., and Paxten, J.W. (2005) Prediction of herb-drug metabolic interactions: a simulation study. Phytotherapy Research. 19:464-471.

Zlocarnik, G., Grootenhuis, P.D.J. and Waston, J.B. (2005) High throughput P450 inhibition screens in early drug discovery. Drug Discovery Today. 10(21):1443-1450.

# CHAPTER 5:
# PLASMA MATRINE PK IN HUMANS
# AFTER RECEIVING ACAPHA®:
# CLASSICAL PK MODELLING

## 5.1 Introduction

Pharmacokinetic processes can be defined as absorption, distribution, metabolism and excretion, giving rise to the often used acronym – ADME. The ADME processes describe the movement of a drug into, within and out of the animal or human body. These processes together with the pharmacological effects and dosage forms of the drug, and the patient's conditions determine the optimal dose and dosing interval of the drug.

During the last several decades, pharmacokinetics (PK) has evolved from its simple origins into a complex discipline with many subdisciplines and applications. Pharmacokinetic modelling has contributed greatly by translating the obvious measures of administered dose to estimate the more relevant measures of tissue dose such as blood or tissue concentration-time profile and urinary excretion. Pharmacokinetic models generally can be grouped into two classes: compartmental and physiological. The compartmental (or classical) model of matrine is described in this chapter. The physiological model will be discussed in the next chapter.

A classical model attempts to relate the blood or tissue concentration of the parent (or metabolite) to the administered dose of the parent chemical by using a set of mathematical equations. Therefore, a typical model might consist of one to three compartments. In a single compartment model, the whole body is treated as a single

79

compartment in which the concentration of the drug is uniform. In a two or three compartment model, a central compartment (blood) is in equilibrium with one or two perpherial compartments whose concentration can be related to the central compartment by rate constants in each direction. In the multicompartment model, the time course of drug concentration in the central compartment is typically curvilinear with a terminal linear portion. The drug concentration-time curve is resolved mathematically into decaying exponential terms to account for curvature of the data. The number of exponential terms corresponds to the number of compartments in the model, each representing an exchange between a peripheral tissue/organ with the central compartment. Obviously, compartmentalization by such rigid curve stripping process is a rather abstract mathematical construct and lacks physiological relevance. Because of a lack of biological constraints with classical models, empirical data can be fitted by freely varying the model parameters. The best estimates of parameter values can then be statistically compared across experimental conditions, treatments, or chemicals to establish if apparent differences are significant. Therefore, although classical models can be used for interpolation, they have only limited extrapolation capability (Leung, 1991; Himmelstein and Lutz, 1979).

Although the clinical evidence of Acapha[®] for esophageal cancer treatment is compelling, practically nothing is known of the PK of Acapha[®]. However, several laboratories have studied the PK of matrine (the chemical marker of Acapha[®]) in rat, rabbit and human (Wu *et al.*, 2003; Luo and Xia, 1991; Zhu *et al.*, 1992; Wang and Huang, 1992; Wang *et al.*, 1994). Wu *et al.*, (2003) reported that total body clearance, elimination half-life and volume of distribution were not changed significantly in the

plasma of rat after a bolus injection of 4 mg/kg or 40 mg/kg matrine *i.v.* However, the AUC of matrine increased proportionally from 4 to 40 mg/kg. These results suggest that matrine PK involves mainly the first-order processes. Wu *et al.*, (2003) also reported that the fraction of dose absorbed was about 0.44 in rat receiving a single oral dose of 40 mg/kg pure matrine. Luo and Xia, (1991), Wang and Huang (1992) and Zhu *et al*, (1992) reported the PK of matrine in the plasma of rabbit after injecting *i.v.* 40 mg/kg of pure matrine as a bolus. The matrine blood concentration profile of the rabbit can be described by a two-compartment open classical PK model. In another study, matrine kinetics were also shown to be a first-order process when rabbit was given an *i.v.* injection of matrine between 10-30 mg/kg. But linear kinetics were replaced by nonlinear kinetics when the administered dose was increased to 60 mg/kg (Zhu *et al*, 1992). Hitherto, there is only one matrine PK study reported in humans (Wang *et al.*, 1994). Serum matrine concentration profiles in humans after infusing 6 mg/kg matrine *i.v.* can be described by a 2-compartment, open classical PK model. The elimination half-life ($t_{1/2}$) and the renal clearance of matrine are $184 \pm 54$ min and 144 ml/min, respectively. About 52% of the administered dose is excreted unchanged in the urine within 32 hours.

The purposes of the present investigation were to study the kinetics of crude matrine in former smokers after receiving a single oral dose of Acapha® and to fit the plasma concentration data to a clearance-volume PK model.

## 5.2 Materials and methods

### 5.2.1 Reagents and chemicals

Chemicals were purchased from the following sources: matrine from the National

Institute for the Control of Pharmaceutical and Biological Products (Beijing, China); toluene and hydrochloric acid from Anachemia Co., (Montreal, PQ, Canada); petroleum ether and sodium sulfate from BDH (Toronto, ON, Canada); sodium hydroxide solution (1 M) from VWR (West Chester, PA, USA); butanol from Caledon (Georgetown, ON, Canada); Sodium deuteroxide (40% in water), deuterium oxide and deuterated chloroform from CDN Isotope (Pointe-Claire, PQ, Canada); deuterated ethyl alcohol and absolute tetrahydrofuran from Aldrich (Milkwankee, WI, USA); human plasma from the blood bank of the Royal Columbian Hospital (New Westminster, BC, Canada).

### 5.2.2 Study design

(a) The single oral dose PK study was conducted at the BC Cancer Agency under Good Clinical Practice. Fifteen former smokers between the ages of 45-74 years previously diagnosed with bronchial dysplasia, were recruited for the study. The subjects were randomly divided into two groups of 6 and 9 volunteers. The group with 6 volunteers was given a single oral dose of 1.2 g (0.02 g/kg) Acapha® tablets. The group with 9 volunteers was given a single oral dose of 2.4 g (0.04 g/kg) Acapha® tablets. Blood samples were collected before dosing and at 0.5, 1, 2, 3, 4, 5, 6, 8, 10, 24, and 48 hr post-dosing. Urine samples also were collected and the volumes recorded in the following time intervals: 0-4, 4-8, 8-12, 12-24, 24-36, and 36-48 hrs post-dosing.

(b) The multiple oral doses study was conducted with each volunteer received a daily oral dose of 4.8 g (0.08 g/kg) Acapha® (2.4 g *b.i.d* or 0.04 g/kg *b.i.d.*) for 6 months. Blood and urine samples were collected during their scheduled biweekly visits to the B.C. Cancer Agency. The exact post-dosing time of urine collection was unknown although attempts were made to collect the samples at 2 hr post-dosing in the morning. Blood

samples were immediately separated at 4 °C by centrifugation and stored at -20 °C until analysed. The study protocol was approved by both the Research Ethics Board of Simon Fraser University and the Clinical Research Ethics Board of the University of British Columbia. Written informed consent was obtained for each subject prior to their participation in the study.

### 5.2.3 Measurement of matrine concentration

#### 5.2.3.1 Extraction and measurement of plasma matrine

Plasma extraction and measurement of matrine were conducted according to the method developed in our laboratory (Sit *et al.*, 2004). Briefly, 50 μl of deuterated matrine solution was taken from a stock solution (5 μg/ml) and put into a screw capped glass centrifuged tube containing 0.5 ml NaOH (1 M) and 1 ml plasma sample. After adding 3 ml of toluene: butanol (v/v 7:3), the centrifuge tube was capped and shaken horizontally on a mechanical shaker for 15 min. The centrifuge tube was centrifuged at 3000 rpm to separate the layers. The organic layer was removed and put into a new 10 ml, screw capped tube containing 0.5 ml HCl (0.25 M). The centrifuge tube was shaken again and then centrifuged to separate the layers. The organic layer was discarded. The remaining aqueous layer was made alkaline with the addition of 0.5 ml NaOH (1 M). After the addition of 200 μl toluene:butanol (v/v 9:1), the mixture was shaken again on the mechanical shaker. The organic layer was separated by centrifugation and transferred to a vial for GC/MS analysis.

A Hewlett-Packard 5890 series II gas chromatograph coupled to a 5971 mass spectrometric detector was used to analyse matrine in the plasma extracts.

Chromatographic separation was performed using a 5% diphenyl-95% dimethylpolysiloxane capillary column (30 m X 0.25 mm X 0.25μm, HP-5 MS). Helium was used as the carrier gas under a head pressure of 50 psi. The injector and transfer line temperatures were set at 250 °C and 280 °C, respectively. The initial oven temperature was set at 110 °C, maintained for 1 min and then increased to 220 °C at a rate of 30 °C /min and maintained for 1 min. The temperature was further increased to 300 °C at a rate of 15 °C/min and maintained for 3 min. Ionization was performed under electronic impact ionization with 70 eV. Matrine and deuterated matrine were analyzed in the selective ion monitoring (SIM) mode. The ions *m/z* 248 and m/z 250 were selected to monitor matrine and deuterated matrine, respectively due to their abundance and specificity. The ion *m/z* 249 also was recorded but was not used in matrine quantification. The intra-day and inter-day precision ranged from 0.4-4.0% and 1.0-3.5%, respectively. The intra-day accuracy was between -7.3 -4.5%. The lower limit of quantition was 13-23 ng/ml and no intereference of endogenous plasma chemicals was found. A linear response was obtained over the range of 10-500 ng/ml matrine standard solutions (Sit *et al.*, 2004). Urine samples were extracted and analysed by the same protocol as the plasma.

### 5.2.3.2   LOQ of GC/MS-SIM

LOQ, defined as the limit of quantitation, is the concentration which produces a signal in the analytical instrument that is 10-fold of the error on the regression line of the calibration curve. The GC/MS-SIM analysis required matrine-d2 as the internal standard. Since matrine-d2 was not available commercially, it was synthesized chemically in our laboratory according to the procedure of Sit *et al*, (2004). The percentage of deuterated matrine in the final product varied from batch to batch. As a result, the LOQ of the

GC/MS-SIM method might vary from 13 - 23 ng/ml.

## 5.2.4  Pharmacokinetic analyses

The plasma concentration-time profiles were analysed by a clearance-volume two-compartment model to obtain estimates of absorption rate constants (KA1, KA2), total body clearance (CL), intercompartmental clearance (CLd),  and the apparent volumes of distribution (VT, VC). WinNonlin (Scientific Consulting, Inc, USA) was used to fit the model. The apparent steady-state volume of distribution (Vdss) was estimated using the equation Vdss = VT +VC. The Vdss relates the amount of chemical in the body to the concentration of matrine in the plasma when an equibrium exists between the peripheral tissues and the plasma (i.e., steady-state conditions). The CL represents the sum of urinary, fecal, and metabolic elimination pathways from humans and can be interpreted as the volume (L) of plasma that is completely cleared of matrine per unit of time.

The plasma matrine PK profiles showed multiple peaks in human after receiving a single oral dose of Acapha®. Multiple peaks in the plasma concentration-time curve could be caused by a reduction in gastric motility, absorption of matrine from several sites, enterohepatic recycling of matrine, etc. Therefore, a 2-compartment clearance-volume PK model which incorporates specific parameters describing two different absorption sites was used to fit the matrine concentration-time curve. This clearance-volume PK model was largely based on a model reported by Gabrielsson and Weiner (2000). A diagrammatic representation of the model is shown in Fig.5.1. The model consists of a central and a peripheral compartment. Input 1 and Input 2 represent, respectively the two first-order absorption processes with lag time (TLAG1 and TLAG2).

**Figure 5.1:    Conceptual model used to describe the plasma PK of matrine in human**
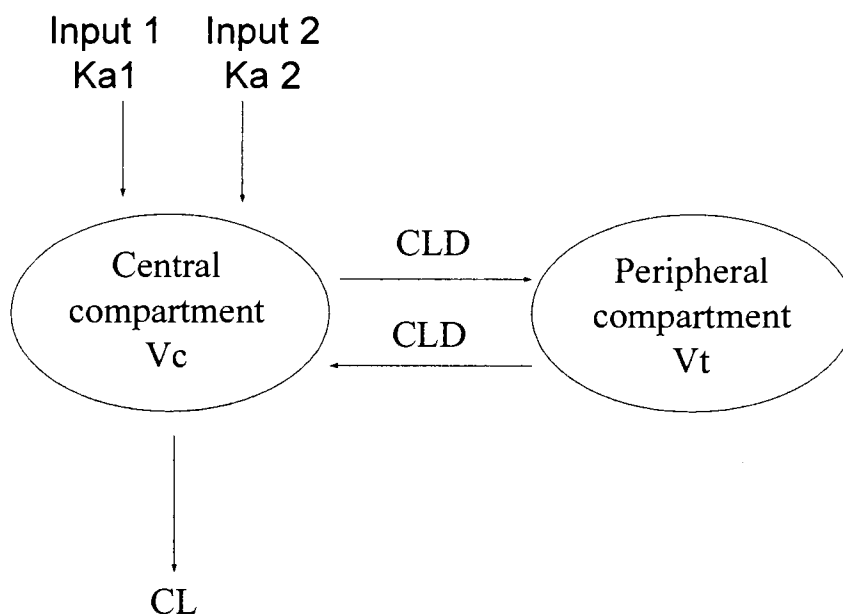


Central compartment:

$$Vc* (dC/dt) = Input\ 1 + Input\ 2 - CL*C - CLD*C + CLD*\ Ct$$

$$Input\ 1 = Dose*(FRCT1)*KA1*\ e^{-KA1\ (T-Tlag1)}$$

$$Input\ 2 = Dose*(FRCT2)*\ KA2\ *\ e^{-KA2\ (T-Tlag2)}$$

Peripheral compartment:

$$Vt* (dCt/dt) = CLD*C-CLD*\ Ct$$

KA1 and KA2 are the absorption rate constants from the gastrointestinal tract. FRCT 1 and FRCT 2 represent, respectively the fractions of absorption by Input 1 and Input 2 from the gastrointestinal tract. CL, Vc, CLD, and Vt, respectively represent the clearance, distribution volume of central compartment, inter-compartmental diffusion and

the distribution volume of the peripheral compartment.

## 5.3 Results

### 5.3.1 Time couse of plasma matrine concentration in human after a single oral dose

Individual plasma concentration-time curves were characterized by several "fluctuations" or "bumps" (data not shown). However, when the individual plasma concentration-time curves were averaged, a smooth plasma concentration-time curve was observed. Figure 5.2 and Figure 5.3, respectively show the time course of mean plasma matrine concentrations in human volunteers after a single oral dose of 2.4 g (0.04 g/kg) and 1.2 g (0.02 g/kg) of Acapha. Crude matrine was detected in the plasma at 0.5 hr post-dosing (the earliest time point of blood sampling), indicating that Acapha® is rapidly absorbed into the systemic circulation of humans. This confirms the results of the Caco-2 cell transport study (Figure 3.6 I-VI) in which crude matrine passes through the Caco-2 cell monolayers rapidly. Figures 5.2 and 5.3 also show that crude matrine concentrations in the plasma increased rapidly with time and peaked at about 3 hr post-dosing. Thereafter, plasma matrine concentration decreased gradually and reached background level at about 48 hr post-dosing. The Cmax of the 2.4 g (0.04 g/kg) and the 1.2 g (0.02 g/kg) dose groups were 65 ng/ml and 30 ng/ml, respectively. The 2.4 g (0.04 g/kg) dose group also differed to the 1.2 g (0.02 g/kg) dose group in a visible second peak appearing at day 1 post-dosing (Figures 5.2 and 5.3). The presence

**Figure 5.2:** Time course of mean matrine plasma concentration for human subjects after receiving a single oral dose of 2.4 g (0.04 g/kg) Acapha®. Note: 2.4 g Acapha® tablets contain 9.6 mg crude matrine.
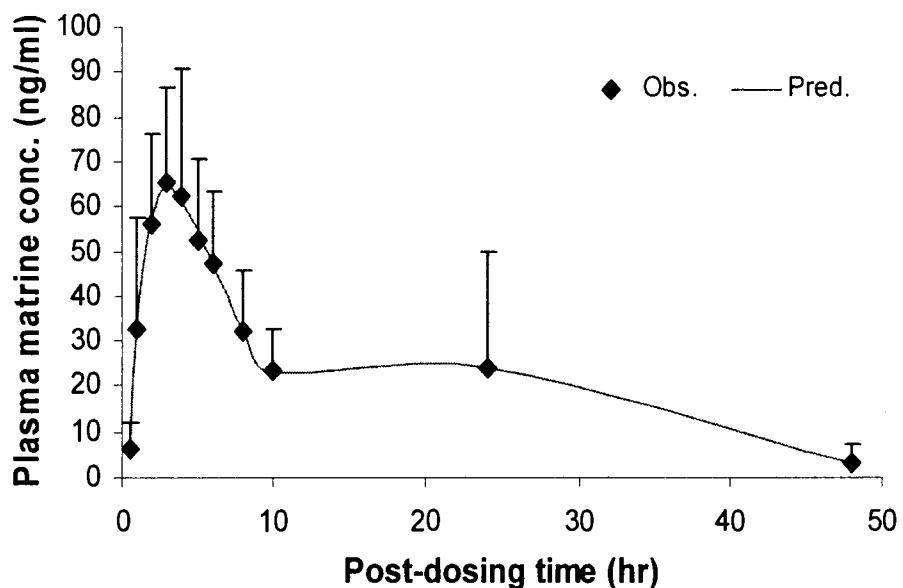


**Figure 5.3:** Time course of mean matrine plasma concentration for human subjects after receiving a single oral dose of 1.2 g (0.02 g/kg) Acapha®. Note: 1.2 g Acapha® tablets contain 4.8 mg crude matrine.
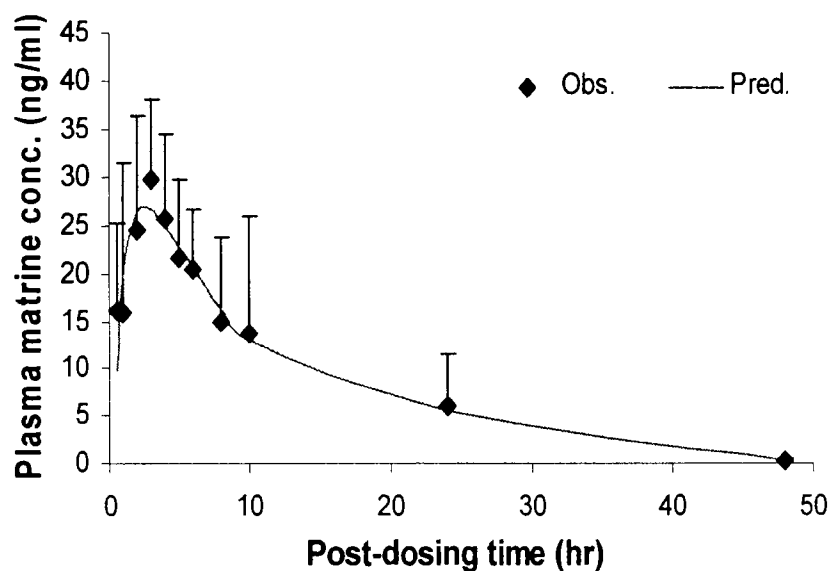
of a second peak in the plasma concentration-time curve is characteristic of enterohepatic recycling and/or protracted absorption of Acapha® (Gabrielsson and Weiner, 2000).

The mean kinetic data of the 1.2 g and 2.4 g dose groups were fitted separately by a 2-compartment volume-clearance model using WinNonlin®. Table 5.1 shows the model derived PK parameters. Since KA1 ranged from 0.31-0.33 1/hr, matrine was absorbed rapidly by the first absorption site. The fraction of dose absorbed was about 30-40% which was much higher than the fraction of dose absorbed by the second absorption site (5-8%). The rate of matrine absorption at the second absorption site was much higher in the 2.4 g (0.04 g/kg) dose group than the 1.2 g (0.02 g/kg) dose group; therefore, only the 2.4 g (0.04g/kg) dose group showed a clear second absorption peak in the plasma concentration-time profile. The KA1 and CL/F of the two dose groups were very similar, suggesting the absorption and elimination processes of matrine mainly involved the first-order kinetic processes. The VC/F and VT/F are 6.83 L and 15.04 L, respectively for the 2.4 g (0.04 g/kg) group; 5.14 L and 7.41 L, respectively for the 1.2 g (0.02 g/kg) dose group (Table 5.1). Since the plasma volume and interstitial space of humans are about 5 and 9 liters, respectively (Tsuji, et al., 1985), the modelled derived VC/F and VT/F are similar to their physiological values. The total distribution volumes (VC/F + VT/F) of the 2.4 g (0.04 g/kg) Acapha® group and 1.2 g (0.02 g/kg) Acapha® group are 21.8 L and 12.6 L, respectively which are much larger than the total blood volume of an adult human (about 5 L). Matrine most likley distributes into the various organs and tissues of humans.

**Table 5.1:** Model-derived PK parameters for human after receiving a single oral dose of Acapha®

| Parameter | Dose, 2.4g (0.04 g/kg) Acapha® | Dose, 1.2 g (0.02 g/kg) Acapha® |
|---|---|---|
| KA1(hr⁻¹) | 0.33 | 0.31 |
| KA2 (hr⁻¹) | 0.41 | 0.28 |
| VC/F (L) | 6.83 | 5.14 |
| VT/F (L) | 15.04 | 7.41 |
| CL/F (L/hr) | 2.00 | 2.20 |
| CLD/F (L/hr) | 1.20 | 2.90 |
| FRCT1 | 0.31 | 0.29 |
| FRCT2 | 0.08 | 0.05 |
| TLAG1 (hr) | 0.40 | 0.20 |
| TLAG2 (hr) | 22.00 | 18.00 |

*KA1 and KA2 are the absorption rate constants from the gastrointestinal tract. FRCT 1 and FRCT 2 represent, respectively the fractions of absorption by the first and second absorption sites of the gastrointestinal tract with lagtime TLAG1 and TLAG2. CL, Vc, CLD, and Vt, respectively correspond to the clearance, distribution volume of central compartment, inter-compartmental diffusion and the distribution volume of the peripheral compartment.

The individual volunteer dataset also was fitted separately using the volume-clearance PK model (Gabrielsson and Weiner, 2000). Tables 5.2 and 5.3 summarize the model-derived PK parameters and their variance. For most parameters, the standard deviation (SD) is very close to the average (mean) and the CVs are > 30%. The VT/F and the TLAG2 in the 2.4 g (0.04 g/kg) dose group show large variance among the subjects.

The plasma concentration-time data was fitted using uniform weighing. Therefore, the WSSR (weighed sum of the squared residual) has the same value as the SSR (sum of the squared residual). The results show good correlation between the predicted and determined concentration for most subjects in the two dose groups

(CORR_(OBS,PRED) > 0.94). The final AIC and SC for all subjects are very similar.

Details of statistic results are summarized in **Appendix II**.

Table 5.2: PK parameters for individual volunteer receiving a single oral dose of 2.4 g (0.04 g/kg) Acapha®

| Parameter | G1(1) | G1(2) | G1(3) | G1(4) | G1(5) | G1(6) | G1(7) | G1(8) | G1(9) | Mean | SD | CV% |
|---|---|---|---|---|---|---|---|---|---|---|---|---|
| KA1(hr⁻¹) | 0.52 | 0.13 | 0.27 | 0.28 | 0.52 | 0.41 | 0.36 | 0.86 | 0.47 | 0.42 | 0.21 | 49.37 |
| KA2 (hr⁻¹) | 0.23 | 1.00 | 0.72 | 0.21 | 0.91 | 0.43 | 0.54 | 1.00 | 0.49 | 0.62 | 0.31 | 50.21 |
| VC/F (L) | 2.37 | 0.52 | 0.65 | 2.63 | 11.91 | 3.74 | 0.59 | 5.79 | 0.50 | 3.19 | 3.74 | 117.19 |
| VT/F (L) | 103.00 | 6.23 | 27.09 | 37.40 | 143.90 | 8.14 | 7.10 | 23.30 | 5.01 | 40.13 | 49.60 | 123.59 |
| CL/F(L/hr) | 0.11 | 1.39 | 0.88 | 2.17 | 0.36 | 1.31 | 1.14 | 1.16 | 0.69 | 1.02 | 0.61 | 59.59 |
| CLD/F (L/hr) | 1.12 | 0.17 | 4.62 | 0.77 | 4.92 | 2.36 | 5.75 | 1.53 | 1.14 | 2.49 | 2.06 | 82.96 |
| FRCT1 | 0.14 | 0.13 | 0.25 | 0.17 | 0.26 | 0.25 | 0.28 | 0.21 | 0.11 | 0.20 | 0.06 | 32.25 |
| FRCT2 | 0.15 | 0.05 | 0.03 | 0.08 | 0.02 | 0.19 | 0.14 | 0.03 | 0.09 | 0.08 | 0.06 | 72.50 |
| TLAG1 (hr) | 0.74 | 0.46 | 0.46 | 0.40 | 0.85 | 0.44 | 0.50 | 1.63 | 0.20 | 0.63 | 0.42 | 66.17 |
| TLAG2 (hr) | 22.00 | 4.50 | 2.50 | 3.50 | 5.50 | 22.00 | 9.00 | 4.50 | 9.00 | 9.17 | 7.61 | 82.99 |

**Table 5.3:** PK parameters for individual volunteer receiving a single oral dose of 1.2 g (0.02 g/kg) Acapha®

| Parameter | G2(1) | G2(2) | G2(3) | G2(4) | G2(5) | G2(6) | Mean | SD | CV% |
|---|---|---|---|---|---|---|---|---|---|
| KA1(hr$^{-1}$) | 1.42 | 0.35 | 0.30 | 0.59 | 0.30 | 0.52 | 0.58 | 0.43 | 73.45 |
| KA2 (hr$^{-1}$) | 0.20 | 0.49 | 0.30 | 0.30 | 0.20 | 0.36 | 0.31 | 0.11 | 35.44 |
| VC/F (L) | 18.64 | 4.11 | 5.62 | 0.52 | 0.51 | 0.50 | 4.98 | 7.04 | 141.24 |
| VT/F (L) | 5.00 | 43.98 | 5.60 | 14.80 | 14.52 | 7.51 | 15.24 | 14.73 | 96.66 |
| CL/F(L/hr) | 3.46 | 1.69 | 0.96 | 1.31 | 3.44 | 1.84 | 2.12 | 1.08 | 50.90 |
| CLD/F (L/hr) | 8.22 | 0.28 | 5.63 | 6.60 | 1.97 | 5.41 | 4.69 | 2.98 | 63.58 |
| FRCT1 | 0.34 | 0.24 | 0.23 | 0.23 | 0.22 | 0.27 | 0.25 | 0.05 | 18.03 |
| FRCT2 | 0.01 | 0.01 | 0.01 | 0.09 | 0.01 | 0.03 | 0.02 | 0.03 | 129.98 |
| TLAG1 (hr) | 0.79 | 0.59 | 1.77 | 0.46 | 2.89 | 0.22 | 1.12 | 1.02 | 91.03 |
| TLAG2 (hr) | 18.00 | 18.00 | 18.00 | 18.00 | 18.00 | 18.00 | 18.00 | 0.00 | 0.00 |

### 5.3.2 Cumulative urine excretion of matrine in human after a single oral dose

Figures 5.4 and 5.5, respectively show the time course of matrine concentrations in the urine of 1.2 g (0.02 g/kg) and 2.4 g (0.04 g/kg) dose groups. Cumulative urine excretion of matrine were about 76% and 62% of the administered dose in 42 hr, respectively for the 1.2 g (0.02 g/kg) and 2.4 g (0.04 g/kg) dose groups (Table 5.4).

**Table 5.4:**    Cumulative urine excretion of matrine as percent of administered dose (%)

| Time (hr) | 2.4 g (0.04 g/kg) Acapha[®] | 1.2 g (0.02 g/kg)Acapha[®] |
|-----------|------------------------------|-----------------------------|
| 2 | 6.8 | 10.8 |
| 6 | 23.4 | 27.1 |
| 10 | 37.9 | 38.8 |
| 18 | 52.1 | 59.4 |
| 30 | 59.3 | 64.3 |
| 42 | 62.7 | 76.4 |

**Figure 5.4:** Cumulative urine excretion of matrine in human after receiving a single oral dose of 1.2 g (0.02 g/kg) Acapha®
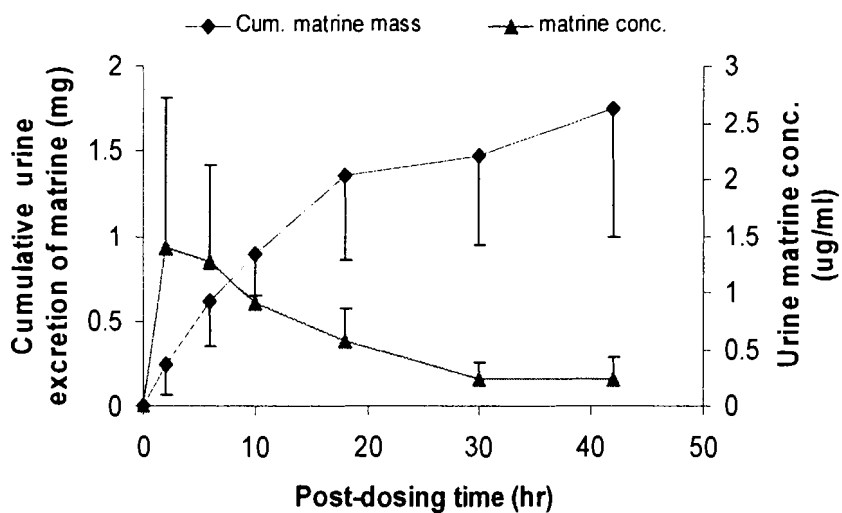


**Figure 5.5:** Cumulative urine excretion of matrine in human after receiving a single oral dose of 2.4 g (0.04 g/kg) Acapha®
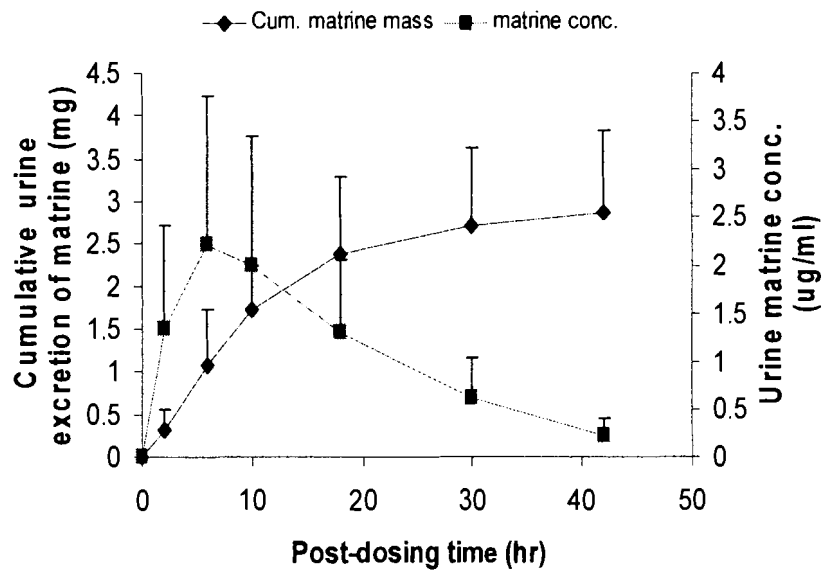
## 5.4 Discussion

The reasons that an herbal product is unable to be developed into a chemopreventive agent include absorption problems by the gastrointestinal tract, rapid metabolism and elimination, and/or unfavourable distribution properties, etc. These ultimately may be manifested clinically as a lack of efficacy (Prentis *et al.*, 1988). Therefore, it is important to perform a PK study on a potential chemopreventive agent at an early stage of its development; a PK study in the preclinical program can be used to support drug discovery, supply the kinetic information for pharmacological and toxicological study, and extrapolate the result from animal to man *via* physiological modeling. On the other hand, a PK study during clinical trials may be used to support the dose-finding and dose escalation studies.

A comparison of the matrine concentration-time profiles of human volunteers shows a large variation in the number of peaks, lagtime and Cmax. A large variation in the model-derived PK parameters is expected because of inter-individual difference and the interaction between crude matrine and other chemicals in Acapha[®]. Interestingly, when the different datasets in a specific dose group were averaged, the mean plasma matrine concentration *vs.* time curves showed fewer "bumps". Furthermore, the plasma concentration-time curves can be fitted using a 2-compartment clearance –volume model (Figures 5.2 and 5.3).

The presence of multiple peaks and shoulders in the plasma matrine concentration-time curve may be the result of several complex processes: absorption from multiple sites in the GI tract at different rates, enterohepatic recycling, gastric emptying, storage and subsequent release of drug from a postabsorptive depot site. These

have been observed in the plasma concentration–time profiles of drugs such as talinolol, ranitidine, cimitidine, furosemide and acebutolol (Tubic, et al, 2006). As suggested by Gabrielsson and Weiner (2000), the most probable reasons for the phenomenon of multiple peaks are enterohepatic recycling and multiple absorption routes. It is unlikely that matrine undergoes enterohepatic recycling since a second peak is not present in the plasma concentration-time curve after *i.v.* infusion (Wang *et al.*, 1994). Also, the majority of the chemicals that undergo enterohepatic recycling are polar molecules with molecular masses in excess of 500 kDa. Because matrine is a small molecule, it would not be a likely candidate for enterohepatic recycling. Therefore, the most likely explanation for the second peak is the multiple absorption sites. Probably, the dissoluion and release of crude matrine from an herbal product such as Acapha® is not a rapid and complete process. As a result, absorption of matrine occurs at different sites throughout the gastrointestinal tract just like a controlled-release formulation (Tubic, et al, 2006).

As shown in Figures 5.2 and 5.3, the mean plasma matrine concentration-time profiles can be fitted by the 2-compartment, clearance-volume model. The 2 peaks observed in the plasma matrine concentration-time curve are well described by the incorporation of 2 absorption phases, in which a portion of the dose was released and absorbed, each with a separate lag time and absorption rate constant. An attempt also has been made to use a zero-order absorption process to represent the first absorption phase of the model but the model takes a long time to run and appears less able to fit the plasma kinetic data well. A zero-order absorption phase also is at odds with the assumptions used in the PBPK model (see Chapter 6), which utilizes 2 linear, first order processes to model the absorption sites.

The matrine concentration-time curve from individual volunteer also was fitted to the 2-compartment volume-clearance model. The "best-fit" PK parameters of the volunteers show large inter-individual variations; many PK parameters have CV% (SD*100/ Mean) greater than 50%. Variance of the model fitted PK parameters is usually less than 40% CV (Hirt, et al, 2006; Garcia, et al, 2006). The high variance between different subjects in this study may be related to the matrix of Acapha®. Other chemicals in Acapha® and plant matrices also make the PK processes very complicated in human.

The sum of central compartment volume and peripheral compartment volume yields a Vdss which is about 3 fold greater than the volume of blood in human. This result indicates that matrine is distributed to many tissues (organs), a conclusion which is consistent with the results of the rat tissue distribution study (Chapter 6). Results of this study also confirms that matrine is eliminated unchanged *via* the urine; urinary excretion at 30 hr post-dosing was found to be about 59 - 64% of the administered dose (Table 5.4) which are in good agreement with the 53% cumulative matrine urine excretion at 32 hr post-dosing reported by Wang *et al.*, (1994).

Several plasma samples in the 1.2 g dose group are very close to the LOQ of the GC/MS-SIM method. At present, there is no concensus among pharmacokinetists on the best way to deal with data which are at or below LOQ. The simplest solution is to discard the data. Alternatively, they can be replaced with a zero or LOQ/2 (Beal, 2001). If the plasma samples close to LOQ were discarded, there would not be enough data available to conduct data fitting. Also, there is the possibility of overestimating matrine plasma concentration if we just keep the higher concentration samples. Therefore, all the results from the low dose group were kept and used in modeling.

In summary, the 2-compartment clearance-volume model with two absorption phases adequately describes the PK of matrine in humans after receiving Acapha® as a single oral dose. The relatively large variance of the model-derived parameters probably is related to the matrix effects of Acapha® on its own absorption and/or inter-subject differences.

## 5.5    References

Beal, S.L. (2001) Ways to fit a PK model with some data below the quantification limit. Journal of Pharmacokinetics and Pharmacodynamics. 28(5):481-504.

Gabrielsson, J. and Weiner, D. (2000) Pharmacokinetic and Pharmacodynamic Data Analysis: Concepts and Applications. 3$^{rd}$ edition. Swedish Pharmaceutical Press, Stockholm, Sweden, pp 654.

Garcia, B., Barcia, E., Perez, F. and Molina, I.T. (2006) Population pharmacokinetics of gentamicin in premature newborns. Journal of Antimicrobial Chemotherapy. 58:372-379.

Himmelstein, K.J. and Lutz, R.J. (1979) A review of the applications of physiologically based pharmacokinetic modeling. Journal of Pharmacokinetics and Biopharmaceutics. 7(2):127-145.

Hirt, D., Treluyer, J.M., Jullien, V., Firtion, G., Chappuy, H., Rey, E., Pons, G., Mandelbrot, L. and Urien, S. (2006) Pregnancy-related effects on nelfinavir-M8 pharmacokinetics: a population study with 133 women. Antimicrobial Agents and Chemotherapy. 50:2079-2086.

Leung, H.W. (1991) Development and utilization of physiologically based pharmacokinetic models for toxicological applications. Journal of Toxicology and Environmental Health. 32:247-267.

Luo, X.Y. and Xia, B. N. (1991), Pharmacokinetic study of matrine. Journal of Guiyang Medical College. 16 (2):180-183.

Prentis R.A., Lis, Y. and Walker, S.R. (1988) Pharmaceutical innovation by the seven UK-owned pharmaceutical companies (1964-1985). British Journal of Clinical Pharmacology. 25:387-396.

Sit, D.S., Gao, G., Law, F.C. and Li, P.C. (2004) Gas chromatography-mass spectrometry determination of matrine in human plasma. Journal of Chromatography B. 808(2):209-214.

Tubic, M, Wagner, D., Spahn-Langguth, H., Weiler, C., Wanitschke, R., Otto Böcher, W. and Langguth, P. (2006), Effects of controlled-release on the pharmacokinetics and absorption characteristics of a compound undergoing intestinal efflux in humans. European Journal of Pharmaceutical Sciences. 29:231-239.

Wang, P.Q., Lu, G.H., Zhou, X.B., Shen, J.F., Chen, S.X., Mei, S.W. and Chen, M.F. (1994) Pharmacokinetics of matrine in healthy volunteers. Acta Pharmaceutica Sinica. 29 (5):326-329.

Wang, X.H. and Huang, S.K. (1992) Pharmacokinetics and pharmacodynamics of matrine and oxymatrine. Acta Pharmaceutica Sinica. 27(8):572-576.

Wu, X., Yamashida, F., Hashida, M., Chen, X., and Hu, Z. (2003) Determination of matrine in rat plasma by high-performance liquid chromatography and its application to pharmacokinetic studies. Talanta. 59:965-971.

Zhu, J.P., Deng, D.M., Huang, H.Z. and He, M.H. (1992) Study on the pharmacokinetics of matrine. Zhong Cheng Yao. 14(6):7-8.

# CHAPTER 6:
# DEVELOPMENT AND VALIDATION
# OF A PBPK MODEL OF MATRINE
# IN RAT AND HUMAN

## 6.1    Introduction

It is generally agreed that the development of natural health product (NHPs) into a supplement or therapeutic agent needs considerable improvement to cope with the rapid changes in research and health care environment. This is particularly true in conducting PK studies for NHPs because most of the PK tools available today are developed for a single chemical entity not for a chemical mixture such as NHPs. Modeling and simulation are techniques that have been widely used in engineering to design and develop products more efficiently. Both modeling and simulation rely on the use of models to simplify descriptions of complex systems under investigation. The concept of modeling and simulation may also be used to deal with complex chemical mixtures such as those seen in NHPs. The purposes of this Chapter were: (1) to develop and validate a physiologically based pharmacokinetic (PBPK) model of matrine for rat and human and (2) to integrate the PBPK model into the development process of Acapha® by making it more rational and efficient.

As mentioned in Chapter 5, classical or data-based PK models remain the preferred approach of drug development because it is simple and therefore easier to perform than the PBPK model. Therefore, the majority of the PK models developed to-date is classical model which is based on the drug concentration-time profiles in the

whole blood, plasma or serum, although these may occasionally include other body fluids such as urine, faeces, and breast milk. However, the blood concentration-time profile of a drug is only a surrogate of the concentration-time profile at the target site of action outside the blood compartment. Also, blood concentration-time profile is a result of, rather than a determinant for, drug distribution in various extravascular tissues. Since the relationship between the blood concentration and drug concentration at the site of action is not simple and straightforward, conclusions derived from blood PK analysis should be conditioned on how well it corresponds to the concentration-time profile at the site of action (Nestorov, et al, 2003)

The earliest study that could be called PBPK modelling described the entry of anaesthetic agents into the brain (Haggard, 1924). Teorell (1937) suggested the application of mechanistic, physiologically based modeling to describe the kinetics of xenobiotics in the body. Although there were other PBPK models reported in the early 1960's, it was not until Bischoff *et al.* (1971) published a series of papers that the scientific community was provided with a more rigorous methodology for PBPK modelling. PBPK was first developed to describe the kinetics of therapeutic drugs (Himmelstein and Lutz, 1979) and then of the environmental chemicals (Menzel, 1987). Through the 1970s, PBPK modelling techniques gradually began to gain acceptance and the number of PBPK publications for therapeutic compounds peaked in the late 1970s. A MEDLINE search on the key phase 'physiologically based pharmacokinetic model', carried out on June, 2006 retrieved 715 publications since 1966, an increase of more than 200 papers over the number of March, 2002 (495 references). Among these publications, the majority of the PBPK models were developed for risk assessment of

environmental chemicals. **Appendix III** lists the published PBPK models for environmental chemicals and drugs. As far as I know, there has been no PBPK model reported for an herbal product.

PBPK models differ to the classical PK models in that PBPK models are based on the actual physiology of an animal. In classical PK models, the compartments are defined by the experimental data itself and the composite rate constants determined by data fitting. In contrast, PBPK models use actual organ or tissue groups with their weights and blood flow to build the model. Actual physical-chemical and biochemical parameters of the chemical also are integrated into the model. The result is a model that predicts the time course of drug concentration in blood and/or tissues without being based on their experimental data. PBPK models can be used for quantitative extrapolation well beyond the range of experimental conditions based on which the model is developed. Therefore, the main advantage of a PBPK model is its greater predictive power. Because physiology parameters are used for modelling, a different species can be modelled by replacing them with those with the species of interest (species-to-species extrapolation). Because metabolic parameters are used in the modelling, it is possible to extrapolate over ranges in which saturation of metabolism occurs. Similarly, route-to-route extrapolation can be easily implemented by writing an equation which describes the nature of the new input function. Perhaps the greatest advantage of the PBPK model is that it provides a conceptual framework to summarize a large amount of PK information and for hypothesis testing. A disadvantage of the PBPK models is the requirement of a large number of parameters and equations to implement the model.

## 6.2 Materials and methods

### 6.2.1 Conceptual PBPK model

A blood flow rate limited PBPK model consisting of 12 compartments was developed to describe the disposition of matrine in rat and human (Figure 6.1). This model is very similar to the generic PBPK model reported by Poulin and Theil (2002). These two models differ primarily in that the matrine PBPK model has 2 absorption phases with different lag times and a gut lumen. Also, the matrine PBPK model uses tissue/plasma partition coefficients derived from the area method of Gallo *et al.*, (1987) whereas Poulin and Theil (2002) uses tissue/plasma partition coefficients derived from the predictive tissue composition-based model. To overcome the lack of experimental data, the bone and skin are lumped with other tissues to form a "rest of the body" compartment. The kidney is considered the only eliminating organ for matrine because the amount of matrine excreted in the bile of rat is only $0.27 \pm 0.024\%$ of the administered dose in 12 hr (Luo and Xia, 1991). Since matrine is eliminated unchanged in the urine, no provision has been made in the model on the metabolism of matrine following hepatic uptake.

**Figure 6.1:    Schematic diagram of PBPK model for matrine in rat and human**
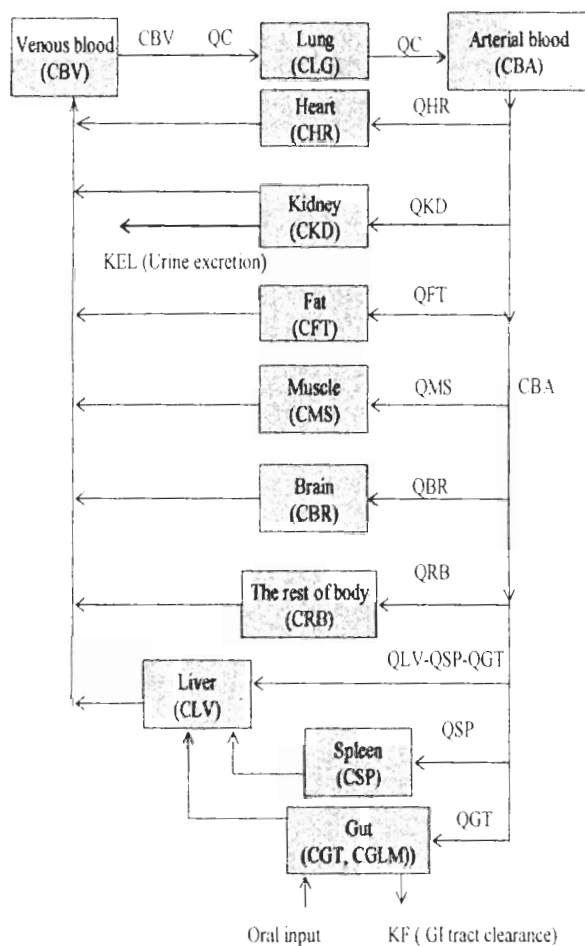


The movement of matrine in each compartment was described by a mass balance equation. The differential and algebraic equations of the PBPK model are described in **Appendix IV**.

## 6.2.2   Model parameterization

### 6.2.2.1   Physiological parameters

Most of the matrine model parameters are parameterized *a priori*. The tissue volume and blood flow were expressed as a fraction of total body volume and cardiac

output, respectively. They were taken from the literature (Luttringer *et al.*, 2003; Brown *et al.* 1997) and summarized in Table 6.1 and Table 6.2.

Table 6.1:     Relative organ weight (percent of body weight) in rat and humans*

| Tissue | Rat | Human |
| --- | --- | --- |
| Adipose | 7.6 | 12.0 |
| Bone | 4.2 | 8.6 |
| Brain | 0.57 | 0.20 |
| Heart | 0.33 | 0.47 |
| Kidney | 0.73 | 0.44 |
| Liver | 3.66 | 2.57 |
| GI tract | 2.7 | 1.7 |
| Lung | 0.50 | 0.76 |
| Muscle | 40.4 | 40.0 |
| Skin | 19.0 | 3.71 |
| Spleen | 0.20 | 0.26 |
| Blood | 8.1 | 7.7 |
| The rest of body | 12.0 | 21.6 |
| Total | 100 | 100 |

*Based on the mean body weight (BW) of a 0.26 kg rat and a 70 kg human

**Table 6.2:**    **Regional blood flow distribution in rats and humans (% of cardiac output)**

| Tissue | Rat | Human |
|---|---|---|
| Adipose | 7.0 | 5.0 |
| Bone | 12.2 | 5.0 |
| Brain | 2.0 | 12.0 |
| Heart | 4.9 | 4.0 |
| Kidney | 14.1 | 19.0 |
| Liver | 17.5 | 25.0 |
| GI tract | 13.1 | 17.0 |
| Muscle | 27.8 | 17.0 |
| Skin | 5.8 | 5.0 |
| Spleen | 2.0 | 2.0 |
| The rest of body | 8.7 | 8.0 |
| Total | 100 | 100 |

Cardiac output for a 0.4 kg rat is 7.08 L/hr; it is calculated from the equation, 14.1*BW **0.75 (L/hr). Cardiac output for a 70 kg human is 390 L/hr; it is calculated from the equation, 16.1*B.W **0.75 (L/hr).

### 6.2.2.2   Biochemical and physico-chemical parameters

Tissue/plasma partition coefficients were determined using the following methods:

(1) *In vivo* tissue/plasma partition coefficients were calculated using the area method of Gallo *et al.*, (1987) from the tissue distribution data of rat after receiving a single oral dose of pure matrine. Briefly, the experimental tissue distribution data were plotted against sampling time. The resulting concentration-time profile of each tissue was fitted by the noncompartmental model, using WinNonlin®. The area under the concentration-time curve (AUC) was calculated using the logarithmic trapezoidal rule. The AUC of a specific tissue divided by the AUC of plasma was used as the initial estimate of tissue/plasma partition coefficient.

(2) Predictive tissue composition-based model. Tissue/plasma partition coefficients also were calculated using the Kow (octanol: water partition coefficient) of matrine according to Poulin et al., (2002). A detailed description of this method is found in **Appendix V.**

(3) In vitro equilibrium dialysis method. Tissue/plasma partition coefficients were calculated based on tissue dialysis data according to Lin et al., (1982). A detailed description of the method is found in **Appendix VI.**

The above tissue/plasma partition coefficients were used initially to develop the matrine PBPK model. The area method of Gallo et al., (1987) was found to be the best in describing the experimental matrine tissue concentration vs. time curves. Table 6.3 shows the final tissue/plasma partition coefficients used in the present matrine PBPK model studies for both rat and humans

Table 6.3:     Tissue/plasma partition coefficients used in the model:

| Tissue | PC |
| --- | --- |
| Kidney | 20 |
| Liver | 10 |
| Spleen | 6.6 |
| Lung | 1.53 |
| Heart | 1.5 |
| Muscle | 1.4 |
| Brain | 2.1 |
| Fat | 0.5 |
| GI tract | 3 |
| Rest of the body | 6 |

### 6.2.2.3 Blood/plasma ratio of matrine

Freshly drawn rat or human blood (2.0 ml to 8.0 ml) was centrifuged at 600 x g for 10 min to generate a small erthrocyte-free plasma layer. The samples were spiked with aliquots of the matrine stock solution added to the erythrocyte-free plasma layer to a final concentration of 10 and 100ug/ml. The blood samples were immediately mixed at 25 $^0$C on a mixer. After incubation for 30 min, aliquots of the blood samples were removed, centrifuged to obtain the plasma (3000 x g for 5 min) at 25 $^0$C. Concentration of matrine in the plasma was measured by GC/MS-SIM. The concentration in blood was assumed to be the theoretical concentration. Blood: plasma concentration ratio was calculated by dividing matrine concentration in the whole blood by matrine concentration in the plasma

### 6.2.2.4 Parameter optimization

The remaining PBPK model parameters, such as the absorption (KA1 and KA2) and elimination rate (KEL) constants that could not be determined *a priori*, were estimated by fitting the kinetic data in the literature (Wu *et al.*, 2003; Luo and Xia 1991; Wang *et al.*, 1994) to a classical 1-compartment PK model using WinNonlin$^®$. Since attempts to obtain the original data were unsuccessful, the mean kinetic data were estimated by inspection from the published graphs. The initial estimates of these parameters were further optimized by the optimization module of AcslXtreme (Aegis Technologies Group, Inc., Huntsville, AL. USA) based on the experimental tissue distribution data of the present study.

### 6.2.3 Simulation of published matrine PK data

The validated PBPK model of rat was run under the experimental conditions reported by Wu *et al.*, (2003) and Luo and Xia (1991) to predict the time course of matine concentrations in the tissues of rat. Both Wu *et al.*, (2003) and Luo and Xia (1991) studies were conducted in rats after receiving a single oral dose of 40 mg/kg pure matrine. Model-predicted results were compared with those observed in the experiments.

### 6.2.4 Animal experiment

#### 6.2.4.1 Preparation of Acapha® suspension and pure matrine solution

A solution of pure matrine was prepared by dissolving matrine in distilled water. Because Acapha® could not be dissolved completely in water or an organic solvent, a suspension of Acapha® was prepared for the rat gavage study. Attempts were made to prepare the suspension with different ratio of Acapha® and water. The best ratio combination appeared to be 0.3 g Acapha® in 1.2 ml water because this ratio yielded the highest extractable matrine concentration. The suspension was sonicated for 20 min before it was used in the rat kinetic studies.

#### 6.2.4.2 Procedures for animal experiment

Sixty male adult Sprague-Dawley rats weighing about 350 g were purchased from Charles River Laboratories, Inc. (Boston, MA. USA). They were quarantined at the Animal Care Facility of Simon Fraser University for 1 week before use. Eighteen rats were randomly selected for each of the high dose study (3.75 g/kg Acapha® or 15 mg/kg pure matrine) and 12 or 15 rats for each of the low dose study (12 rats for 0.375 g/kg Acapha® or 15 rats for 1.5 mg/kg pure matrine). The night before the experiment, food

was removed and only water was available *ad libidum.*

The rats were weighed and subdivided into groups of 3 according to their body weights and the amount of matrine or Acapha® administered was adjusted accordingly. The volume of dosing solution administered was about 1.5 ml/100 g body weight. Rats receiving a high dose of Acapha® were kept individually in metabolic cages for urine and feces collection. Other rats were kept in groups of 3 per cage because urine and feces were not collected from these rats. The rats were euthanized by $CO_2$ asphyxiation at different post-dosing time points: 0.25, 1, 3, 6, 12, and 24 hr for the high dose study; 0.25, 1, 2, 4, and 6 hr for the low dose study. After $CO_2$ asphyxiation, a blood sample was withdrawn immediately by cardiac acupuncture from the rat. The blood sample was centrifuged at 3000 rpm for 5 min to collect the plasma. Major organs such as heart, liver, spleen, lung, kidney, fat, muscle, and brain were removed from the carcass. The tissues and organs were washed in distilled water, wiped dry with tissue paper, and stored in vials at -20 $^0C$ until analysis. The study protocol was approved by the Simon Fraser University Animal Care Committee.

### 6.2.4.3   Analysis of tissue samples

About 1.0 g of tissue samples (0.5 g for spleen) were weighed and put into test tubes. The tissue samples were homogenized in 3 ml of distilled water in a Kinemetica GmbH homogenizer (PCU-2-110, Switzerland) for about 2 min. The final volume of the tissue homogenate was recorded using a glass cylinder.

An aliquot (1 ml) of the tissue homogenate was transferred to a screw capped centrifuge tube for extraction. Matrine was extracted from the tissue homogenates using

a procedure described in section 5.2.3.1. Briefly, matrine-d2 (250 ng), 3 ml of toluene: butanol (v/v 7:3), and 0.5 ml NaOH (1 M) were added to the tissue homogente. The centrifuge tube was capped and shaken horizontally on a mechanical shaker for 15 min and centrifuged at 3000 rpm to separate the layers. The organic layer was removed and put into a new 10-ml, screw capped tube containing 0.5 ml HCl (0.25 M). The centrifuge tube was shaken again and then centrifuged to separate the layers. The organic layer was discarded. The remaining aqueous layer was made alkaline with the addition of 0.5 ml NaOH (1 M). After the addition of 200 µl toluene:butanol (v/v 9:1), the mixture was shaken again on the mechanical shaker. The organic layer was separated by centrifugation and transferred to a vial for GC/MS-SIM analysis. Matrine concentration in the tissue or organ was calculated after correcting for dilution volumes and tissue weights.

### 6.2.4.4   Recovery of matrine from tissue extraction

Two rats were sacrificed for these studies. The heart, liver, spleen, lung, kidney, muscle, brain, and fat were removed, rinsed in water and blotted dry with papers. A 25% v/v homogenate was prepared in water using a Kinemetica GmbH homogenizer (PCU-2-110, Switzerland).

#### 6.2.4.4.1   Absolute recovery

Absolute recovery represents the recovery due to the extraction procedure. Quadruple samples were prepared from each tissue homogenate by pipetting an aliquot (1 ml) of the (25% v/v) tissue homogenate into separate centrifuge tubes. Matrine was added to the tissue homogenate to obtain a final concentration of 1 µg/ml. Matrine-d2 (250 ng) was added to two of the centrifuge tubes which served as the recovery samples. All 4

tubes were extracted as described above (section 6.2.4.3). After extraction, matrine-d2 (250 ng) was added to the two remaining centrifuge tubes which did not contain the internal standard. These samples served as the control samples.

The toluene/butanol (9:1; v/v) extracts of the tissue samples were analysed for matrine using GC/MS-SIM. Matrine concentrations in the tissue samples were calculated from the standard curve. Absolute recovery was calculated by the equation: (measured matrine concentration in recovery sample/ measured matrine concentration in control sample) x 100%.

### 6.2.4.4.2 Relative recovery

Relative recovery represents the recoveries of matrine from the different tissues. An aliquot (1 ml) of the tissue homogente (25% v/v) was pipetted into a centrifuge tube containing a final matrine concentration of 100 ng/ml (or 500 ng/ml). Duplicate samples were used for each matrine concentration and a total of 4 samples were prepared for each tissue homogenate. The samples were extracted by a solution of toluene:butanol as described above (section 6.2.4.3) after adding 250 ng of matrine-d2. The toluene:butanol extract was analysed using GC/MS-SIM. Matrine concentrations in the tissue samples were calculated from the standard curve. Relative recovery was calculated by the equation, (measured matrine concentration in a specific tissue/measured matrine concentration in the 100 ng/ml (or 500 ng/ml) standard solution) x 100%. The 4 relative recoveries from each tissue sample were averaged.

### 6.2.5 Measure of goodness of fit

**6.2.5.1.** The log-likelihood (LL) of the data was used to measure the goodness of fit for the PBPK model. LL is calculated by the following equation (Bois *et al*, 1991):

$$LL = \Sigma(1,N) \, [-N_i/2 \cdot \ln(1 + (yi - yi^*)^2/ Si^2)]$$

Where N is the total number of mean experimental data points used; $N_i$ and $Si^2$ are, respectively, the number of experimental repetitions and the variance for each data point; yi is the experimental data point value, and yi* is the corresponding model-predicted value. In LL analysis, the squared differences between the log-transformed model predictions and the corresponding log-transformed experimental data are minimized and weighed by the variance of each experimental data point. The input data with a higher log-likelihood value represents a better fit of the data with the model.

**6.2.5.2.** The prediction error was also used to measure the goodness of fit of individual tissue data. Prediction error was calculated by the following equation (Bjorkman, 2003):

$$Prediction\ error = \log(C_{pred}) - \log(C_{meas})$$

where $C_{pred}$ represents model-predicted matrine concentration and $C_{meas}$ represents the measured matrine concentration. Prediction error is analogous to the calculation of "n-fold" deviations.

### 6.2.6  Sensitivity of PBPK model to variation in model parameters

Sensitivity analysis characterizes the variability of model-simulated outputs when the model inputs (*e.g.*, physiological, biochemical and physico-chemical parameters) are varied. The partial derivatives (analytical sensitivity) of model output with respect to the model output parameters are calculated using AcslXtreme®. This approach of sensitivity analysis for PBPK models does not predict an overall model output variability but will allow ranking of model parameters in order of their sensitivity. Also, the sensitivity coefficients are log-normalized to eliminate bias due to the magnitude of the parameter

values which would otherwise emphasize the sensitivity coefficients calculated when the parameters values are small. In the presnt study, sensitivity coefficients were calculated for F1, F2, KA1, KA2, TLAG, KEL, BLPLR, and KF in the rat when the output was matrine concentrations in the venous blood.

## 6.2.7 Scaling to human

The PBPK model developed for the rat was scaled to human by using the tissue/plasma partition coefficients determined in the rat and the tissue volumes and plasma flow rates of a standard human. Initial estimate of the elimination rate constant for matrine (KEL) in humans was obtained by fitting the serum matrine kinetic data of Wang *et al.* (1994) to a 1-compartment classical PK model using the WinNonlin®. The KEL, BLPLR, and RRB were then optimized to the kinetic data of Wang *et al* (1994) using AcslXtreme®. As it was impossible to scale absorption rate constants (KA1, KA2, F1, F2 and KF) from the rat, they were also obtained by optimization of the human plasma kinetic data obtained by the BC Cancer Agency.

The apparent volume of distribution at steady state (Vdss) for matrine in humans was predicted by summing the total V x R for all tissues in the PBPK model (Benowitz *et al.*, 1974); where V is the tissue volume of a standard man (Table 6.1) and R is tissue/plasma partition coefficients determined in rat.

## 6.2.8 Simulation software

The differential and algebraic equations of the PBPK model were solved numerically with the aid of AcslXtreme®. PBPK model parameter optimization and sensitivity determination also were conducted using the AcslXtreme®.

## 6.3 Results

### 6.3.1 Recovery of the tissue samples

Table 6.4 shows that absolute recoveries for rat tissues range from 38% (plasma) to 62.5 % (fat). In other words, about 38- 63% of matrine were lost during the extraction procedure. In contrast, similar relative recoveries were observed in different rat tissues. A similar relative recovery value for different tissues indicates that matrine concentrations determined in different tissues can be compared directly without corrections for recoveries.

**Table 6.4:    Recovery of matrine from tissues (%)**

| Tissue | Absolute recovery | Relative recovery |
| --- | --- | --- |
| Heart | 59.6 | 103.5 |
| Liver | 43.1 | 100.2 |
| Spleen | 45.8 | 97.4 |
| Lung | 38.9 | 99.6 |
| Kidney | 55.2 | 105.4 |
| Fat | 62.5 | 100.4 |
| Muscle | 53.2 | 98.6 |
| Brain | 58.2 | 101.7 |
| Plasma | 38.0* | 100 |

\* From Sit et al., 2004

### 6.3.2 Development of rat PBPK model

#### 6.3.2.1 Pharmacokinetic parameter estimation

The optimized PK parameters are shown in Table 6.5. Both pure matrine and crude matrine are absorbed by the rat from two different sites each with a different

absorption rate constant (KA1, KA2), bioavailability (F1, F2) and time delay (TLAG1, TLAG2). Pure matrine and crude matrine are eliminated from the rat with an elimination rate constant and fecal clearance represented by KEL and KF, respectively. BLPLR represents the blood/plasma partition ratio of matrine and was determined experimentally to be 0.68 for the rat. Since KF was not a sensitive parameter, 1.5 $hr^{-1}$ was used in all studies.

Table 6.5:    Optimized pharmacokinetic parameters for the rat

| Parameter | Acapha® | | Matrine | |
|---|---|---|---|---|
| | 3.8 g/kg* | 0.38 g/kg** | 15 mg/kg | 1.5 mg/kg |
| F1 | 0.45 | 0.72 | 0.8 | 0.65 |
| F2 | 0.15 | 0.01 | 0.01 | 0.01 |
| KA1($hr^{-1}$) | 21.7 | 40 | 50 | 33 |
| KA2($hr^{-1}$) | 1.0 | 0.05 | 1.25 | 0.1 |
| KEL($hr^{-1}$) | 300 | 300 | 400 | 450 |
| TLAG1 (hr) | 0.2 | 0.15 | 0.15 | 0.15 |
| TLAG2 (hr) | 11 | 11 | 11 | 11 |
| BLPLR | 0.68 | 0.68 | 0.68 | 0.68 |
| KF ($hr^{-1}$) | 1.5 | 1.5 | 1.5 | 1.5 |

*3.8 g/kg Acapha® is equivalent to 15.2 mg/kg crude matrine
**0.38 g/kg Acapha® is equivalent to 1.52 mg/kg crude matrine

### 6.3.2.2    Comparison of model predicted and experimental concentrations in the rat

Figure 6.2:    compares the predicted and observed matrine concentrations in the different tissues of rats after receiving a single oral dose of pure matrine or Acapha®. A high dose study (15 mg/kg for matrine; 3.8 g/kg for Acapha®) and a low dose study (1.5 mg/kg for matrine and 0.38 g/kg for Acapha®) each were conducted for pure matrine and

Acapha®. An attempt has been made to ensure that the doses of crude matrine in the Acapha® studies matched closely to those of the pure matrine *i.e.*, 3.8 g/kg and 0.38 g/kg Acapha® contained about 15 mg/kg and 1.5 mg/kg crude matrine, respectively.

Figure 6.2 shows that matrine is absorbed rapidly into the blood and distributes to various tissues after oral administration to the rat. Highly perfused organs such as liver, kidney, and spleen had a relatively high Cmax. Lean tissues, such as skeletal muscle, heart, brain, and lung had a lower Cmax. The highest matrine levels were found in most of the tissues at 15 min post-dosing (the first time point of sampling). Matrine concentrations in the tissues were found to decrease in the order of liver>kidney >spleen>>brain>heart, lung, plasma> muscle >fat. The matrine concentration-time profiles of the various tissues were found to be exceedingly similar (Figure 6.2) which render credence to the assumption of a blood flow rate limited PBPK model for matrine.

Figure 6.2:    Matrine concentration in the tissues of rat. The two top curves of each figure represent the time course of matrine concentration of a specific tissue in the high dose studies (3.8 g/kg Acapha and 15 mg/kg pure matrine) and the two bottom curves represent the tissue concentrations for the two low dose studies (0.38 g/kg Acapha and 1.5 mg/kg pure matrine). Each symbol represents the observed mean value for 3 rats while the lines represent PBPK model-predicted values.
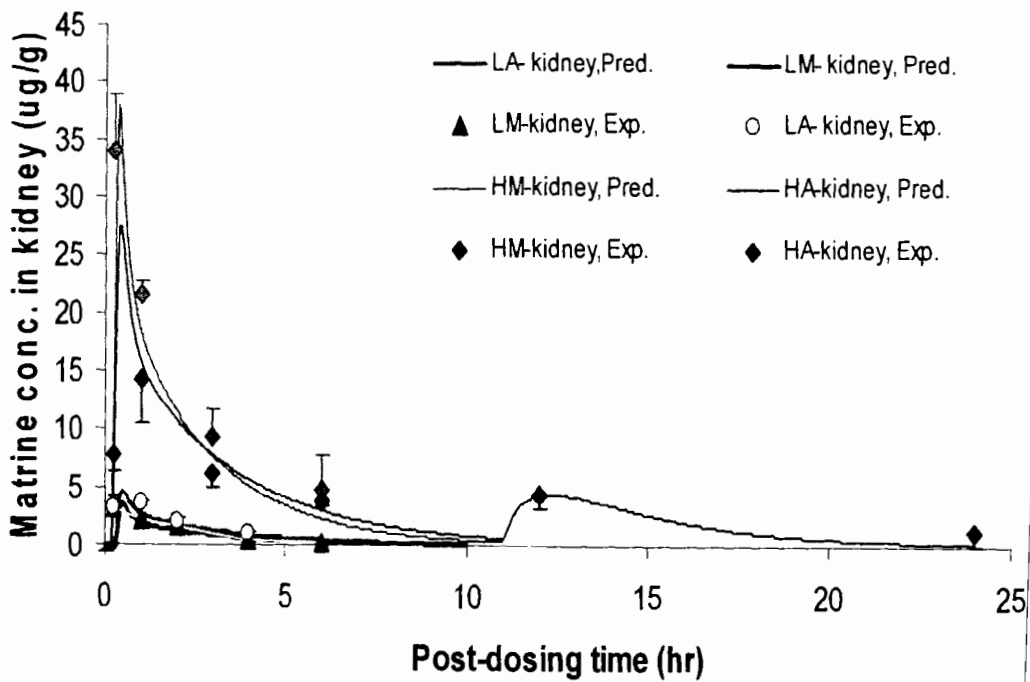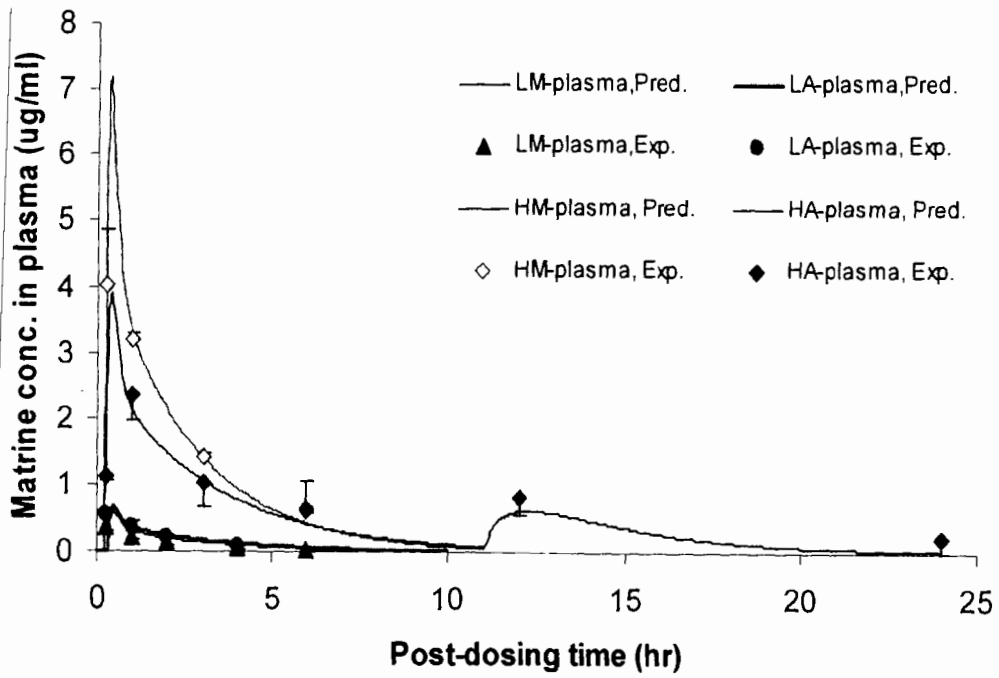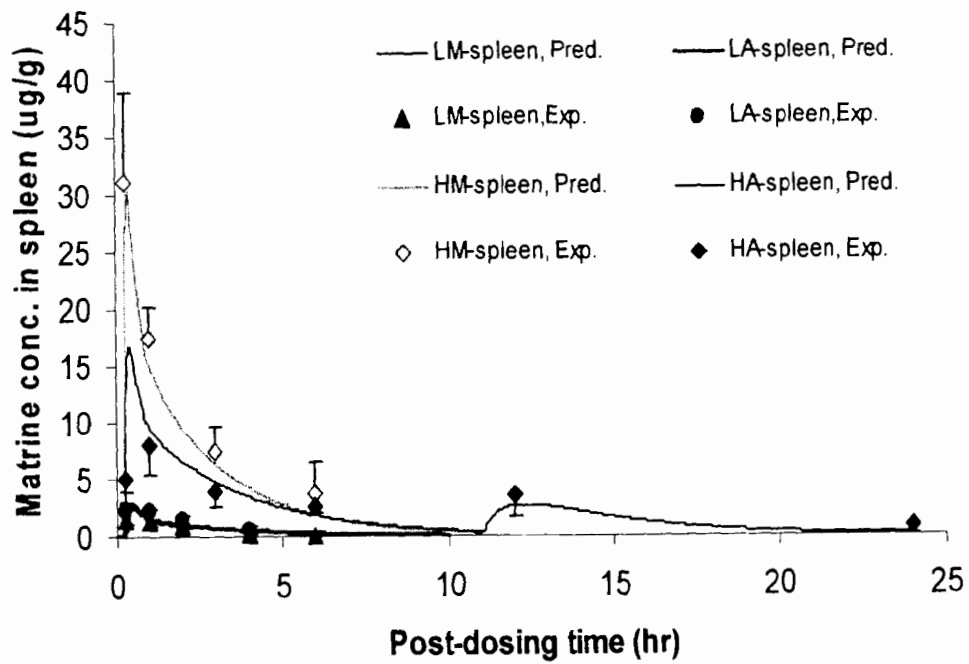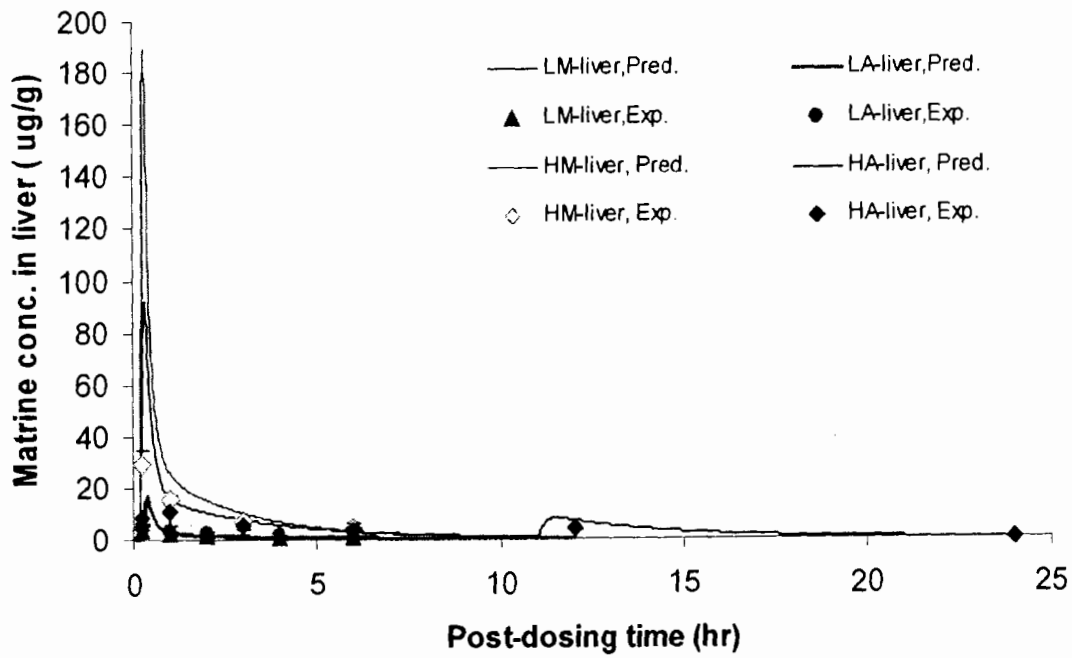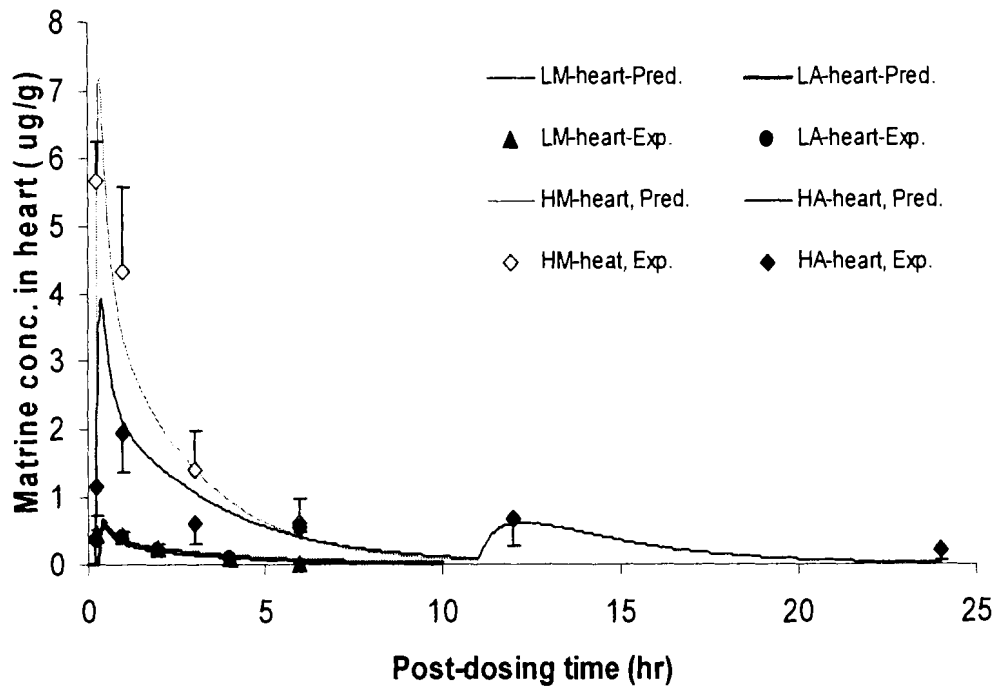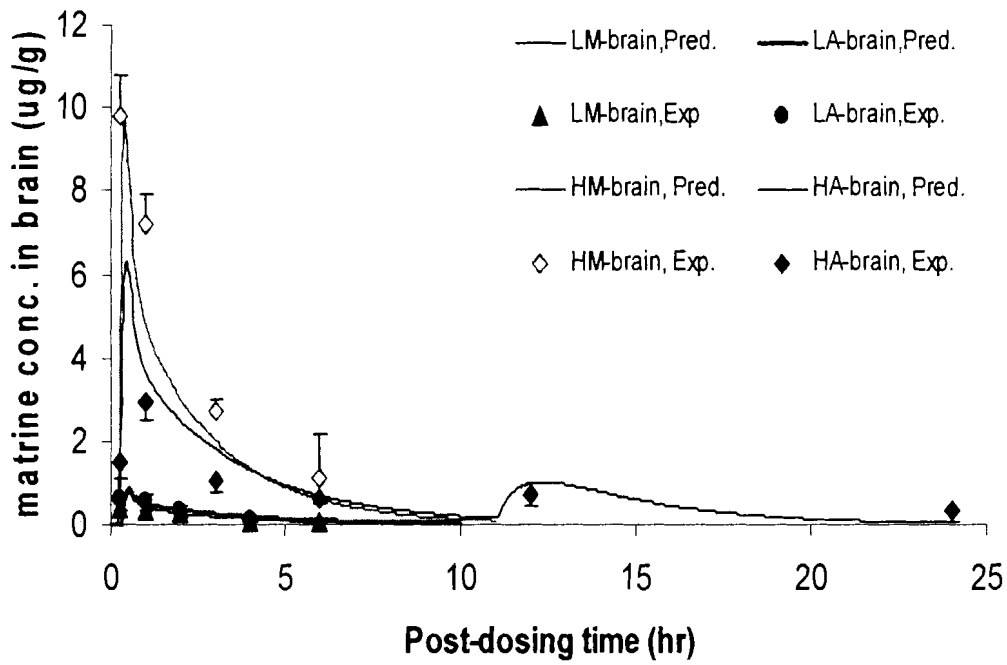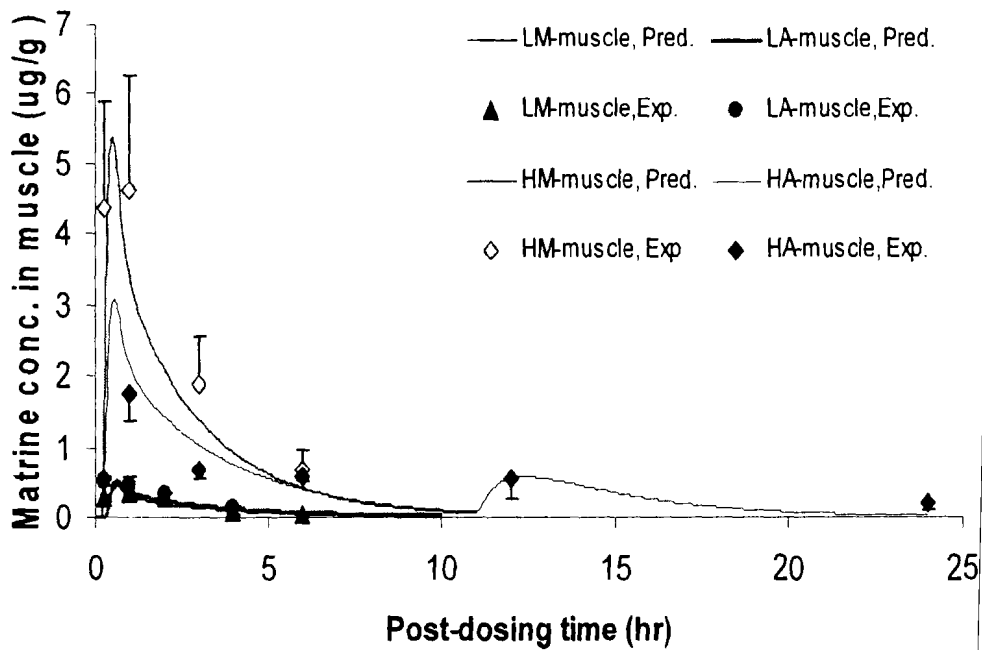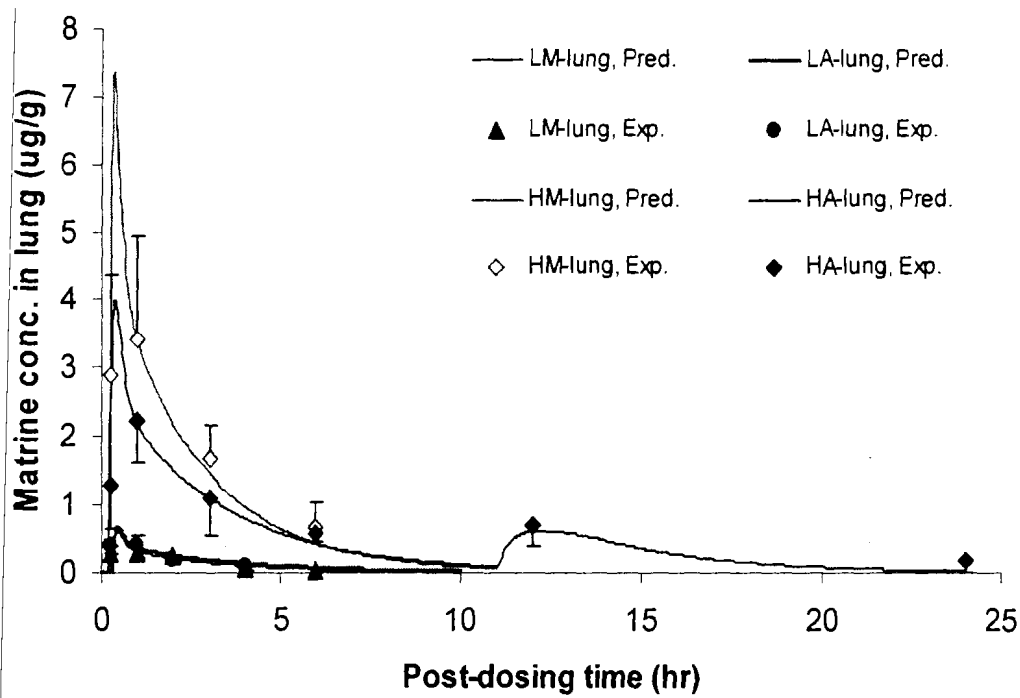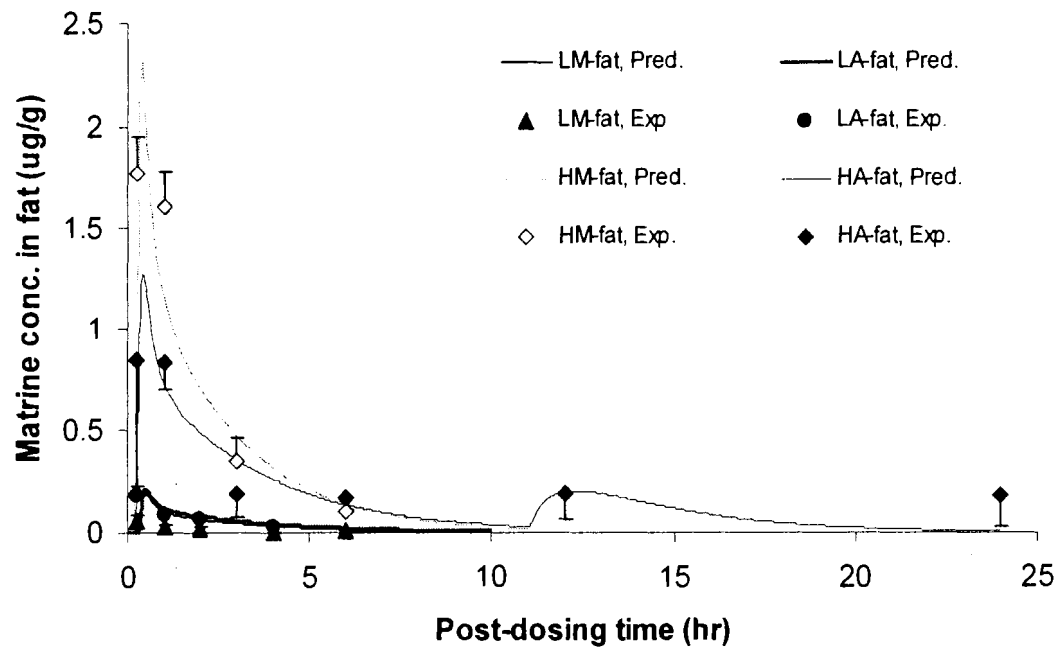
As shown in Figure 6.2, model predicted tissue matrine concentrations are in excellent agreement with the experimental data for both pure and crude matrine. However, pure matrine appeared to be absorbed at a much faster rate than crude matrine. This is consistent with the results of the Caco-2 cell monolayer study in which pure matrine is transported at a higher rate than crude matrine (Table 3.1). In addition, only the kinetic profiles of high crude matrine dose study showed a second peak at about 12 hr post-dosing (Figure 6.2).

### 6.3.3 Cumulative urine excretion

Table 6.6 shows the cumulative urine excretion of matrine in rat after receiving a single oral dose of 3.8 g/kg Acapha® or 40 mg/kg pure matrine. Model predicted urine excretion was 60% in 24 hr; it was 3 fold higher than the observed urinary excretion (20.8%) after Acapha® administration. An explanation for the discrepancy in results is not readily available but Luo and Xia (1991) have reported that about 53.7% of an i.g. administered dose of pure matrine (40 mg/kg) is excreted by the rat in 24 hr.

Table 6.6: Cumulative urine excretion of matrine in rat after receiving a single oral dose of pure matrine or Acapha®

| Time (hr) | Acapha* Mean± SD (%) | Model Predicted % | Pure matrine** % excretion |
|---|---|---|---|
| 6 | 11.8 ± 6.9 | 37.8 | 29*** |
| 12 | 16.8 ± 5.5 | 45.5 | 52.2 ± 3.3 |
| 24 | 20.8 ±6.7 | 60 | 53.7 ± 3.4 |

*Acapha® 3.8 g/kg (15.2 mg crude matrine/kg) p.o.; ** Pure matrine 40 mg/kg (Luo and Xia, 1991); ***Estimated from the published graph (Luo and Xia, 1991).

### 6.3.4 Log-likelihood analysis of the dataset: evaluation of goodness of PBPK model fitting

Figure 6.3 shows the LL and the linear relationship between predicted and determined tissue concentrations in each dataset. The LL integrates the differences between model prediction and experimental data. The LL of the high pure matrine group is -61.1 which is the highest among the 4 datasets, indicating a better fit of the data with the model.

The "identity line" of the plot represents the ideal situation that each predicted value is identical with its experimental counterpart. Therefore, the data points above the "identity line" represent overestimates and the data points below the line represent underestimates. Since most of the data points of the present study fall on or near the "identity line", model predicted values are very close to their empirical counterparts. The data points at 0.25 hr and 24 hr post-dosing, in particular those of the liver, are the most scattered data points around the "identity line" because these data points are very close to the LOQ and cannot be determined accurately.

Figure 6.3: Model predicted tissue concentrations versus observed values for the four datasets. Each data point represents an average of triplicate samples. Variance is not presented. For a perfect fit, the points would fall on the identity line.

High dose matrine
( LL:-61.1)

LN (predicted matrine tissue conc.)

LN ( observed matrine tissue conc.)

High dose Acapha
( LL:-84.2)

LN (predicted matrine tissue conc.)

LN ( observed matrine tissue conc.)

Low dose matrine
( LL:-86.1)

LN (predicted matrine tissue conc.)

LN ( observed matrine tissue conc.)

Low dose Acapha
( LL:-79.9)

LN (predicted matrine tissue conc.)

LN ( observed matrine tissue conc.)
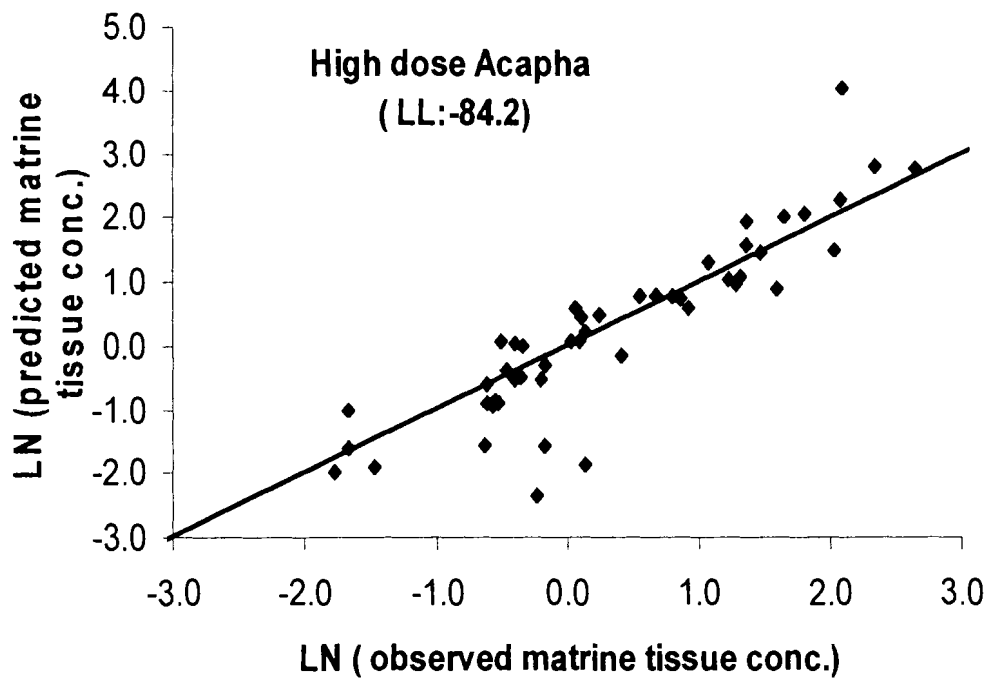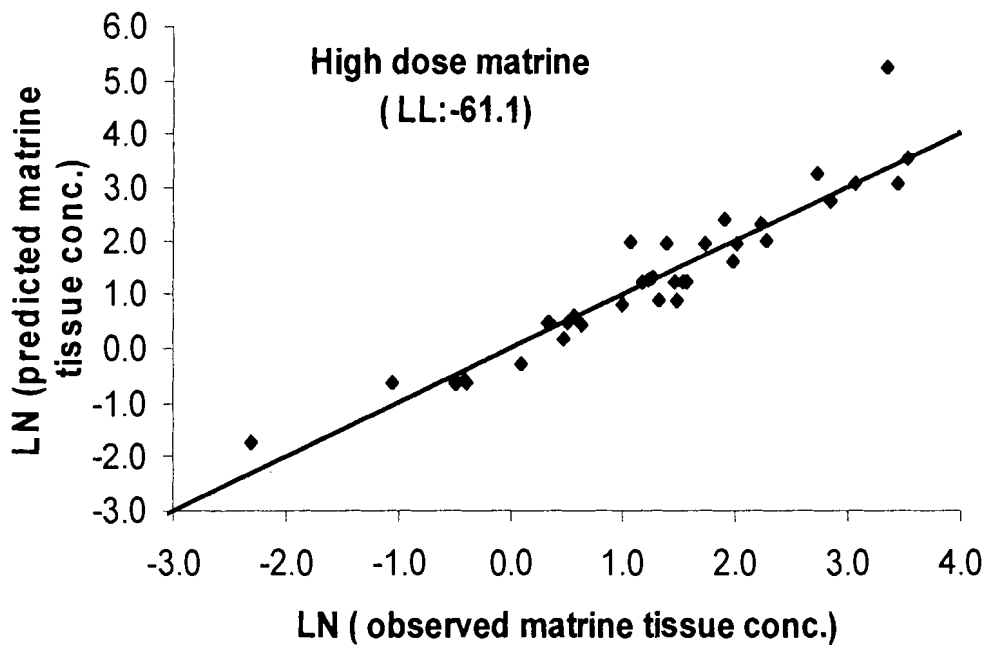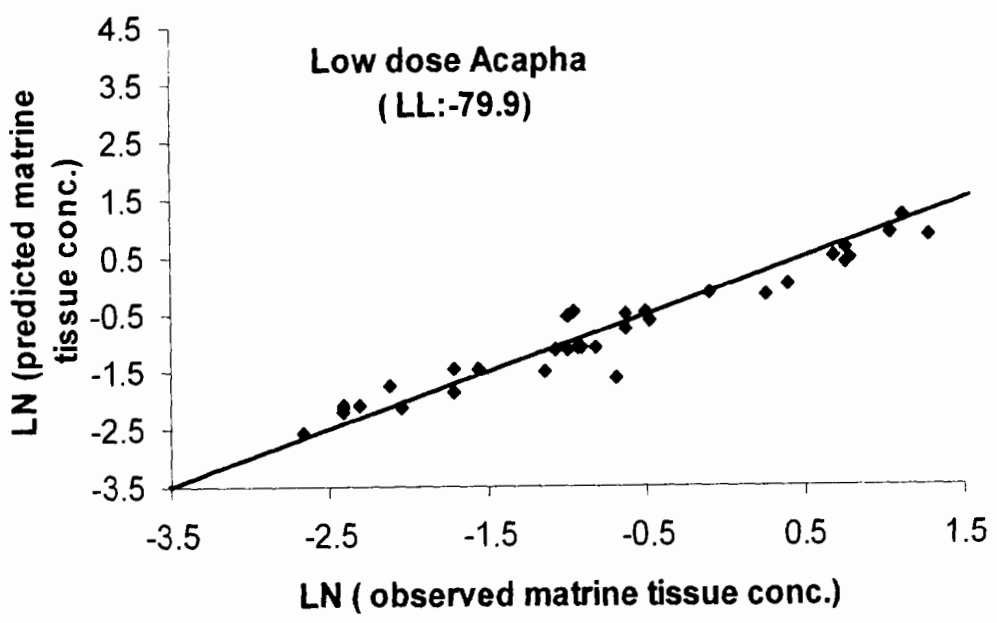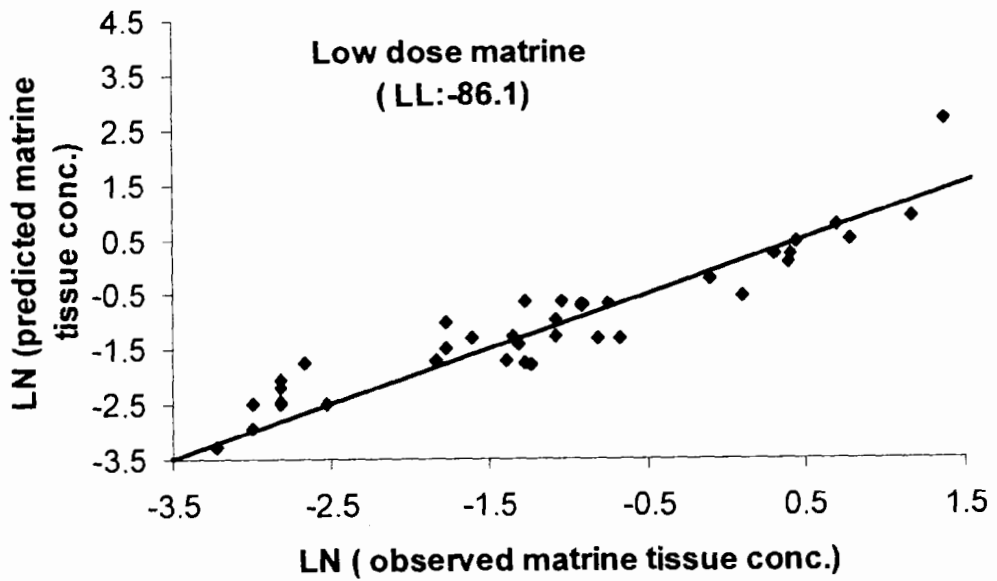
### 6.3.5 Parameter sensitivity analysis

Figure 6.4 and Figure 6.5 show the time-dependent sensitivity (partial derivative) of model-predicted venous blood matrine concentration to F1, F2, KA1, KA2, TLAG, KEL, BLPLR, and KF in rats after receiving a single oral dose of 3.8 g/kg Acapha®. If the sensitivity of a model parameter is high in absolute value, the parameter will have an important effect on the model. If the sensitivity is very close to zero, the model parameter will have only a small effect on the model. As shown in Figures 6.4 and 6.5, the normalized sensitivity coefficients calculated for this study ranged between -9.6 and 2.6. Also, the sensitivity coefficients of most parameters were less than 1 in absolute value and changed in a smooth fashion with time. Presumably these were related to the instability associated with the finite difference calculations at times when blood matrine concentrations were very low. In contrast, the sensitivity coefficients of F1 and KA1 were found to fluctuate rapidly and severely with time. Thus they were the most sensitive parameters of the PBPK model and the individual input errors in F1 and KA1 are greatly amplified in the output.

**Figure 6.4:** Normalized sensitivity coefficients for PK parameters in rat after receiving a single oral dose of 3.8 mg/kg when the output is the venous blood concentration
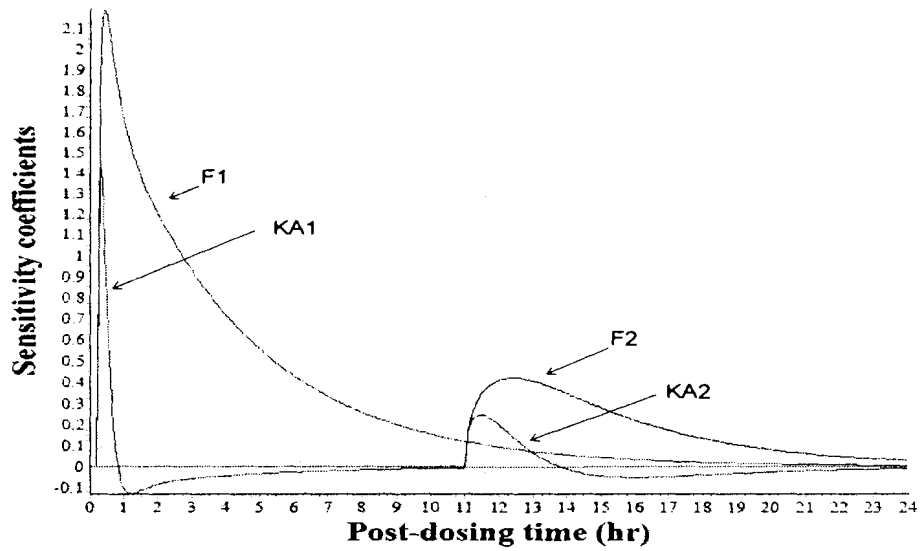


**Figure 6.5:** Normalized sensitivity coefficients for PK parameters in rat after receiving a single oral dose of 3.8 mg/kg when the output is the venous blood concentration



132
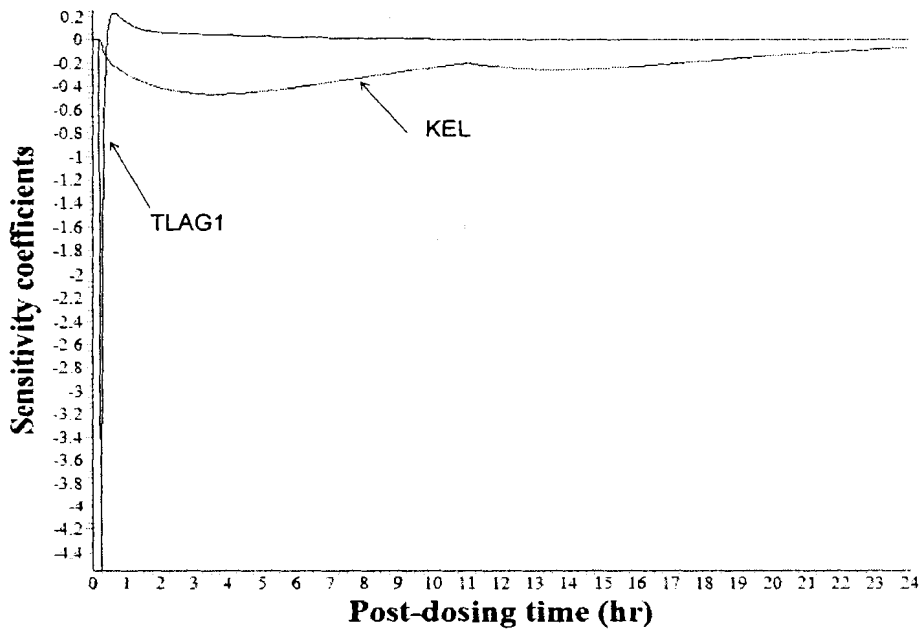
### 6.3.6 Validation of rat PBPK model

Model validation is conducted by running the developed model with an experimental dataset other than the one used for model development. If the simulated results match the experimental data closely, the model is termed "validated". The PBPK model was validated using the plasma matrine concentration dataset of the rat dosed with a single dose of 40 mg/kg pure matrine by gavage (Wu *et al.*, 2003). Simulation was run using the parameters listed in Table 6.5 with the exception of the parameters which are related to the absorption and elimination of matrine by the rat. The optimized parameters are: F1 (0.3), KA1 (3.0 $hr^{-1}$), KEL (357 $hr^{-1}$) and TLAG (1.5 hr). These parameters are different to those listed in the Table 6.5 because Wu *et al.*, (2003) use a high dose of pure matrine in their study and there are large inter-individual differences in both kinetic studies. Nevertheless, Figure 6.6 shows that the rat PBPK model is validated because model predicted plasma matrine concentrations describe closely the experimental data of Wu *et al.*, (2003).

**Figure 6.6:** Time course of matrine plasma concentrations in rat after receiving a single oral dose of 40 mg/kg pure matrine. Symbols represent experimental data of Wu *et al.*, (2003); solid line represents model simulation.



The tissue distribution data of Luo and Xie (1991) also was used to validate the PBPK model of matrine in rats dosed with a single oral dose of pure matrine (40 mg/kg). Luo and Xie (1991) determined matrine concentrations in the brain, kidney, liver, heart and plasma samples at different time points post-dosing using HPLC/UV. Simulation was run using the parameters listed in Table 6.5 with the exception of the absorption and elimination parameters which were optimized to F1 (0.63), KA1 (3.7 hr⁻¹), KEL (444 hr⁻¹) and TLAG (0.61 hr). Figure 6.7 shows the results of the validation study; the PBPK model is able to simulate the experimental matrine concentrations in the different tissues very well (prediction error < 50%). The only exception is the lung of which the model underestimates matrine concentration by about 2-fold (prediction error > 50%) (data not shown). If the partition coefficient of the lung were increased from 1.5 to 3.0, model-prediction would closely describe the experimental matrine concentrations in the lung (prediction error < 50%) (Figure 6.7).

Figure 6.7:     PBPK model validation with the datasets of Luo and Xia. Symbols represent
experimental data of Luo and Xie (1991); solid line represents model simulation.
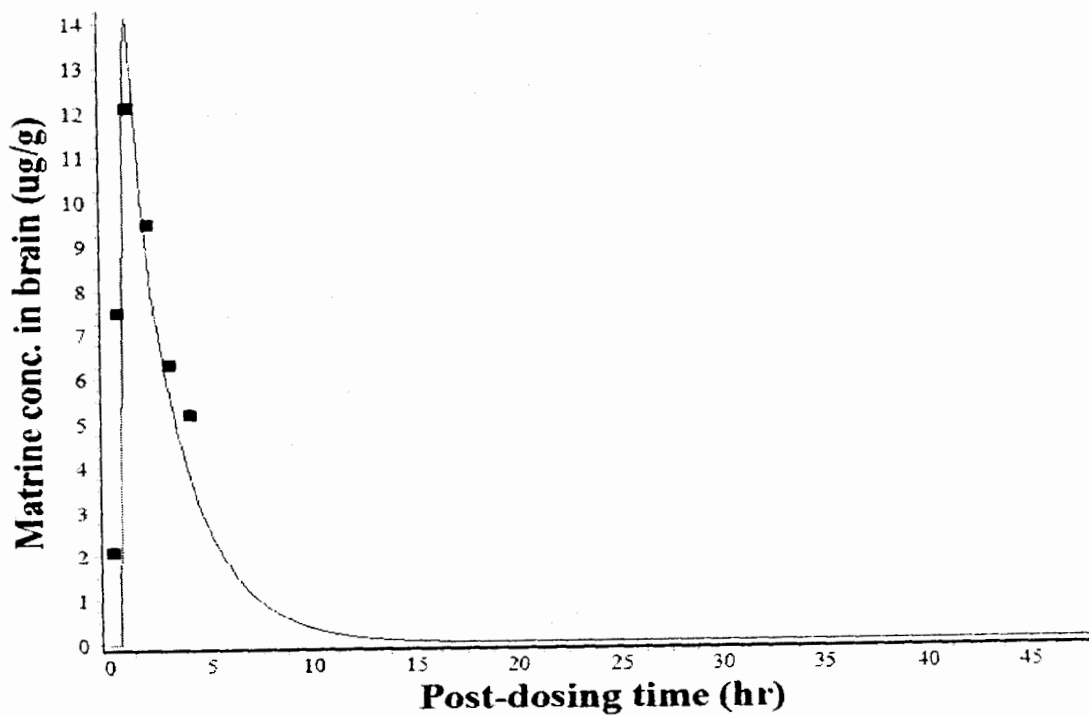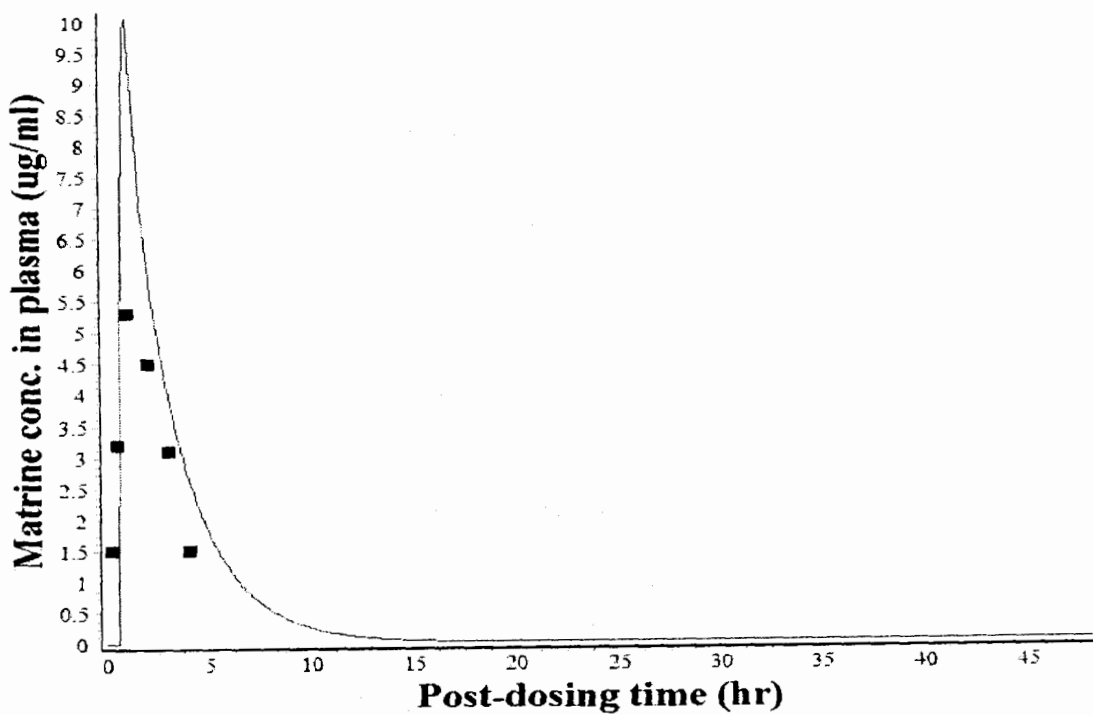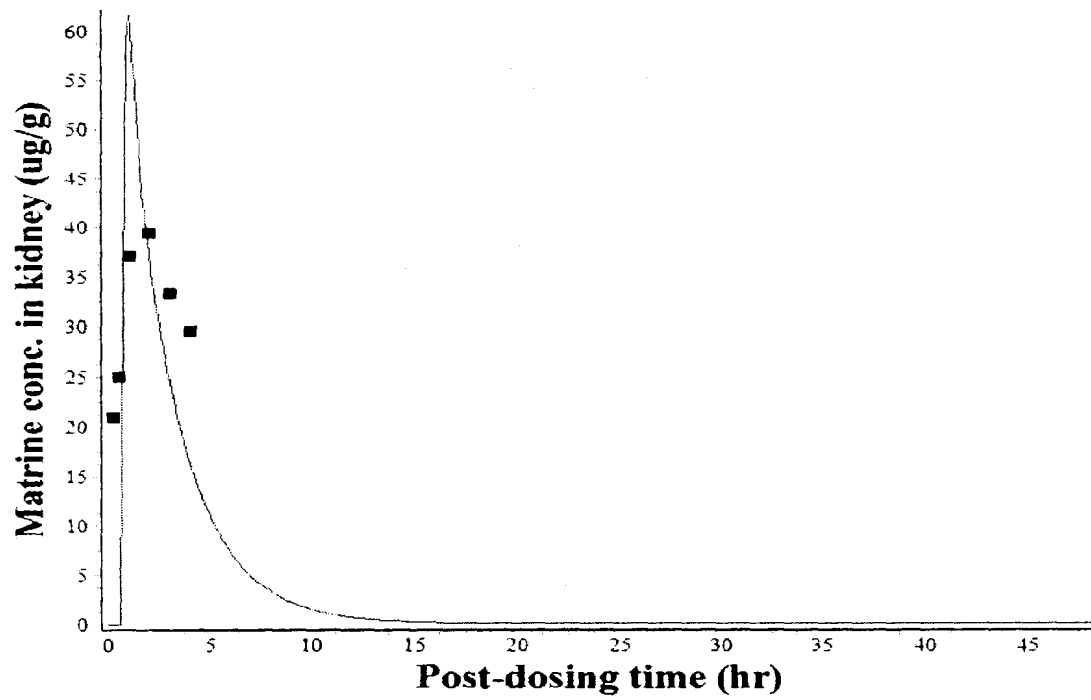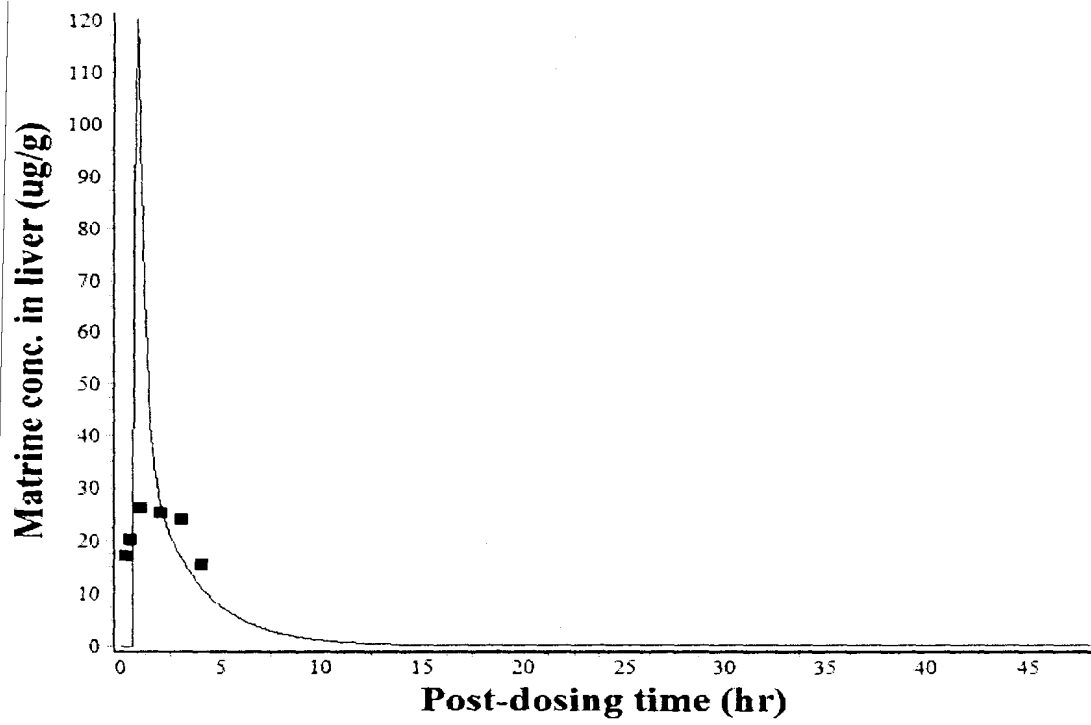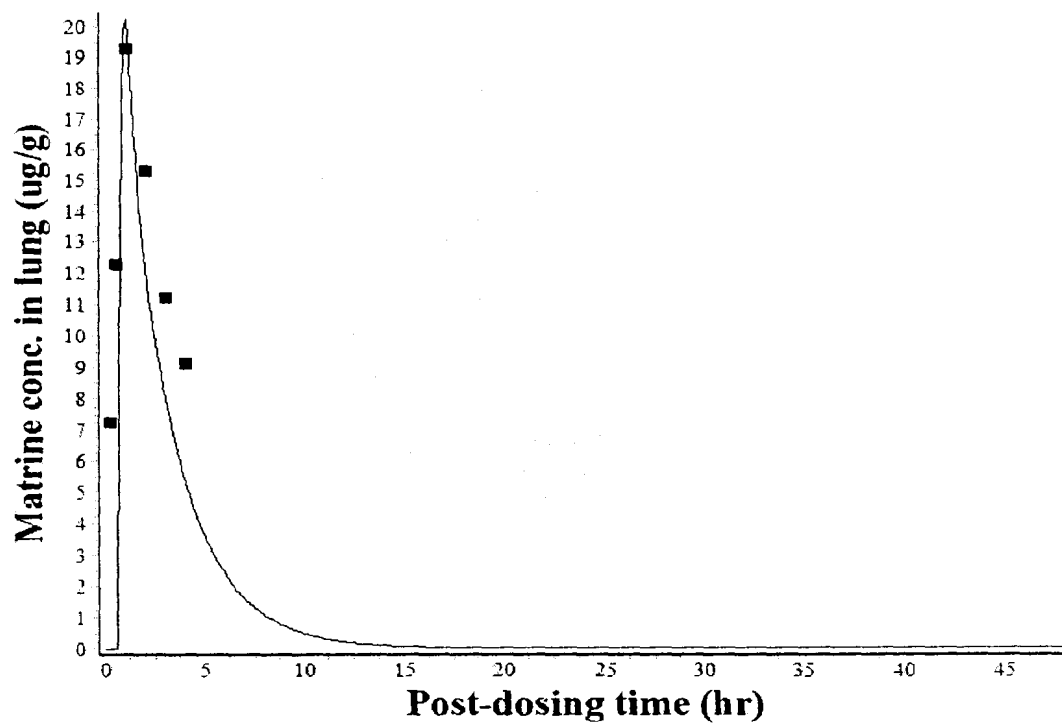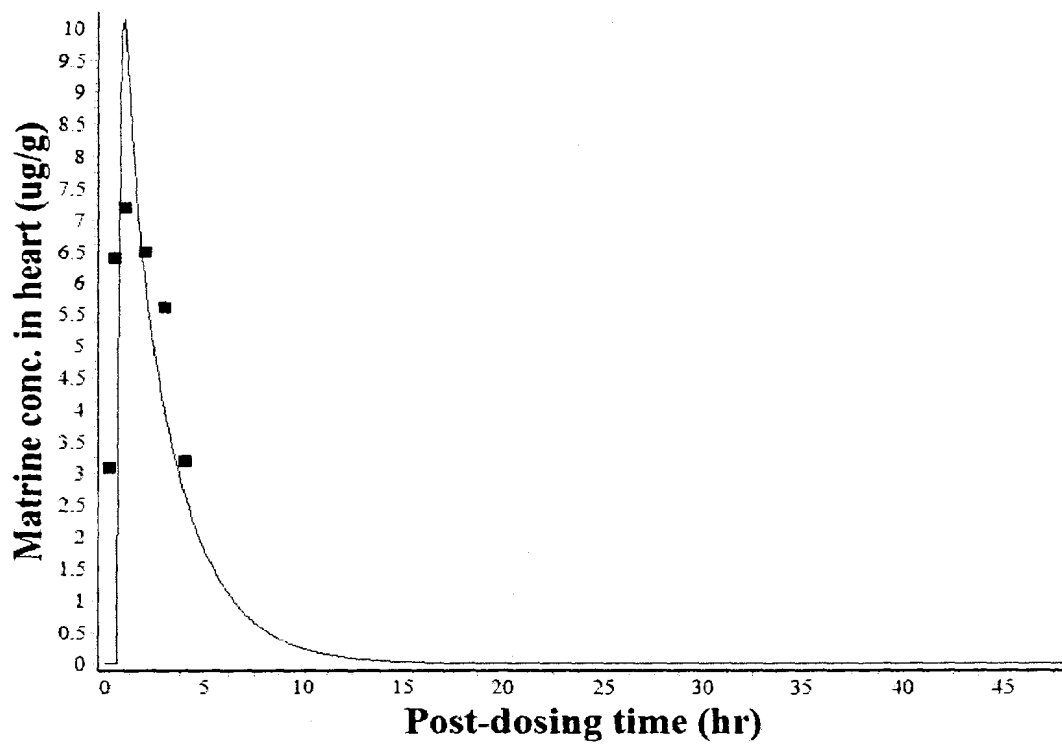
### 6.3.7 Scaling to human PBPK model

The PBPK model developed for the rat was scaled to human by using the tissue/plasma partition coefficients determined in the rat (Table 6.3) and the tissue volumes and plasma flow rates of a standard human (Tables 6.1 and 6.2). In addition, the oral input function of the human PBPK model was replaced with $i.v.$ infusion. The elimination rate constant (KEL) and blood/plasma ratio (BLPLR) were optimized based on the serum and urine matrine kinetic data of human after $i.v.$ infusion of 6 mg/kg pure matrine (Wang $et\ al.$, 1994). The optimized KEL and BLPLR were 39.8 $hr^{-1}$ and 1.8, respectively. Figures 6.8 and 6.9 show the modeled predicted serum matrine concentration and cumulative urine excretion, respectively; model prediction described closely the experimental data of Wang $et\ al.$, (1994).

Figure 6.8:   Time course for serum matrine concentrations in human during and following a 0.5 hr $i.v.$ infusion of 6 mg/kg pure matrine solution
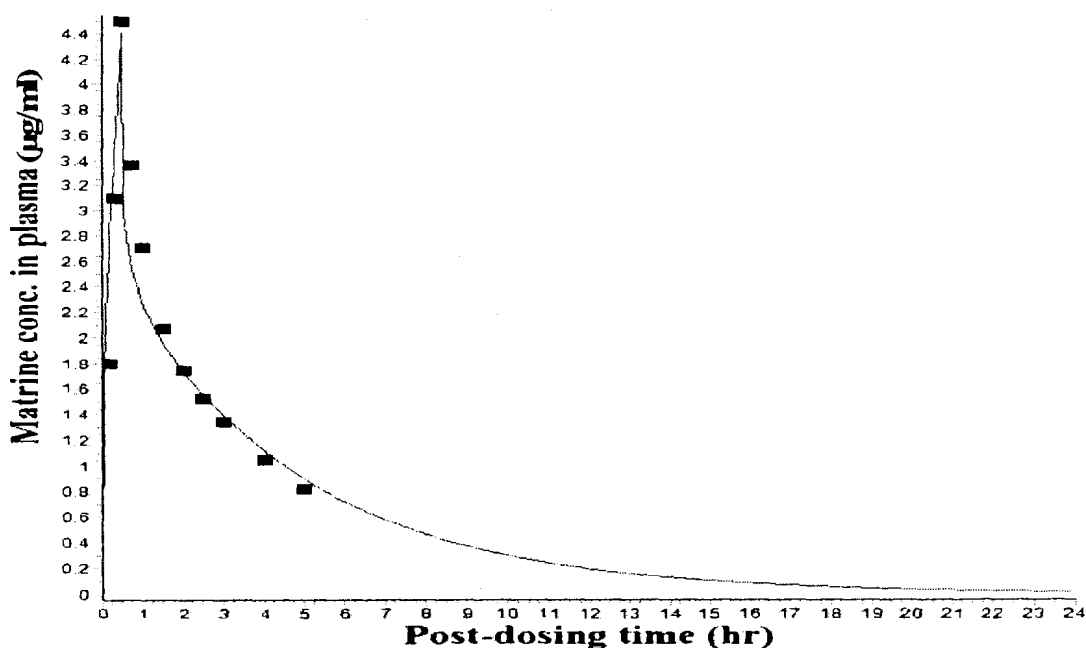
Figure 6.9:     Cumulative urine excretion of matrine in human following a 0.5 hr *i.v.* infusion of 6 mg/kg pure matrine solution. Symbols represent experimental data of Wang *et al.*, (1994); solid line represents model simulation.
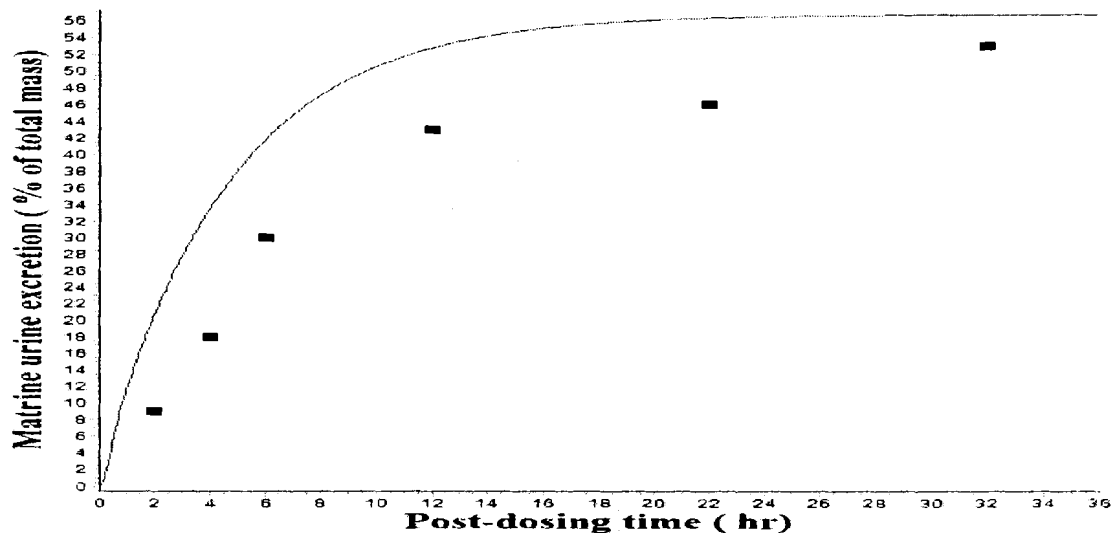


## 6.3.8   Calibration of matrine PBPK model for human dosed with Acapha®

The human PBPK model was also calibrated for human receiving Acapha® ( crude matrine) *p.o.* The KEL and BLPLR were fixed initially at  39.8 hr$^{-1}$ and 1.8, respectively but model prediction did not provide a good fit for the experimental data. KEL and BLPLR together with the oral input parameters (F1, F2, KA1, KA2, TLAG1 and TLAG2) were finally optimized according to the experimental data of the high Acapha® dose study. Table 6.9 shows the pharmacokinetic parameters of crude matrine in former smokers after receiving a single oral dose of 1.2 g (0.02 g/kg) or 2.4 g (0.04 g/kg) Acapha®  tablets. The optimized KEL of the Acapha® studies are very similar to that observed in the *i.v.* infusion study of Wang *et al.*, (1994). The BLPLR of the Acapha® studies are much smaller than the the *i.v.* infusion study of Wang *et al.*, (1994). The oral input parameters (F1, F2, KA1, KA2, TLAG1 and TLAG2) are not compared because

Wang *et al.*, (1994) is an *i.v.* infusion study.

Table 6.7:    Optimized pharmacokinetic parameters for Acapha®

| Parameter | Acapha® | |
|---|---|---|
| | 2.4 g (0.04 g/kg) | 1.2 g (0.02 g/kg) |
| F1 | 0.8 | 0.8 |
| F2 | 0.15 | 0.2 |
| KA1($h^{-1}$) | 1.5 | 0.9 |
| KA2($h^{-1}$) | 19.0 | 0.11 |
| KEL($h^{-1}$) | 40 | 60 |
| TLAG1 (hr) | 1.4 | 1.0 |
| TLAG2 (hr) | 24 | 24 |
| BLPLR | 0.5 | 0.5 |
| KF ($h^{-1}$) | 0.5 | 0.5 |

Figure 6.10 and Figure 6.11 show the model predicted as well as the experimental plasma matrine concentrations in human after receiving a single oral dose of 2.4 g (0.04 g/kg) and 1.2 g (0.02 g/kg) Acapha®, respectively. Model predicted plasma matrine concentrations were in close agreement with the experimental data. The human PBPK model was able to describe the kinetic data of the 1.2 g (0.02 g/kg) Acapha® dataset closely even though the experimental concentrations (Figure 6.11) were very close to the LOQ of the GC/MS-SIM analytical method.

Figure 6.10: Venous matrine plasma concentration in human volunteers receiving 2.4 g (0.04 g/kg) Acapha®
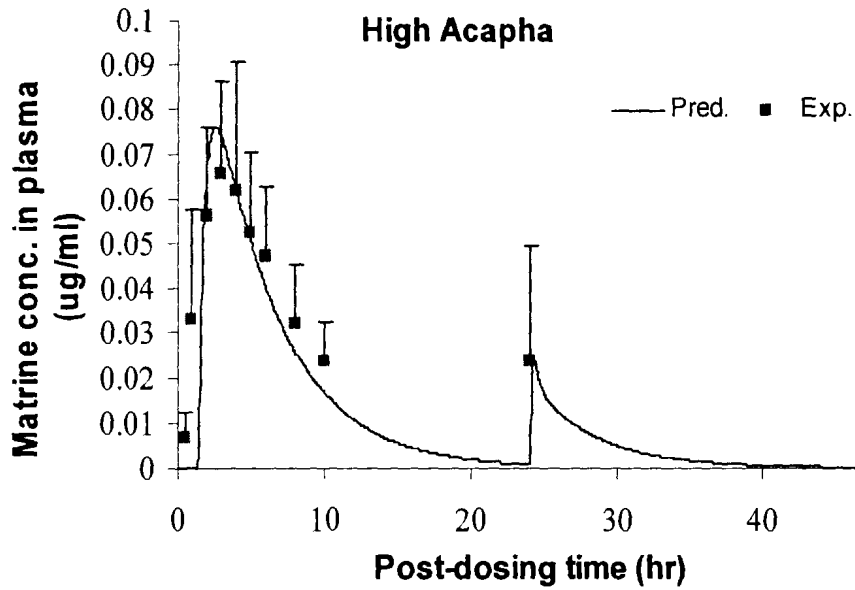


Figure 6.11: Venous matrine plasma concentration in human volunteers receiving 1.2 g (0.02 g/kg) Acapha®
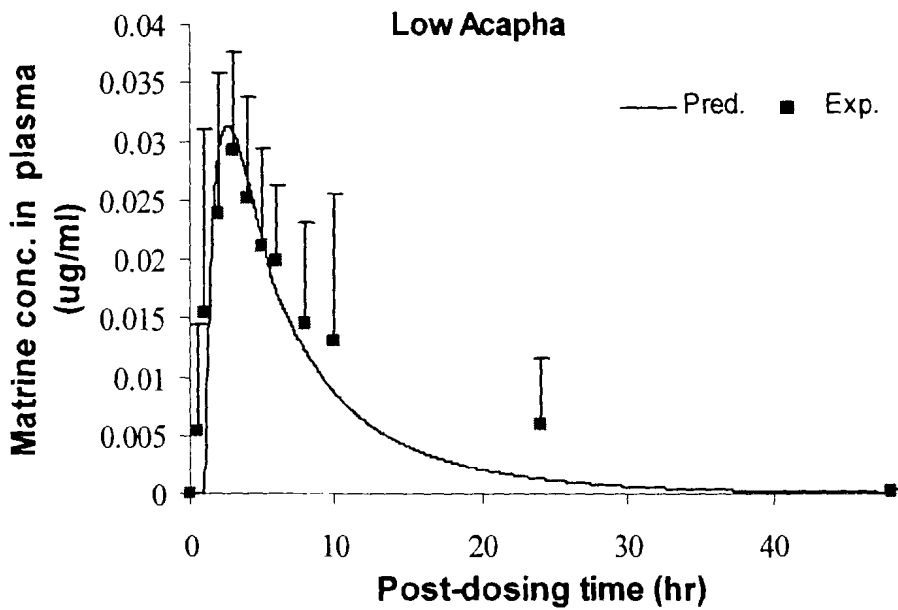
LL was used to evaluate the goodness of fit for the combined datasets of the Acapha® studies. The LL was found to be -18. Figure 6.12 displays the model predicted plasma concentrations versus the actual experimental matrine concentrations for the combined datasets. The two data points at the bottom of the "identity line" are more dispersed around the line because they are the last time points of the datasets and below the LOQ of the analytical method. The rest of the data points fall on the "identity line" indicating the closeness of model simulation and the experimental data.

Figure 6.12:  Model predited tissue concentrations versus observed values for the Acapha® datasets. The first two timepoints in Figure 6.10 and Figure 6.11 are excluded.
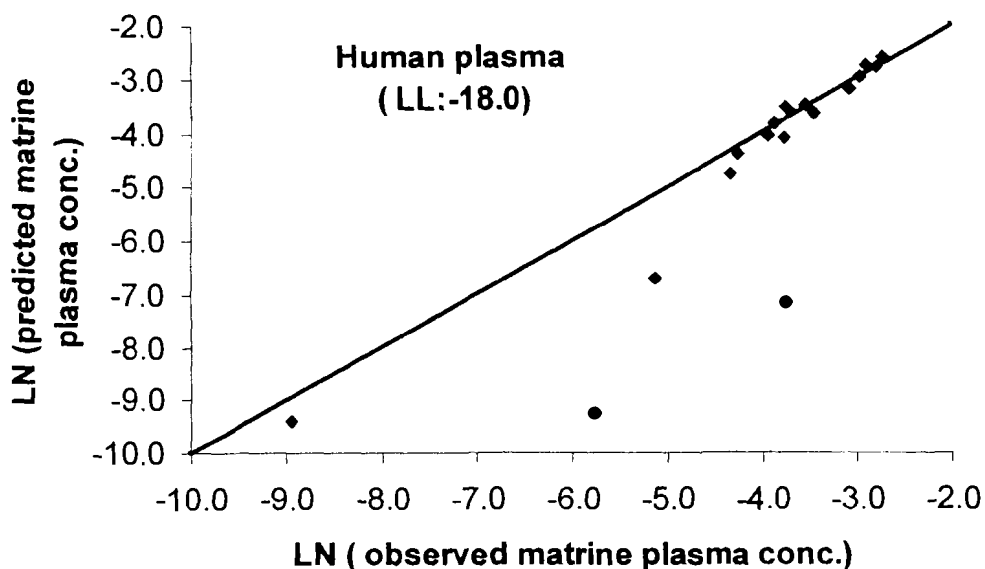


The calibrated human PBPK model also was used to simulate cumulative urine excretion of matrine in humans after receiving a single oral dose of Acapha®. Figure 6.13 and Figure 6.14 show the cumulative urine excretion of matrine in human volunteers after

receiving 2.4 g (0.04 g/kg) and 1.2 g (0.02 g/kg) Acapha®, respectively. Model predicted

cumulative urine excretion of matrine were in close agreement with the observed

cumulative urine excretion of the human volunteers.

Figure 6.13: Cumulative urine excretion of matrine in human volunteers receiving 2.4 g (0.04 g/kg) Acapha®

High Acapha
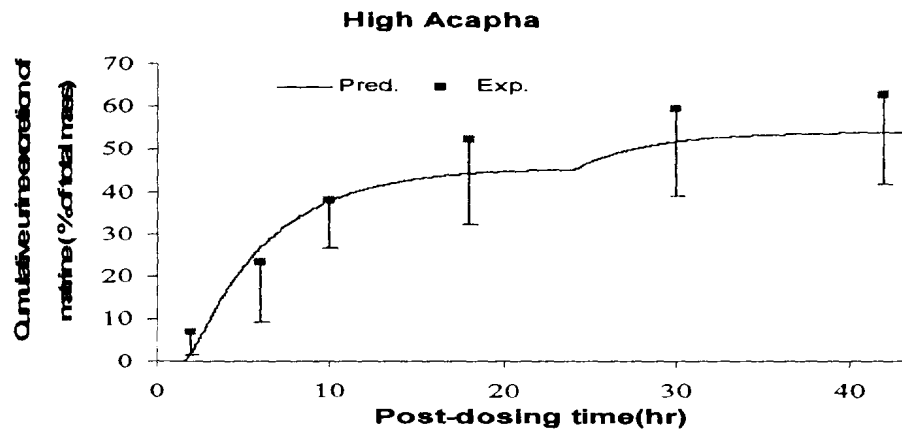


Figure 6.14: Cumulative urine excretion of matrine in human volunteers receiving 1.2 g (0.02 g/kg) Acapha®

Low Acapha
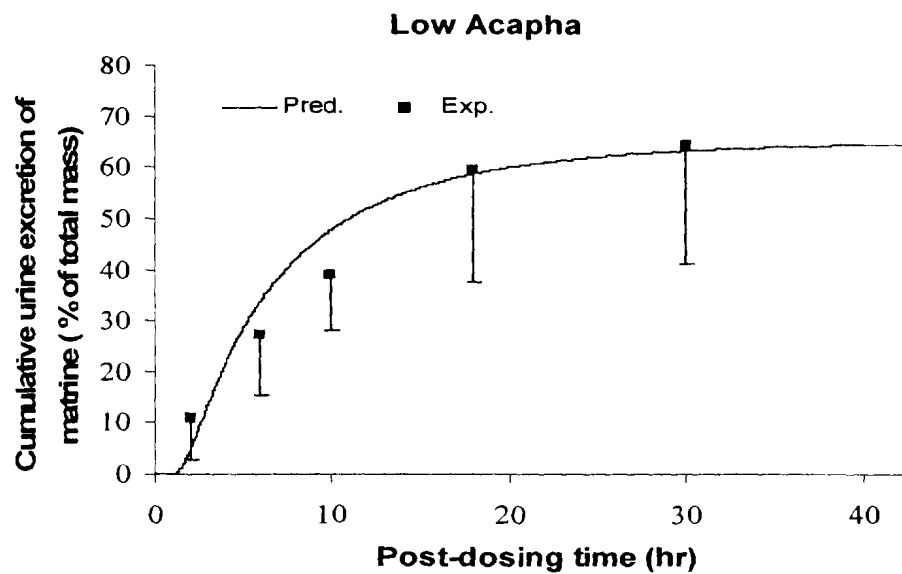
### 6.3.9 Matrine concentration in the plasma and urine of human after receiving multiple daily doses of Acapha®
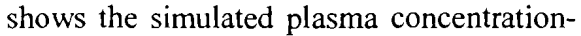
In the BCCA clinical trial studies, human volunteers were treated with a daily oral dose of 2.4 g (0.04 g/kg) Acapha® *b.i.d.* (or 0.08 g/kg/day) for 6 months. As with any clinical studies, patient compliance was a concern. Therefore, blood and urine samples were collected biweekly from the volunteers during their scheduled visits and analysed for matrine by GC/MS-SIM to monitor compliance. A parallel study was conducted using the human PBPK model. Figure 6.15:   shows the simulated plasma concentration-time profile of matrine during a 3-month dosing period. A steady-state plasma matrine concentration is established in 3 days after the initiation of Acapha® treatment. There is no evidence that matrine accumulates in the body. Once a steady state condition was established, simulated matrine plasma concentrations were found to fluctuate between 0.02-0.115 µg/ml. The range of plasma matrine concentration bracketed the mean matrine concentrations (N = 25) measured in the volunteers' biweekly visit plasma samples.

**Figure 6.15: Plasma matrine concentration in humans receiving 0.08 g/kg/day Acapha® for 3 months. Each square symbol represents the mean plasma matrine concentration of 25 experimental subjects.**
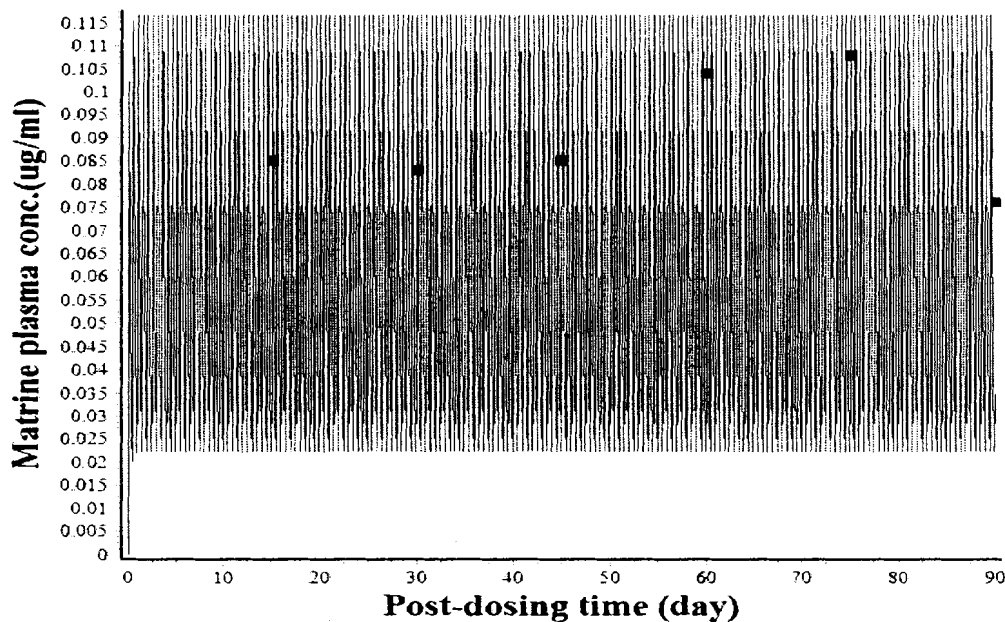


Figure 6.16 shows the urinary concentration of matrine in humans receiving a daily dose of 0.08 g/kg Acapha® for 6 months. Mean matrine concentrations in the urine are relatively constant; they stayed at about 4 µg/ml level during the 6-month treatment period. These results confirm that matrine concentration in these volunteers has reached a steady state.

**Figure 6.16:** Matrine concentrations in the urine of humans receiving 0.08 g/kg/day Acapha for 6 months
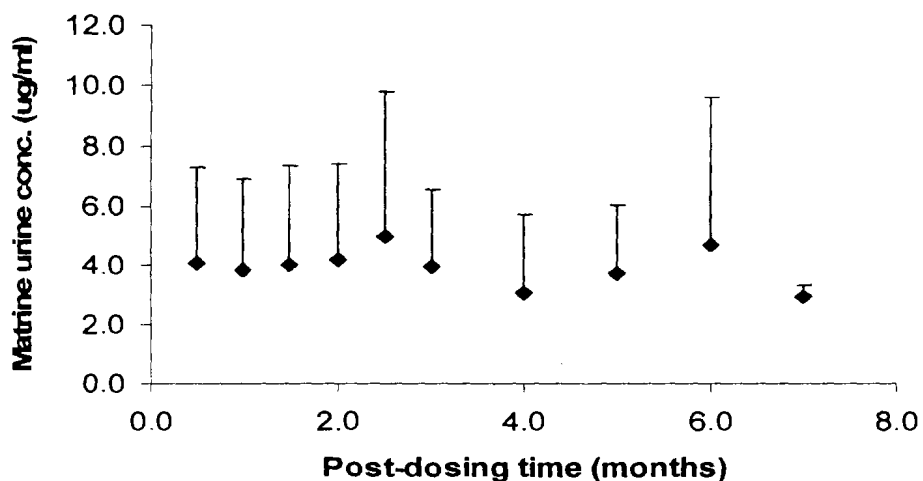


## 6.4 Discussion

A PBPK model for matrine was developed, based on the experimental data from our laboratory and the published kinetic data in the literature. The model provides an appropriate qualitative and quantitative description of pure matrine and crude matrine (in Acapha®) concentrations in the tissues and plasma of rats and the plasma and urine of humans. Both pure and crude matrine (in Acapha®) are absorbed rapidly from the gastrointestinal tract of rat into the systemic circulation. They are also available for uptake by the major organs throughout the body. The PK profiles of pure matrine and crude matrine in the rat tissues are very similar (Figure 6.2). The exception being that crude matrine is absorbed at a slower rate than pure matrine (Table 6.4) perhaps due to the matrix effects of Acapha®.

Matrine concentrations in the rat tissues are found to decrease in the order of liver>kidney>spleen>>brain>heart, lung, plasma> muscle >fat. Because matrine is a

small, uncharged, and lipid-soluble chemical, it diffuses easily through the capillary and cell membranes. This also may explain why the Tmax of matrine in most rat tissues are < 15 min post-dosing (Figure 6.2). The uptake of matrine by a tissue/organ probably is governed by the dose, the perfusion rate and the lipid content of the organ. Thus the liver, kidney and spleen exhibit high matrine concentrations; these organs are highly perfused and, with exception of the kidney, have relatively high lipid content. Two other lean but highly perfused organs, the heart and lung show rapid matrine uptake but lower matrine concentrations. Skeletal muscle, a tissue with a moderate perfusion rate and low lipid content, exhibit relatively slow and limited uptake of matrine. Luo and Xie (1991) examined tissue distribution in Wistar rats after administering 40 mg/kg pure matrine $i.g.$ Matrine concentrations in the tissues were found to be higher than those in the blood; they decreased in the order of kidney >liver >lung > brain > heart. The order of liver and kidney matrine concentrations are reversed of that observed in the present study. An explanation for the discrepancy in results is not readily available but may be related to the rat species or the dose of matrine used in these studies. .

A comparison of high dose and low dose kinetic data in rat shows that the Cmax in the high dose groups are about 10-fold higher than those of the low dose groups (Figure 6.2). This is consistent with the 10-fold difference in the administered doses and the assumption that matine kinetics in rat and human involve the first-order processes.

In general, the PK parameters of pure matrine were found to be equal or higher than that of crude matrine especially those in the high dose groups (Table 6.5) which are in agreement with the $in$ $vitro$ Caco-2 cell transport study (Figure 3.9). These results probably are related to the matrix effects of Acapha® which could reduce the absorption

of crude matrine by the rat. Because KA2 and F2 are relatively small when compared to KA1 and F1, the second absorption phase plays only a limited role in matrine absorption and thus matrine PK in the rat. The bioavailabilities of matrine in the rat range from 0.6-0.8 (Table 6.5); they are higher than the 0.44 bioavailability at 8 hr post-dosing in rats after receiving 40 mg/kg pure matrine *p.o.* (Wu *et al.* 2003).

Matrine is excreted unchanged *via* the urine and feces which are represented by KEL and KF, respectively. Initially, KEL and KF values were estimated from the literature and from the experimental data of the present study. KEL was further optimized using the urinary excretion data. Since KF was not a sensitive model parameter and only 0.36 ± 0.064% of the administered dose to rat was excreted in the feces in 24 hr (Luo and Xia, 1991), it was fixed at 0.5 $hr^{-1}$ and 1.4 $hr^{-1}$, respectively for human and rat PBPK models.

In the present study, tissue/blood partition coefficients for matrine in the rat were estimated using 3 different methods: (a) the tissue-composition model (Poulin *et al*, 2002, Luttringer *et al*, 2003), (b) *in vitro* equilibrium dialysis method (Lin *et al.*, 1982), and (c) *in vivo* AUC method (Gallo *et al.*, 1987). There was some dissimilarity among the tissue/blood partition coefficients determined by these methods:

(a) The tissue-composition model (Poulin *et al*, 2002, Luttringer *et al*, 2003) was unable to provide a reasonable simulation for most of the rat tissue data; it overestimated matrine concentrations in the fat, brain, muscle, and heart but underestimated matrine concentration in kidney, liver, and spleen (data not shown), although it provided an adequate simulation for matrine concentration in the plasma (Table 6.8). The main assumption of the tissue-composition model is the homogenous distribution of matrine

into the tissues *via* the passive diffusion, soluble or lipophilic (lipid and water) and binding (specific and non-specific) processes. This approach of tissue/blood partition coefficients determination fails if an error is made in estimating or calculating one of these parameters.

(b) The *in vitro* equilibrium dialysis method (Lin *et al.*, 1982) improves the simulation for lung, heart, brain, and fat but was unable to improve kidney, liver, spleen, and muscle prediction (Table 6.8). The *in vitro* equilibrium dialysis procedure involves the use of tissue homogenates, in which normal tissue architecture and cellular structure are disrupted. These may introduce changes in the portioning of matrine in some tissues.

(c) In our hands, the area method of Gallo *et al.*, (1987) provided the best simulation for the experimental data. The tissue/plasma partition coefficients are related to many *in vivo* factors such as blood flow, organ volume, tissue components, non specific binding-proteins and active transporter, and barrier between different tissues. Therefore, prediction of *in vivo* PC with an *in vitro* system is limited by the above factors and it is best to obtain these parameters with an *in vivo* study (Igari *et al*, 1983). The PCs of our rat PBPK model were derived from an *in vivo* tissue distribution study; they were further improved using the optimization procedure of AcslXtreme®. Thus, they are preferable to the PCs derived from an *in vitro* equilibrium study or a tissue composition model because these partition coefficients are the most accurate estimates.

**Table 6.8:** The log-likelihood of the tissue distribution data for 3.8 g/kg Acapha® from three sets of PCs

| Tissue | Tissue composition- based | *In vitro* dialysis-based | AUC-based |
|---|---|---|---|
| Fat | -48.7 | -23.6 | -5.4 |
| Kidney | -21.3 | -22.2 | -8.1 |
| Spleen | -10.8 | -11.8 | -6.8 |
| Liver | -16.2 | -12.6 | -17.1 |
| Brain | -38.9 | -15.6 | -9.4 |
| Heart | -24.6 | -3.8 | -6.6 |
| Plasma | -21.0 | -10.1 | -14.8 |
| Muscle | -28.5 | -20.6 | -13.3 |
| lung | -23.3 | -6.0 | -2.7 |

The volume of distribution at steady state (Vdss) represents the equivalent plasma volume in which a drug is distributed into the body. In the present study, two different methods were used to calculate the Vdss: (a) it was calculated from the non-compartmental model analysis of the matrine plasma concentration-time curve, and (b) it was also estimated from the sum of the products of tissue masses and partition coefficients of the PBPK model (Bjorman *et al*, 2001). Table 6.4 shows the Vdss of matrine in rat and human calculated by these methods. The closeness between the Vdss calculated from the plasma matrine concentration data and that derived from the sum of the products of the tissue masses and partition coefficients suggest that the AUC-based partition coefficients are reasonable estimates of the true values in rat and human.

**Table 6.9:** Vdss estimates of matrine using two different methods

| | Vdss calculated by non-compartmental model | Vdss calculated by summing Vi x Pt:p |
|---|---|---|
| Human | 58.3 L | 69.5 L |
| Rat | 1.45 L | 1.32 L |

In the PBPK model, it is assumed that 1 kg of body weight is equal to 1 liter of body volume. As shown in Table 6.4, the Vdss of matrine in human is about 58-70 liters which is very close to the body volume of a standard human. Therefore, matrine is distributed not only in the plasma (about 5 liters) and the interstitial space (about 9 liters) (Tsuji, et al, 1985) but also the intracellular space in human body. In contrast, the Vdss of rat is almost 4x greater than the body volume of the rat (0.35 liter). A higher Vdss in the rat may be related to the higher protein fraction in the rat tissues than human tissues. The ratio of interstitial albumin to plasma albumin in rat is about 3 (Katz *et al.*, 1970), whereas the corresponding ratio in man is about 1.4 (Jusko *et al.*, 1976). Therefore, relative more albumin is present in the interstitial space of rat than human for binding with matrine thus increasing the Vdss of the rat.

A long-term goal of this study was to develop a PBPK model of matrine to help implementing the clinical trials of Acapha®. This goal has been achieved. I have developed and validated a PBPK model of matrine in rat dosed with a single oral dose of pure matrine or Acapha®. The rat model was extrapolated to human by replacing the physiological and biochemical parameters of the rat model with those of the human. The human PBPK model was calibrated against available experimental data before being used

in predicting the plasma PK of matrine in human after receiving a single dose or multiple doses of Acapha® *p.o.* As shown in Figure 6.15:    , matrine plasma concentrations in the biweekly blood samples of the volunteers are bracketed by the model predicted plasma matrine concentrations. Presumably the model also is able to predict accurately matrine PK in the major organs of humans after receiving multiple daily oral doses of Acapha®.

Among the human plasma samples analysed by GC/MS-SIM, four samples were found to exceed the upper limit (0.115 µg/ml) of the model-predicted plasma concentration (data not shown). A close look at the medical history of these volunteers reveals that their physiology and biochemistry have been compromised. It is not known whether the physiological or biochemical change results from Acapha® treatment or whether the effects of other health problems. However, the model predicted upper limit on plasma matrine concentration may serve as a signal or trigger for the volunteers' health status. In other words, a volunteer's health should be examined more closely when his/her plasma matrine concentration exceeds the model predicted upper limit.

## 6.5 References

Anderson, M.E., Sarangapani, R., Reitz, R.H., Gallavan, R.H., Dobrev, I.D., and Plotzke, K.P. (2001) Physiologically modelling reveals novel pharmacokinetic behavior for inhaled octamethylcyclotetrasiloxane in rats. Toxicological Sciences. 60:214-231.

Bellman, R., Kalaba, R., and Jacquez, J.A. (1960) Some mathematical aspects of chemotherapy. Bulletin of Mathamatical Biophysics. 22: 181-190.

Benowitz, N.M., Forsyth, R.P., Melmon, K.L. and Rowland, M. (1974) Lidocaine disposition kinetics in monkey and man. I. Prediction by a perfusion model. Clinical Pharmacology and Therapeutics. 16:87-98.

Bischoff, K.B., Dedrick, R.L., Zaharko, D.S., and Longstreth, J.A.(1971) Methotrexate pharmacokinetics Journal of Pharmaceutical Sciences. 60:1128-1133.

Bischoff, K.B., Dedrick, R.L. and Zaharko, D.S. (1970) Preliminary model for methotrexate pharmacokinetics. Journal of Pharmaceutical Sciences. 59:149-154.

Bischoff, K.B. and Dedrick, R.L. (1968) Thiopental pharmacokinetics. Journal of Pharmaceutical Sciences. 57:1346-1351.

Bjorkman, S., Wada, R., Berling, B.M. and Benoni, G. (2001) Prediction of the disposition of midazolam in surgical patients by a physiologically based pharmacokinetic model. Journal of Pharmaceutical Sciences. 90(9):1226-1241.

Bjorkman, S. (2003) Reduction and lumping of physiologically based pharmacokinetic models: prediction of the disposition of fentanyl and pethidine in humans by successively simplified models. Journal of Pharmacokinetics and Pharmacodynamics. 30(4):285-307.

Bois, F.Y., Woodruff, T.J. and Spear, R. (1991) Comparison of three physiologically based pharmacokinetic models of benzene disposition. Toxicology and Applied Pharmacology. 110:79-88.

Bonate, P.L., Swann, A. and Silverman, P.B. (1996) Preliminary physiologically based pharmacokinetic model for cocaine in the rat: model development and scale-up to humans. Journal of Pharmaceutical Sciences. 85(8):878-883.

Brown, R.P., Delp, M.D., Linstedt, S.L., Rhomberg, L.R., and Beliles, R.P. (1997) Physiological parameter values for physiological based pharmacokinetic models, Toxicology and Industrial Health. 13(4):407-484.

Carlton, L.D., Pollack, G. M. and Brouwer, K.L. (1996) Physiologic pharmacokinetic modeling of gastrointestinal blood flow as a rate-limiting step in the oral absorption of digoxin: implications for patients with congestive heart failure receiving epoprostenol. Journal of Pharmaceutical Sciences. 85(5):473-477.

Chan, K.K., Cohen, J.L., Gross, J.F., Himmelstein, K.J., Bateman, J.R, Tsu-Lee, Y. and Marlis, A.S. (1978) Prediction of adriamycin disposition in cancer patients using a physiologic, pharmacokinetic model. Cancer Treatment Reports. 62(8):1161-1171.

Chen, H.S. and Gross, J.F. (1979) Physiologically based pharmacokinetic models for anticancer drugs. Cancer Chemotherapy and Pharmacology. 2(2):85-94.

Clewell, R.A., Merril, E.A., Yu, K.O., Mahle, D.A., Sterner, T.R., Mattie, D.R., Robinson PJ., Fisher, J.W. and Gearhart, J.M. (2003) Predicting fetal perchlorate dose and inhibition of iodide kinetics during gestation: a physiologically-based pharmacokinetic analysis of perchlorate and iodide kinetics in the rat. Toxicological Science. 73(2):235-55.

Dallas, C.E., Chen, X.M., O'Barr, K., Muralidhara, S., Varkonyi, P. and Bruckner, J.V. (1994) Development of physiologically based pharmacokinetic model for perchloroethylene using tissue concentration-time data. Toxicology and Applied Pharmacology. 128(1):50-9.

Dedrick, R.L., Forrester, D.D. and Ho, D.H. (1972) In vitro-in vivo correlation of drug metabolism-deamination of $1$-D-arabinofuranosylcytosine. Biochemical Pharmacology. 21(1):1-16.

Dedrick, R.L., Zaharko, D.S. and Lutz, R.J. (1973) Transport and binding of methotrexate *in vivo*. Journal of Pharmaceutical Sciences. 62 (6):882-890.

Dedrick, R.L., Forrester, D.D., Cannon, J.N., el-Dareer, S.M. and Mellett, L.B. (1973) Pharmacokinetics of 1-beta-D-arabinofuranosylcytosine (ARA-C) deamination in several species. Biochemical Pharmacology. 22(19):2405-2417.

Dedrick, R.L., Myers, C.E., Bungay, P.M. and DeVita, V.T. Jr. (1978) Pharmacokinetic rationale for peritoneal drug administration in the treatment of ovarian cancer. Cancer Treatment Reports. 62(1):1-11.

Eickoff, C.V. (2004) Studies of polycyclic aromatic hydrocarbons in Dungeness crabs: biomonitoring, physiologically based toxikinetic model, and human health risk assessment. Thesis.

Grillo, J.A., Venitz, J. and Ornato, J.P. (2001) Prediction of lidocaine tissue concentrations following different dose regimes during cardiac arrest using a physiologically based pharmacokinetic model. Resuscitation. 50(3):331-340.

Hagard, H.W. (1924) The absorption, distribution, and elimination of ethyl ether. II. Analysis of the mechanism of the absorption and elimination of such a gas or vapor as ethyl ether. Journal of Biological Chemistry. 59:753-770.

Harris, P.A. and Gross, J.F. (1975) Preliminary pharmacokinetics model for adriamycin (NRC-123127). Cancer Chemotherapy Reports, Part 1. 59:819-825.

Himmelstein, K.J. and Gross, J.F. (1977) Mathematical model for cyclocytidine pharmacokinetics. Journal of Pharmaceutical Sciences. 66(10):1441-1444.

Himmelstein, K.J. and Lutz, R.J. (1979) A review of the applications of physiologically based pharmacokinetic modeling. Journal of Pharmacokinetics and Biopharmaceutics. 7(2):127-145.

Igari, Y., Sugiyama, Y., Sawada, Y., Iga, T., Hanano, M. (1983) Prediction of diazepam disposition in the rat and man by a physiologically based pharmacokinetic model. Journal of Pharmacokinetics and Biopharmaceutics. 11(6):577-593.

Ishida, S., Sakiya, Y., Ichikawa, T., Taira Z. and Awazu, S. (1990) Prediction of glycyrrhizin disposition in rat and man by a physiologically based pharmacokinetic model. Chemical & Pharmaceutical Bulletin. 38(1):212-218.

Jusko, W.J. (1976) Pharmacokinetics in disease state changing protein binding. In the Effect of Disease State on Drug Pharmacokinetics. Ed. Benet, L.Z. American Association, Washington, DC, pp.99-123.

Kang, H.J., Wientjes, M.G. and Au, J.L. (1997) Physiologically based pharmacokinetic models of 2',3'-dideoxyinosine. Pharmaceutical Research. 14(3):337-344.

Katz, J., Bonnarris., G., Golden., S., and Sellers., A.L.( 1970) Extravascular albumin mass and exchange in rat tissues. Clinical Science (Lond.). 39:705-724

Kawai, R., Lemaire, M., Steimer, J.L., Bruelisauer, A., Niederberger, W. and Rowland, M. (1994) Physiologically based pharmacokinetic study on a cyclosporin derivative, SDZ IMM 125. Journal of Pharmacokinetics and Biopharmaceutics. 22(5):327-365.

Kawai, R., Mathew, D., Tanaka, C. and Rowland, M. (1998) Physiologically based pharmacokinetics of cyclocporine A: extension to tissue distribution kinetics in rats and scale-up to human. Journal of Pharmacology and Experimental Therapeutics. 287:457-468.

Kim, J.Y., Lee, S.Y., Kim, D.H.(2002) Effects of flavonoids isolated from Scutellariae Radix on cytochrome P-450 activities in human liver microsomes. Journal of Toxicology and Environmental Health, Part A. 65:373-381.

Lagneau, F., Marty, J., Beyne, P. and Tod, M. (2005) Physiologically modelling for indirect evaluation of drug tissular pharmacokinetics under non-steady- state conditions, an example of antimicrobial prophylaxis during liver surgery. Journal of Pharmacokinetics and Pharmacodynamics. 32(1):1-31.

Lee, S.K., Ou, Y.C., Yang, R.S. (2002) Comparison of pharmacokinetic interactions and physiologically based pharmacokinetic modeling of PCB 153 and PCB 126 in nonpregnant mice, lactating mice, and suckling pups. Toxicological Sciences. 65(1):26-34.

Levitt, D.G. and Schnider, T.W.(2005) Human physiologically based pharmacokinetic model for propofol. BMC Anesthesiology. 5(4):1471-2253.

Levitt, D.G. and Schoemaker, R.C.(2006) Human physiologically based pharmacokinetic model for ACE inhibitors: ramipril and ramiprilat. BMC Clinical Pharmacology. 6:1-27.

Li, J. and Gwilt, P. (2002) The effect of malignant effusions on methotrexate disposition. Cancer Chemotherapy and Pharmacology. 50(5):373-382.

Lin, J.H., Sugiyama, Y., Awazu, S., and Hanano, M. (1982) In vitro and in vivo evaluation of the tissue-to blood parttion coefficient for physiological pharmacokinetic models. Journal of Pharmacokinetics and Biopharmaceutics. 10(6):637-647.

Luo, X.Y. and Xia, B.N. (1991) Pharmacokinetic study of matrine. Journal of Guiyang Medical Journal. 16(2):180-183.

Luttringer, O, Theil, F.P., Poulin, P, Schmitt-Hoffmann, A.H., Guentert, T.W., and Lave T. (2003) Physiologically based pharmacokinetic (PBPK) modeling of disposition of epiroprim in humans. Journal of Pharmaceutical Sciences. 92(10): 1990-2007.

Lutz, R.J., Galbraith, W.M., Dedrick, R.L., Shrager, R. and Mellett, L.B. (1977) A model for the kinetics of distribution of actinomycin-D in the beagle dog. Journal of Pharmacology and Experimental Therapeutics. 200(3):469-478.

Mapleson, W.W. (1963) An electric analogue for uptake and exchange of inert gases and other agents. Journal of Applied Physiology. 18:197-204.

Maruyama, W, Yoshida, K., Tanka, T. and Nakanishi, J. (2002) Determination of tissue-blood partition coefficients for a physiological model for humans and estimation of dioxin concentration in tissues. Chemosphere. 46:975-985.

Maruyama, W., Yoshida, K., Tanka, T. and Nakanishi, J. (2003) Simulation of dioxin accumulation in human tissues and analysis of reproductive risk. Chemosphere. 53(4):301-313.

Menzel, D.B. (1987) Physiological pharmacokinetic modeling. Environmental Science & Technology. 21:944-950.

Moghadamnia, A.A., Rostami-Hodjegan, A., Abdul-Manap, R., Wright, C.E., Morice, A.H. and Tucker, G.T. (2003) Physiologically based modelling of inhibition of metabolism and assessment of the relative potency of drug and metabolite: dextromethorphan vs. dextrorphan using quinidine inhibition. British Journal of Clinical Pharmacology. 56(1):57-67.

Morrison, P.F., Lincoln, T.L. and Aroesty, J. (1975) Disposition of cytosine arabinoside (NSC-63878) and its metabolites: a pharmacokinetic simulation. Cancer Chemotherapy Reports, Part 1. 59(4):861-876.

Nagata, O., Murata, M., Kato, H., Terasaki, T., Sato, H. and Tsuji, A. (1990) Physiological pharmacokinetics of a new muscle-relaxant, inaperisone combined with its pharmacological effect on blood flow rate. Drug Metabolism and Disposition. 18(6):902-910.

Nestorov, I.A., Aarons, L.J., Rowland, M. (1997) Physiologically based pharmacokinetic modelling of a homologous series of barbiturates in the rat: a sensitivity analysis, Journal of Pharmacokinetics and Biopharmaceutics. 25 (4): 413-47.

Nestorov, I. (2003) Whole body pharmacokinetic models, Clinical Pharmacokinetics. 42(10):883-908.

Perleberg, U.R, Keys, D.A. and Fisher, J.W. (2004) Development of a physiologically based pharmacokinetic model for decane, a constituent of jet propellent-8. Inhalation Toxicology. 16(11-12):771-783.

Plowchalk, D.R., Teeguarden, J.   (2002) Development of a physiologically based pharmacokinetic model for estradiol in rats and humans: a biologically motivated quantitative framework for evaluating responses to estradiol and endocrine- active compounds. Toxicological Sciences. 69 (1):60-78.

Poulin, P. and Theil, F. P. (2002) Prediction of pharmacokinetics prior to in vivo studies II. Generic physiologically based pharmacokinetic models of drug disposition. Journal of Pharmaceutical Sciences. 91(5): 1358-1370.

Rao, H.V., Beliles, R.P., Whitford, G.M. and Turner, C.H. (1995) A physiologically based pharmacokinetic model for fluoride uptake by bone. Regulatory Toxicology and Pharmacology. 22:30-42.

Sarangapani, R., Teeguarden, J., Anderson, M.E., Reitz, R.H. and Plotzke, K.P. (2003) Route-specific   differences   in   distribution   characteristics   of octamethylcyclotetrasiloxane  in rats: analysis using PBPK models. Toxicological Sciences. 71:41-52.

Simmons, J.E., Boyes, W.K., Bushnell, P.J., Raymer, J.H., Limsakun, T., McDonald, A., Sey, Y.M. and Evans, M.V. (2002) A physiologically based pharmacokinetic model for trichloroethylene in the male long-evans rat. Toxicological Sciences. 69(1):3-15.

Sit, D.S., Gao, G., Law, F.C. and Li, P.C. (2004) Gas chromatography-mass spectrometry determination of matrine in human plasma. Journal of Chromatography B. 808(2):209-214.

Teorell, T. (1937) Kinetics of the distribution of substances administered to the body. Archives Internationales de Pharmacodynamie et de Therapie. 57:205-240.

Trachsel, D., Tschudi, P., Portier, C.J., Kuhn, M., Thormann, W., Scholtysik, G. and Mevissen, M. (2004) Pharmacokinetics and pharmacodynamic effects of amiodarone in plasma of ponies after single intravenous administration. Toxicology and Applied Pharmacology. 195:113-125.

Tsuji, A., Nishide, K., Minami, H., Nakashima, E., Terasaki, T. and Yamana, T. (1985) Physiologically based pharmacokinetic model for cefazolin in rabbits and its preliminary extrapolation to human. Drug metabolism and Disposition. 13(6):729-739

Wang, P.Q., Lu, G.H., Zhou, X.B., Shen, J.F., Chen, S.X., Mei, S.W., and Chen M.F. (1994) Pharmacokinetics of matrine in healthy volunteers. Acta Pharmaceutica Sinica. 29(5):326-329.

Wang, P.Q., Lu, G.H., Zhou, X.B., Shen, J.F., Chen, S.X., Mei, S.W. and Chen, M.F. (1994) Pharmacokinetics of matrine in healthy volunteers. Acta Pharmaceutica Sinica. 29 (5):326-329.

Wang, X.F., Santostefano, M.J., Evans, M.V., Richardson, V.M., Diliberto, J.J. and Birnbaum, L.S. (1997) Determination of parameters responsible for pharmacokinetic behavior of TCDD in female Sprague-Dawley rats. Toxicology and Applied Pharmacology. 147:151-168.

Williams, R.J., Vinegar, A, McDougal, J.N., Jarabek, A.M. and Fisher, J.W. (1996) Rat to human extrapolation of HCFC-123 kinetics deduced from halothane kinetics: a corollary approach to physiologically based pharmacokinetic modelling. Fundamental and Applied Toxicology. 30:55-66.

Wu, X., Yamashida, F., Hashida, M., Chen, X., and Hu, Z. (2003) Determination of matrine in rat plasma by high-performance liquid chromatography and its application to pharmacokinetic studies. Talanta. 59:965-971.

Zaharko, D.S., Dedrick, R.L. and Oliverio, V.T. (1972) Prediction of the distribution of methotrexate in the sting rays Dasyatidae sabrina and sayi by use of a model developed in mice. Comparative Biochemistry and Physiology. A, Comparative Physiology. 42(1):183-194.

Zaharko, D.S., Dedrick, R.L., Peale, A.L., Drake, J.C. and Lutz, R.J. (1974) Relative toxicity of methotrexate in several tissues of mice bearing Lewis lung carcinoma. Journal of Pharmacology and Experimental Therapeutics. 189(3):585-592.

# CHAPTER 7:
# CONCLUSION

Acapha® is an herbal mixture prepared from six common Chinese herbs. Little is known of the pharmacokinetics (PK) of Acapha®. The purposes of the present study were to determine the possible use of matrine as a chemical marker to study the PK of Acapha®, to compare the PK of pure matrine with that of crude matrine (in Acapha®), to elucidate the underlying mechanism of matrine absorption and metabolism, and to develop and validate a physiologically based pharmacokinetic (PBPK) model of matrine for rats and humans. All these goals have been achieved.

Although Acapha® has been manufactured in China under the guidance of Good Agricultural Practice and Good Manufacturing Practice, the quality of the product may still change during storage and transportation. Therefore, the quality of the Acapha® tablets was reassessed before the initiation of the pharmacokinetic (PK) studies. The Acapha® tablets were extracted by 70% ethanol and analysed using GC/MS and HPLC/UV. Results of the analyses show that the chemical profiles of Acapha® were consistent with those provided by the manufacturer and that a standardized level of matrine was found in each of the Acapha® tablets.

In the present study, matrine was selected as a marker chemical for the Acapha® PK studies although the active components of Acapha® remained largely unknown at present. However, evidence is accumulating to indicate that matrine possesses many of the chemopreventive and/or anticancer properties of Acapha®. As matrine is also used in

China for treatment of heart arrhythmias and other problems, pure matrine PK studies are readily available in the Chinese medicine literature. However, it is not known how much of this pure matrine PK information is applicable to the PK of crude matrine in Acapha® matrices. In the present studies, the PK of pure matrine and crude matrine (in Acapha®) were compared using the following *in vitro* and *in vivo* techniques:

## 7.1 *In vitro* absorption and metabolism studies of pure and crude matrine

The absorption and biotransformation of pure matrine and crude matrine in Acapha® were compared using *in vitro* preparations such as the Caco-2 cell transport and human liver microsomes (*i.e.,* matrine metabolism and CYP isoenzyme inhibition studies). The *in vitro* experiments were conducted to provide information on the rate and extent of matrine absorption by the human gastrointestinal tract, metabolism of matrine by the human liver and the possible occurrence of drug-Acapha® interactions in humans. This information was needed not only for elucidating the underlying mechanism of matrine absorption and metabolism but also for the development of a generic PBPK model for matrine. The results of these studies are summarized as follows:

### 7.1.1 Transport of pure and crude matrine in Caco-2 cell monolayers

Results of the Caco-2 cells transport studies showed that only a few of the chemical components in Acapha® were transported across the Caco-2 cell monolayer. Both pure and crude matrine were found to across the Caco-2 cell monolayer easily using the passive diffusion mechanism. However, the transport rate of pure matrine was always higher than those of crude matrine suggesting the retardation of matrine transport by

Acapha® matrices. P-glycoprotein did not appear to play an important role in matrine transport because verapamil, an inhibitor of P-glycoprotein did not have any effect on matrine transport. This conclusion is supported by the observation that similar apparent permeability coefficients ($P_{app}$) were observed whether matrine was transported from A to B (apical side to basolateral side) or from B to A (basolateral side to apical side). The relatively high $P_{app}$ (0.6-2.2 x 10$^{-6}$ cm/s) of transport suggests that matrine is bioavailable to humans after oral administration.

### 7.1.2 Human liver microsomal incubation

Matrine was not found to be metabolized by human liver microsomes. Acapha® extract was not a potent inhibitor of CYP 1A2, 3A4, 2C9, 2C19, and 2D6 probe substrates i.e., caffeine, erythromycin, naproxen, dextromethorphen, and diazepam metabolism because the $IC_{50}$ of Acapha® extract were > 2000μM for all probe substrates. Since human plasma matrine concentration usually is < 1μM after treatment with Acapha®, it is highly unlikely that Acapha® may interact with drugs that are metabolized by these CYP isoenzymes.

## 7.2 Pure and crude matrine PK studies *in vivo*

### 7.2.1 Tissue distribution of pure and crude matrine in the rat

The time course of pure matrine and crude matrine in the rat tissues were compared after administering, respectively 15 mg/kg and 1.5 mg/kg of pure matrine or 3.8 g/kg and 0.38 g/kg of Acapha® orally to the rat. Results of the studies indicated that both pure matrine and crude matrine were absorbed rapidly by the rat and distributed to the various tissues. Matrine concentrations in the tissues were found to decrease in the

order of liver>kidney>spleen>>brain>heart, lung, plasma> muscle >fat. Highly perfused

organs such as liver, kidney, and spleen appeared to have a relatively high Cmax. Lean

tissues, such as skeletal muscle, heart, brain, and lung had a lower Cmax. The highest

matrine levels were found in most of the tissues at 15 min post-dosing (the first time

point of sampling). Matrine tissue concentrations in rats after receiving pure matrine were

higher than that of rats after receiving crude matrine or Acapha®. The difference in tissue

concentrations was the most obvious after comparing the results of 15 mg/kg pure

matrine group with that of 3.8 g/kg Acapha® group. The finding of different tissue

concentrations for pure and crude matrine is in agreement with the results observed in the

*in vitro* Caco-2 cell transport study in which pure matrine is shown to have a higher $P_{app}$

than crude matrine.


### 7.2.2 Development and validation of a generic PBPK model for pure and crude matrine in the rat

In a parallel study, a blood flow rate limited PBPK model consisting of 12 tissue

compartments was developed to describe the PK of matrine in the rat. The assumption of

blood flow rate limitation for the tissue compartment was supported by the observation

that the experimental matrine tissue concentration-time profiles were very similar to

those of the plasma. The tissue compartments of the PBPK model included the heart,

liver, spleen, gut, lung, kidney, fat, brain, muscle, venous blood, arterial blood, and the

"rest of the body". Oral absorption of Acapha® was simulated using an input function

consisting of 2 absorption phases with different lag times. It was assumed that no matrine

was metabolized in the liver and matrine was eliminated unchanged by the kidney. The

PBPK model was able to describe all the experimental datasets of matrine obtained from

the rat closely and a PBPK model of matrine was developed and validated.

### 7.2.3 Plasma matrine kinetics in humans after receiving Acapha®

In a separate study, fifteen former smokers between the ages of 45-74 years previously diagnosed with bronchial dysplasia, were randomly divided into two groups of 6 and 9 volunteers. The group with 6 volunteers was given a single oral dose of 1.2 g (0.02 g/kg) Acapha® tablets. The group with 9 volunteer was given a single oral dose of 2.4 g (0.04 g/kg) Acapha® tablets. Blood and urine samples were collected at different time points post-dosing. Results of the studies showed that matrine appeared in the plasma as early as 0.5 hr post-dosing although plasma concentrations peaked at about 3 hr after receiving Acapha®. Also, the matrine plasma concentration-time profiles were characterized by multiple peaks which probably were due to the multiple absorption sites in the gastrointestinal tract. The plasma profile also showed large inter-individual variance. Matrine was excreted unchanged in the urine; cumulative urine excretion was about 62-76% of the administered dose in 42 hr.

### 7.2.3.1 Fitting of plasma matrine-time curve using a 2-compartment clearance-volume PK model

The human matrine concentration-time profiles obtained above were analyzed using a 2-compartment clearance-volume PK model. The experimental data of both doses of Acapha® (0.02 g/kg and 0.04 g/kg) could be fitted by a 2-compartment clearance-volume PK model. Total distribution volume (Vc + Vt) of matrine for the 0.02 g/kg and 0.04 g/kg doses were respectively, 13 L and 22 L. These are larger than the total blood volume of a human adult indicating wide distribution of matrine into the different organs

and tissues in the body.

### 7.2.3.2 Simulation of plasma matrine-time curve using PBPK model

The human matrine concentration-time profiles also were analyzed using the rat PBPK model which was scaled to a human by replacing the tissue volumes and plasma flow rates of the rat model with those of a standard human. The human PBPK model described the experimental data closely; the Loglikelihood of the model-predicted results and the experimental results was about -18.0 indicating close agreement between the model prediction and the empirical results.

### 7.2.3.3 Application of the PBPK model: extrapolation from a single oral dose to multiple daily dosing scenarios

The PBPK model was used to predict the time course of matrine plasma concentrations in humans after receiving multiple daily oral doses of Acapha®. A steady-state plasma matrine concentration was reached in about 3 days after the initiation of the study. There was no evidence of matrine accumulation in the body. Simulated matrine plasma concentrations were found to fluctuate between 0.02-0.115 µg /ml after the steady state condition was established. Matrine concentration in urine stayed at a steady level throughout the studied period.

## 7.3 Final words

Results of the present studies show that the PK behaviour of an herbal mixture can be derived from those of the marker chemical in a complex herbal mixture. The correct selection of a marker chemical for the PK study is important because if the marker chemical is an active component of the herbal mixture, the PK model can be

combined with a pharmacodynamic model to predict the effects of the herbal product as well. The PBPK model is more advantageous than the classical PK model in PK studies for an herbal mixture because several marker chemical models can be joined together to form a global model to simulate the PK of an herbal mixture.

# APPENDICES

# Appendix I. Gas chromatography-mass spectrometry determination of matrine in human plasma

## 1. Preparation of the deuterated internal standard

Deuterated derivative of matrine (14, 14-$D_2$-matrine) was prepared as follows: matrine (100 mg), 40% sodium deuteroxide (0.5 ml), deuterium oxide (5 ml), deuterated ethyl alcohol (5 ml) and absolute tetrahydrofuran (15 ml) were mixed in a 50 ml round bottom flask equipped with a reflux condenser. The mixture was refluxed for 4 days. After cooling to room temperature, the mixture was dried in a rotatory evaporator. The residues were re-dissolved in 5 ml of deuterated chloroform and the isotopic composition of matrine was assessed by GC/MS. The procedure was repeated until both hydrogens at position 14 of the matrine molecule were replaced by deuterium. The reaction mixture was extracted with deuterated chloroform, passed through a column of sodium sulfate, and dried in a rotary evaporator. The residues were re-dissolved in petroleum ether for recrystallization. The crystals were collected and stored in a desiccator.

## 2. Equipment and chromatographic conditions

A Hewlett-Packard 5890 series II gas chromatograph coupled to a 5971 mass spectrometric detector was used in the study. Chromatographic separation was performed using a 5% diphenyl-95% dimethylpolysiloxane capillary column (30 m × 0.25 mm × 0.25 μm, HP-5 MS). Helium was used as the carrier gas under a head pressure of 50 psi. The injector and transfer line temperatures were set at 250 and 280 °C, respectively. The initial oven temperature was set at 110 °C, maintained for 1 min and then increased to 220 °C at a rate of 30 °C/min and maintained for 1 min. The temperature was further increased to 300 °C at a rate of 15 °C/min and maintained for 3 min. Ionization was

performed by electron impact with 70 eV.

Matrine and deuterated matrine were analyzed in the selected ion monitoring (SIM) mode; the ions $m/z$ 248 and $m/z$ 250 were selected to monitor matrine and deuterated matrine, respectively, due to their abundance and specificity. The ion $m/z$ 249 also was recorded but was not used in matrine quantification.

## 3. Analytical procedure

### Calibration curve and quality control samples

Standard solutions of matrine were prepared in doubly distilled water. A new set of standard solutions was prepared for each batch of samples. Calibration and quality control (QC) standards were prepared by mixing various amounts of unlabeled matrine with a fixed amount of deuterated matrine (250 ng) in 1 ml of human plasma. Standard concentrations of 10, 15, 25, 50, 100, 250, and 500 ng/ml were used to prepare the calibration curve. QC sample concentrations were 10, 50, 100, and 250 ng/ml.

### Extraction procedure

An aliquot (50 µl) was removed from a stock solution of deuterated matrine (5000 ng/ml) and put into a 10-ml screw-capped glass centrifuged tube containing either a calibration or a QC standard (Section 2.4.1). NaOH (0.5 ml, 1 M) was added to make the solution alkaline. After adding 3 ml of toluene:butanol (v/v 7:3), the centrifuge tube was capped and shaken on a mechanical shaker for 15 min. The centrifuge tube was centrifuged at 3000 rpm to separate the layers. The organic layer was removed and put into a new screw-capped tube containing 0.5 ml HCl (0.25 M). The centrifuge tube was

shaken on a mechanical shaker and then centrifuged to separate the layers. The organic layer was discarded. The remaining aqueous layer was made alkaline with the addition of 0.5 ml NaOH (1 M). After the addition of 200 μl toluene:butanol (v/v 9:1), the mixture was shaken again on the mechanical shaker. The organic layer was separated by centrifugation and transferred to a GC vial for GC/MS analysis.

## Validation of the method

## Linearity

The area ratios of matrine ($m/z$ 248) and deuterated matrine ($m/z$ 250) peaks in the GC/MS chromatograms of the calibration standards were calculated. These ratios were plotted against their nominal concentrations to generate the calibration curve in Excel® using the un-weighted least-squares linear regression analysis.

## Precision and accuracy

Precision and accuracy of the method were determined by the reproducibility of the QC samples within and between different batches of samples. Precision was determined by the coefficients of variation (% CV). Accuracy of the method was determined by the relative error (% RE), which was calculated by the equation: (mean of determined concentration − actual concentration)/mean of determined concentration) × 100.

**Specificity**

Specificity of the method was performed by comparing the chromatograms from a blank plasma sample with a plasma sample spiked with either matrine or deuterated matrine.

**Limits of quantitation (LOQ)**

The LOQ was determined as the concentrations to produce a signal that is 10-fold of the error on the regression line.

**Recovery**

To determine the recovery of matrine by the liquid–liquid extraction method, 1 ml of plasma was spiked with deuterated internal standard (250 ng) and extracted using the above procedure (see Section 2.4.2). Matrine (50 or 250 ng) was added either before or after extraction. Recovery was calculated by comparing the area ratios of the matrine and deuterated matrine peaks obtained from adding matrine before and after extraction.

**Stability**

*Autosampler stability*

QC samples from the first day were kept on the autosampler of the GC/MS at room temperature for 24 h and injected again the next day. Matrine was quantified using the calibration curve constructed on the next day.

*Stock solution stability*

Aqueous stock solutions of matrine (1.1, 2.2, and 5.5 µg/ml) were stored in the refrigerator for 7–14 days at 4 °C. On days 7 and 14, these stock solutions were spiked

into human plasma samples and extracted as described above (see Section 3.2). Matrine was quantified using the calibration curves constructed with stock solutions freshly prepared on days 7 and 14.

### *Freeze–thaw stability*

Matrine was spiked into human plasma at 50, 100, and 250 ng/ml and stored at $-80$ °C temperature. The samples were subjected to three freeze–thaw cycles and then extracted. The amount of matrine in the plasma samples after three freeze–thaw cycles was determined using a newly prepared calibration curve.

### *Short-term stability*

Matrine was spiked into human plasma at 50, 100, and 250 ng/ml and stored at $-80$°C for 14 days and then extracted. The amount of matrine in the plasma samples after 14 days was determined using a newly prepared calibration curve.

# Appendix II. Goodness-of-fit assessment for classical models

| Subjects* | WSSR | CORR_ (OBS,PRED) | AIC | SC |
|---|---|---|---|---|
| G1(A) | 11.6 | 0.99 | 44.9 | 48.5 |
| G1(1) | 956.6 | 0.96 | 93.5 | 97.1 |
| G1(2) | 1008.1 | 0.95 | 94.1 | 97.6 |
| G1(3) | 41.2 | 0.98 | 55.2 | 57.9 |
| G1(4) | 3.5 | 0.99 | 30.4 | 33.1 |
| G1(5) | 70.7 | 0.98 | 60.6 | 63.3 |
| G1(6) | 264.0 | 0.98 | 79.3 | 82.9 |
| G1(7) | 115.4 | 0.96 | 95.6 | 99.1 |
| G1(8) | 114.4 | 0.99 | 65.4 | 68.1 |
| G1(9) | 360.3 | 0.98 | 76.9 | 79.6 |
| | | | | |
| G2(A) | 71.2 | 0.95 | 64.9 | 68.5 |
| G2(1) | 41.6 | 0.97 | 55.3 | 58.0 |
| G2(2) | 339.9 | 0.94 | 82.1 | 85.7 |
| G2(3) | 140.5 | 0.96 | 77.3 | 81.7 |
| G2(4) | 38.2 | 0.98 | 58.1 | 61.6 |
| G2(5) | 217.7 | 0.86 | 71.8 | 74.5 |
| G2(6) | 159.5 | 0.97 | 73.8 | 77.4 |

*G1 group rats were dose with 4.8 g Acapha®; G2 group rats were dosed with 2.4 g Acapha®. WSSR is the weighed sum of residues. CORR_(OBS,PRED) is the correlation coefficient between the predicted and determined concentrations, AIC and SC are Akaike Information Criteria and Schewarz Criteria, respectively.

# Appendix III. PBPK models of selected environmental chemicals and clinical drugs

## PBPK models of environmental chemicals

| Chemical | Subjects studied | References |
|---|---|---|
| Perchloroethylene ( PCE) | Rat | Dallas *et al*, 1994 |
| Tricholoroethylene (TCE) | Rat | Simmons *et al*, 2002 |
| Decane | Rat | Perleberg, 2004 |
| Polychlorinated biphenyls (PCB) | Mice | Lee *et al*, 2002 |
| Estradiol | Rat, human | Plowchalk *et al*, 2002 |
| 2,3,7,8-tetrachlorodibenzo-p-dioxin (TCDD) | Rat | Wang, 1997 |
| | Human | Kim *et al*, 2002; Maruyama *et al*, 2002, Maruyama *et al*, 2003 |
| Perchlorate | Rat | Clewell *et al*, 2003 |
| Octamethylcyclotetrasiloxane | Rat | Sarangapani *et al*, 2003 |
| Fluorides | Rat, human | Rao *et al*, 1995 |
| Hydrochlorofluorocarbons (HCFCs) | Rat, human | Williams, 1996 |
| Octamethylcyclotetrasiloxane (D4) | Rat | Anderson *et al*, 2001 |

## PBPK models of clinical drugs

| Drug classification | Chemical | Subjects studied | References |
|---|---|---|---|
| Anti-cancer drug | Actinomycin D | Beagle dog | Lutz *et al.*, 1977b |
| | Adriamycin | Rabbit, human | Harris and Gross, 1975 |
| | | Human | Chan *et al.*, 1978 |
| | Ara-c | Mouse, monkey, human | Dedrick *et al.*, 1972, 1973a |
| | | Mouse | Morrison *et al.*, 1975 |
| | | Human | Dedrick *et al.*, 1978 |
| | Cyclotimidine | Human | Hemmelstein and Gross, 1977 |
| | Cis-platinum | Dog | Chen and Gross, 1979 |
| | Mercaptopurine | Rat, human | Tterlikkis *et al.*, 1977 |
| | Methotrexate | Mouse, rat, dog | Bischoff *et al.*, 1970,1971 |
| | | Fish | Chen and Gross, 1979 |
| | | Dog | Chen and Gross, 1979 |
| | | Rat | Dedrick *et al.*, 1973b |
| | | Mouse | Zaharko *et al*, 1974 |
| | | Human | Dedrick *et al.*, 1978 |
| | | Human | Zaharko *et al.*, 1971 |
| | | Human | Li, 2002 |
| Other drugs | Cephalosporin | Human | Chen and Gross, 1979 |
| | Digoxin | Rat | Chen and Gross, 1979 |
| | | Dog, human | Chen and Gross, 1979 |
| | | Human | Carlton *et al.*, 1996 |
| | Dextromethorphan | Human | Moghadamnia, 2003 |

| Drug classification | Chemical | Subjects studied | References |
|---|---|---|---|
| | Halothane | Human | Chen and Gross, 1979 |
| | | | Chen and Gross, 1979 |
| | | | Chen and Gross, 1979 |
| | | | Chen and Gross, 1979 |
| | Lidocane | Monkey, human | Chen and Gross, 1979 |
| | | Human | Grillo, 2001 |
| | Methohexital | Human | Chen and Gross, 1979 |
| | Salicylate | Dog | Chen and Gross, 1979 |
| | Sulfobromophthalein | Rat, human | Chen and Gross, 1979 |
| | Thiopental | Dog, human | Bischoff and Dedrick, 1968 |
| | | | Chen and Gross, 1979 |
| | | Human | Chen and Gross, 1979 |
| | | Dog | Chen and Gross, 1979 |
| | Pentobarbital | Human | Chen and Gross, 1979 |
| | Polychlorinated biphenyls | Rat | Chen and Gross, 1979 |
| | Barbiturates | Rat | Nestorov et al., 1997 |
| | Diazepam | Rat, human | Igari, 1983 |
| | Cefazolin | Rat, human | Tsuji et al, 1985 |
| | | Human | Lagneau, 2005 |
| | Propofol | Human | Levitt et al, 2005 |
| | Epiroprim | Human | Luttringer, 2003 |
| | Glycyrrhizin | Rat , human | Ishida et al., 1990 |
| | Cyclosporine A and its derivative | Rat, human | Kawai, 1994; 1998 |

| Drug classification | Chemical | Subjects studied | References |
|---|---|---|---|
| | Cocaine | Rat, human | Bonate *et al.*, 1995 |
| | 2',3'-dideoxyinosine | Rat, human | Kang *et al.*, 1997 |
| | Ramipril, ramiprilat | Human | Levitt, 2006 |
| | Inaperisone | Rat | Nagata, 1990 |
| | Amiodarone | Pony | Trachsel, 2004 |
| | Midazolam | Human | Bjorkman, 2001 |

## Appendix IV. Model codes for matrine PBPK model in rats

Physiological parameters

| | | |
|---|---|---|
| CONSTANT | QCC = 14.0 | ! Cardiac output scaling constant (14 L/hr) |
| CONSTANT | QFTC = 0.07 | ! Fraction of blood flow to fat |
| CONSTANT | QBNC = 0.122 | ! Fraction of blood flow to bone |
| CONSTANT | QBRC = 0.02 | ! Fraction of blood flow to brain |
| CONSTANT | QHRC = 0.049 | ! Fraction of blood flow to heart |
| CONSTANT | QKDC = 0.141 | ! Fraction of blood flow to kidney |
| CONSTANT | QMSC = 0.278 | ! Fraction of blood flow to muscle |
| CONSTANT | QSKC = 0.058 | ! Fraction of blood flow to skin |
| CONSTANT | QLVC = 0.175 | ! Fraction of blood flow to liver |
| CONSTANT | QGTC = 0.131 | ! Fraction of blood flow to gut |
| CONSTANT | QSPC = 0.02 | ! Fraction of blood flow to spleen |
| CONSTANT | QRBC = 0.087 | ! Fraction of blood to rest of body |
| CONSTANT | QLGC = 0.021 | ! Fraction of blood to lung |

| | | |
|---|---|---|
| CONSTANT | BW = 0.35 | ! Body weight of rat (Kg) |
| CONSTANT | VFTC = 0.076 | ! Fraction of fat tissue |
| CONSTANT | VBNC = 0.0415 | ! Fraction of bone tissue |
| CONSTANT | VBRC = 0.0057 | ! Fraction of brain tissue |
| CONSTANT | VHRC = 0.0033 | ! Fraction of heart tissue |
| CONSTANT | VKDC = 0.0073 | ! Fraction of kidney tissue |
| CONSTANT | VMSC = 0.404 | ! Fraction of muscle tissue |
| CONSTANT | VSKC = 0.19 | ! Fraction of skin tissue |
| CONSTANT | VLVC = 0.0366 | ! Fraction of liver tissue |
| CONSTANT | VGTC = 0.027 | ! Fraction of gut tissue |
| CONSTANT | VSPC = 0.002 | ! Fraction of spleen tissue |
| CONSTANT | VLGC = 0.005 | ! Fraction of lung tissue |
| CONSTANT | VBAC = 0.0272 | ! Fraction of arterial blood |
| CONSTANT | VBVC = 0.0544 | ! Fraction of venous blood |
| CONSTANT | VRBC = 0.12 | ! Fraction of rest of body |

```
!--------------Experimental parameters


CONSTANT  BLPLR = 0.67
CONSTANT  EH = 1.0e-30              ! No matrine metabolism
CONSTANT  PDOSE = 15               ! Oral dose
CONSTANT  IVDOSE = 1.0e-30         ! IV dose (mg/kg)
CONSTANT  KA1 = 4.3               ! Oral uptake rate constant hr-1
KA1_INPUT = KA1
CONSTANT  KA2 = 1                 ! Oral uptake rate constant (hr-1).
KA2_INPUT = KA2
CONSTANT  VGLM = 0.0176
CONSTANT  KF = 1.4
CONSTANT  HT = 1.0e-30
CONSTANT  KEL = 189               ! Elimination rate constant hr-1
CONSTANT  F1 = 0.45               ! Total urine excretion of matrine at 4 hr =
                                      20%, 48 hr= 54% (Luo et al, 1991)

CONSTANT  F2 = 0.15
CONSTANT  TLAG1 = 0.2
CONSTANT  TLAG2 = 11.0            ! No lag time in Luo and Xia study
CONSTANT  KRA = 1.0e-30


!-----------------------------Timing commands


CONSTANT  TSTOP = 24.0            ! Length of experiment (hr)
CONSTANT  TINF = 0.001           ! Length of IV infusion (hr)
CONSTANT  CINT = 0.05            ! Communication interval (hr)
CONSTANT  MAXT = 0.005           ! Integration control (hr)


!-----------------------------Scaled parameters


DOSE = PDOSE*BW                  ! Oral dose (mg)
IVR = IVDOSE*BW/TINF             ! Intravenous infusion rate (mg/hr)


QC = QCC*BW**0.75                ! Cardiac output (L/hr)
QFT = QFTC*QC                    ! Blood flow to fat
!QBN = QBNC*QC                   ! Blood flow to bone
```

QBR = QBRC*QC         ! Blood flow to brain
QHR = QHRC*QC         ! Blood flow to heart
QKD = QKDC*QC         ! Blood flow to kidney
QMS = QMSC*QC         ! Blood flow to muscle
!QSK = QSKC*QC         ! Blood flow to skin
QLV = QLVC*QC         ! Blood flow to liver
QGT = QGTC*QC         ! Blood flow to gut
QSP = QSPC*QC         ! Blood flow to spleen
QRB = (QRBC + QBNC + QSKC)*QC         ! Blood flow to rest of body


VLG = VLGC*BW         ! Volume of lung (Kg)
VFT = VFTC*BW         ! Volume of fat
!VBN = VBNC*BW         ! Volume of bone
VBR = VBRC*BW         ! Volume of brain
VHR = VHRC*BW         ! Volume of heart
VKD = VKDC*BW         ! Volume of kidney
VMS = VMSC*BW         ! Volume of muscle
!VSK = VSKC*BW         ! Volume of skin
VLV = VLVC*BW         ! Volume of liver
VGT = VGTC*BW         ! Volume of gut
VSP = VSPC*BW         ! Volume of spleen
VRB = (VRBC + VBNC+ VSKC)*BW         ! Volume of rest of body
VBA = VBAC*BW         ! Volume of arterial blood
VBV = VBVC*BW         ! Volume of venous blood


! ------------------------ Tissue/blood partitioning from experimental AUCs


RFT = 0.5         ! Fat/blood partitioning coefficient
RLG = 1.53         ! Lung/blood partitioning coefficient
RBR = 2.1         ! Brain/blood partitioning coefficient
RHR = 1.5         ! Heart/blood partitioning coefficient
RKD = 20         ! Kidney/blood partitioning coefficient
RMS = 1.4         ! Muscle/blood partitioning coefficient
RLV = 10         ! Liver/blood partitioning coefficient
RRB = 6         ! Rest of body/blood partitoning coefficient
RGT = 3.0         ! Gut/blood partitiong coefficient

```
RSP = 6.6                          ! Spleen/blood partitioning coefficient

END                                ! End of initial section
DYNAMIC                            ! Beginning of execution section
ALGORITHM IALG = 2                 ! Use Gear integration algorithm
DERIVATIVE                         ! Beginning of derivative definition block


!--------MR1 = Amount remaining in site 1 (mg)
IF (T .GT. TLAG1) THEN
        RMR1 = -KA1_INPUT*MR1
        MR1 = F1*DOSE*EXP((-KA1_INPUT*(T-TLAG1)))
        ELSE
        MR1 = 0.0
        END IF


!--------RAO1 = Rate of mass input for site 1 (mg)
        RAO1 = KA1_INPUT*MR1


!---------RAO2 = Rate of mass input for site 2 (mg)
        RAO2 = KA2_INPUT*MR2


!--------MR2 = Amount remaining in site 2. Note: No site 2 for Luo's data


        IF (T .GT. TLAG2) THEN
        RMR2 = -KA2_INPUT*MR2
        MR2 = F2*DOSE*EXP((-KA2_INPUT*(T-TLAG2)))
        ELSE
        MR2 = 0.0
        END IF

!--------CLG = Concentration in the lung
        CLG=INTEG((QC/VLG)*(CBV-CLG/RLG),0.)


!--------CFT = Concentration in adipose tissue
        CFT=INTEG((QFT/VFT)*(CBA-CFT/RFT),0.)
```

!--------CBN = Concentration in the bone

!CBN = INTEG ((QBN/VBN)*(CBA-CBN/RBN),0.)


!--------CBR = Concentration in the brain

CBR = INTEG ((QBR/VBR)*(CBA-CBR/RBR),0.)


!--------CHR = Concentration in the heart

CHR = INTEG ((QHR/VHR)*(CBA-CHR/RHR),0.)


!--------CKD = Concentration in the kidney (mg/L)

CKD = INTEG ((QKD/VKD) * (CBA - CKD/RKD)

KEL*VKD*CKD/(RKD*VKD),0.)


!--------AMURINE = Amount of matrine excreted in the urine (mg)

AMURINE = INTEG ((KEL*CKD/RKD)*VKD,0.)


!---------PERCENTURINE = Percent dose excretd in the urine

PERCENTURINE = 100*AMURINE/(PDOSE*BW)


!--------CMS = Concentration in the muscle

CMS = INTEG ((QMS/VMS)*(CBA-CMS/RMS),0.)


!--------CSP = Concentration in the spleen

CSP = INTEG ((QSP/VSP)*(CBA-CSP/RSP),0.)


!--------CSK = Concentration in the skin

!CSK = INTEG ((QSK/VSK)*(CBA-CSK/RSK),0.)


!--------CRB = Concentration in the rest of body

CRB = INTEG ((QRB/VRB)*(CBA-CRB/RRB),0.)


!--------CLV = Concentration in the liver.


CLV = INTEG ((((QLV-QGT-QSP)*CBA + QGT*CGT/RGT + QSP*CSP/RSP −

QLV*CLV/RLV)/VLV) - R/VLV,0.)

R =((QLV-QGT-QSP)*CBA + QGT*CGT/RGT + QSP*CSP/RSP)*EH

!--------R = Secretion rate of matrine out of the liver cells into the bile duct(mg/hr)

R1 = INTEG ((R-R1)/HT,0.)
R2 = INTEG ((R1-R2)/HT,0.)
R3 = INTEG ((R2-R3)/HT,0.)

!--------CGLM = Concentration in the gut lumen or content compartment(mg/L or mg/kg)
!--------Note: KRA is re-absorption rate constant (/hr); KF is GI clearance (L/HR).
!--------Separate absorption compartments are not working

CGLM = INTEG ((R3 - KF*VGT*CGLM - KRA*VGT*CGLM)/VGLM,0.)

!--------CGT = Concentration in the gut wall (mg/L or mg/Kg)

CGT = INTEG ((QGT/VGT)*(CBA-CGT/RGT)+(KRA*VGT*CGLM + RAO1 +
        RAO2)/VGT,0.)

!--------CBA = Concentration of matrine in arterial blood
        CBA = INTEG(QC*(CLG/RLG-CBA)/VBA,0.)

!--------CBV = Concentration in mixed venous blood
CBV =INTEG((QFT*CFT/RFT+QHR*CHR/RHR+QKD*CKD/RKD+QMS*CMS/RMS
+ & QLV*CLV/RLV+QBR*CBR/RBR+QRB*CRB/RRB+IV-QC*CBV)/VBV,0.)

!--------CPV = Concentration in mixed venous plasma
        CPV = CBV/BLPLR

!--------IV = Intravenous infusion rate (mg/min)
        IVZONE = RSW(T.GE.TINF, 0.,1.)
        IV = IVR*IVZONE
TERMT(T.GE.TSTOP)        ! Condition for terminating simulation
END                      ! End of derivative block
END                      ! End of dynamic section
END                      ! End of program

183

## Appendix V. Tissue composition method to estimate tissue/plasma partition coefficients

Tissue composition method to determine tissue/plasma partition (Pt:p) coefficients were conducted according to Poulin *et al.*, (2002). Briefly, the tissues and plasma were considered as mixtures of total lipids, water, and proteins with a global pH of 7.4. Therefore, a drug is partitioned into lipid and water fractions (nonspecific binding), as well as a specific reversible binding to proteins. The following tissue composition-based equations were used to estimate the Pt:p values:

$$\text{Pt:p nonadipose} = \frac{[\text{Po:w} \times (\text{Vnt} + 0.3 \times \text{Vpht})] + [1 \times (\text{Vwt} + 0.7 \times \text{Vpht})] \times \text{fup}}{[\text{Po:w} \times (\text{Vnp} + 0.3 \times \text{Vphp})] + [1 \times (\text{Vwp} + 0.7 \times \text{Vphp})] \times \text{fut}}$$

$$\text{Pt:p adipose} = \frac{[\text{Dvo:w*} \times (\text{Vnt} + 0.3 \times \text{Vpht})] + [1 \times (\text{Vwt} + 0.7 \times \text{Vpht})] \times \text{fup}}{[\text{Dvo:w*} \times (\text{Vnp} + 0.3 \times \text{Vphp})] + [1 \times (\text{Vwp} + 0.7 \times \text{Vphp})] \times 1}$$

where, $fu_t = 1/(1 + (((1 - fu_p)/fu_p) \times 0.5))$, fu = unbound fraction, t = tissue, p = plasma, $P_{o:w} = n$-octanol-buffer partition coefficient (PC) of the non-ionized species at pH 7.4, $D_{vo:w}* =$ olive oil: buffer PC of both the non-ionized and ionized species at pH 7.4, $V =$ fractional tissue volume content of neutral lipids (nl), phospholipids (ph), and water (w). The $V_n$, $V_{ph}$, $V_w$ for the tissues are summarized in next table. Data on matrine lipophilicity ($P_{o:w}$, $D_{vo:w}*$) came from literature, plasma protein binding ($fu_p$) of matrine were obtained from *in vitro* studies .

**Tissue composition data for different tissues in rat (fraction of wet tissue weight)**

| Tissue | Water (Vw) | Neutral Lipids (Vn) | Phospholipids (Vph) |
|---|---|---|---|
| Adipose | 0.12 | 0.853 | 0.002 |
| Bone | 0.446 | 0.0273 | 0.0027 |
| Brain | 0.778 | 0.0392 | 0.0533 |
| Heart | 0.779 | 0.014 | 0.0118 |
| Kidney | 0.771 | 0.0123 | 0.0284 |
| Liver | 0.705 | 0.0138 | 0.0303 |
| GI tract | 0.749 | 0.0292 | 0.0138 |
| Lung | 0.79 | 0.0219 | 0.014 |
| Muscle | 0.756 | 0.01 | 0.009 |
| Skin | 0.651 | 0.0239 | 0.018 |
| Spleen | 0.771 | 0.0077 | 0.0136 |
| Plasma | 0.96 | 0.00147 | 0.00083 |

## Appendix VI. *In vitro* dialysis method to estimate tissue/plasma partition coefficients

The tissue: phosphate buffered saline (PBS) partition coefficient was determined for each of the following nine tissues: heart, liver, spleen, lung, kidney, fat, muscle, brain, plasma (thesis of Eickhoff, 2004).

Dialysis tubing (Spectro/Por®3 MWCO 3500, Spectrum Laboratories Inc, Rancho Dominguez, CA) was pretreated according to the procedures provided by the Spectrum Product Instruction Booklet. Briefly, the tubing was cut into 5 cm lengths and soaked in distilled water at room temperature for 30 minutes to remove the glycerine or sodium azide preservative. The dialysis tubing was rinsed thoroughly with distilled water and soaked in PBS (Dulbecco's PBS from Sigma, St Louis, MO, USA) buffer pH 7.4 overnight.

Tissue homogenates were put into the dialysis tubing separately as follows: one end of the dialysis tube was tightly tied with thread. An aliquot (1 ml) of the freshly prepared tissue homogenate was pipetted into the dialysis bags and sealed carefully by tying the upper open end to prevent the inclusion of air bubbles. Excess thread was cut off but a length of thread should be left to suspend the dialysis bag in a 22-ml glass vial. Twenty ml of PBS was added nto a 22-ml glass vial. Two matrine solutions with 2000 ng/ml and 400 ng/ml concentrations were prepared and an aliquot (20 ml) of each matrine solutions was pipetted into each glass vial equipped with a micro stirring bar (Fisher). The spinning rate of the stirring bar was adjusted to ensure that the bag was submerged in the buffer but not disturbed by the stir bar at the bottom of vials. The vial was placed on a

stirring plate and the stirring condition should be same for each vial.

Duplicate samples were prepared for each tissue homogenate. For each matrine concentration, one reference and one control were prepared: the reference vial consisting of dialysis bags filled with 1 ml of matrine PBS; this was used to determine background binding. The control vial contained only matrine PBS solution without the dialysis tube inside; this was the total matrine concentration before partition. The experiment was conducted at 9°C in a temperature controlled room for 48hrs. At the end of experiment, 1 ml aliquot was taken from the PBS solution outside the bag. All the samples were extracted and then analyzed for matrine by GC/MS.

The concentration of matrine in the tissues was calculated as the difference in the concentration of matrine in the PBS of the control vial without dialysis bag minus the concentration of matrine in the PBS of each vial with dialysis bag. If necessary the concentration in the tissues can be corrected by the background which comes from the reference vial. The tissue:PBS partition coefficient was calculated as the matrine concentration in each tissue over the matrine concentration in the PBS. Tissue: plasma partition coefficients were calculated as the tissue:PBS partition coefficient over the plasma: PBS partition coefficient.